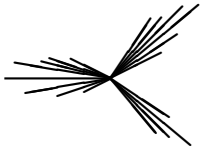

Instituto de Física Teórica
Universidade Estadual Paulista

Master's Dissertation IFT–D.011/2014

Complex Scalar Dark Matter in a B-L Model

Ernany Rossi Schmitz

Advisor

Prof. Dr. Juan Carlos Montero Garcia

Co-advisor

Dr. Bruce Lehmann Sánchez Vega

May, 2014

Acknowledgements

There are many people who I must especially thank because without them this master's thesis wouldn't be possible. First of all, I thank my mother Nelci, father Argídio and brother Fabian for all the support, love, trust, kindness I always got from them.

I thank my master's advisor, Juan Montero, for the patience, the humor, the humble way he treats people and willingness for explaining and discussing. Thanks to him, I started my master's at IFT, because despite his obligations and lack of free time as IFT director, he was willing to advise me. Also, I must thank my co-advisor Bruce Sánchez for his enthusiasm, patience, humor and pratical and intelligent way to solve problems.

I thank IFT for all the structure I enjoyed throughout these two years and for having the opportunity to learn with great professors.

Thanks to the friends I made in IFT and to my long-time friends which I made in my hometown, who I hardly meet but mean a lot to me. I won't say names because someone may be left out of the list. However, the ones with who I shared my life will identify themselves.

Lastly, I thank CAPES for supporting financially my studies.

Resumo

Na primeira parte deste trabalho, fornecemos a história que constitui a base para a evidência de matéria escura. Também, apresentamos aqui alguns dos candidatos à matéria escura mais estudados. Depois, mostramos as ferramentas necessárias ao entendimento dos cálculos de densidade de relíquia, tais como a base de Relatividade Geral e da cosmologia do universo primordial (termodinâmica do universo primordial, média térmica da seção de choque de aniquilação vezes a velocidade, e as soluções analítica e numérica para a equação de Boltzmann). Finalmente, dentro desta parte de fundamentação, discutimos brevemente alguns dos experimentos de detecção direta e indireta e vínculos impostos por eles sobre a matéria escura.

Na segunda parte, analisamos uma extensão, do Modelo Padrão, obtida adicionando-se à simetria de gauge um grupo U(1) local de carga B-L, número bariônico menos número leptônico. Nós mostramos que esta extensão, chamada de modelo B-L, pode conter dois candidatos viáveis à matéria escura e estudamos as condições sobre o espaço de parâmetros do potencial escalar que não só resulta na densidade de relíquia observada, mas também está em acordo com os vínculos provenientes de experimentos de detecção direta.

Palavras-chave: Universo primordial, produção termal de WIMPs, equação de Boltzmann, cosmologia FRW, modelo B-L, matéria escura escalar complexa, detecção direta e indireta.

Áreas do conhecimento: Física de Partículas, Cosmologia, Termodinâmica.

Abstract

In the first part of this work, we provide the historical background that underlies the evidence of dark matter. Also, we present here some of the most studied dark matter candidates. Later, we show the necessary tools for the understanding of relic density calculation, such as the basics of General Relativity and the early Universe Cosmology (thermodynamics of the early Universe, the thermal average of the annihilation cross section times the velocity, and both the approximated analytical and numerical solutions to the Boltzmann equation). Finally, in this grounding part, we discuss briefly some of both direct and indirect detection experiments and constraints imposed by them on dark matter.

In the second part, we analyze an extension of the Standard Model (SM) obtained by adding to the gauge symmetry a local U(1) group of charge B-L , baryon minus lepton numbers. We show that this extension, called B-L Model, can contain two viable cold dark matter candidates and we study the conditions on the space of parameters of the scalar potential that both yields the observed relic density and is in agreement with constraints which come from direct detection experiments.

Keywords: Early universe, thermal production of WIMPs, Boltzmann equation, FRW cosmology, B-L model, complex scalar dark matter, direct and indirect detection.

Areas of knowledge: Particle Physics, Cosmology, Thermodynamics.

Contents

1 Introduction v

2 Background 1

2.1 Motivations 1

2.2 Candidates 4

3 Dark Matter Abundance Calculation 13

3.1 Basic General Relativity 13

3.1.1 Introduction 13

3.1.2 Robertson-Walker metric 14

3.2 Λ-CDM Cosmological Model 17

3.3 Thermodynamics of the early Universe 17

3.4 The Boltzmann equation 25

3.5 Thermalized cross section 30

3.5.1 $\langle \sigma v_{\text{Møl}} \rangle$ expansion in x^{-1} 35

3.5.2 Non-relativistic $\langle \sigma v_{\text{Møl}} \rangle$ ($\langle \sigma v_{\text{Møl}} \rangle_{n.r.}$) and its expansion 35

3.6 Obtaining the DM mass density 37

3.6.1 Numerical solution 37

3.6.2 Approximated solution 40

3.7 An example: How Boltzmann equation works 41

4 Detection of Dark Matter 45

4.1 Direct detection of Dark Matter 45

4.1.1 Theoretical description 47

4.2 Indirect detection of Dark Matter 50

5 Scalar Dark Matter in a B-L Model 53

5.1 Brief review of the $B - L$ model 53

5.2 The vacuum structure and the scalar sector spectrum 55

5.3 Gauge Bosons 58

5.4 Dark Matter 60

5.4.1 Thermal Relic Density 61

5.4.2 Direct Detection 63

6 Conclusions 67

A The Minimization Conditions 69

References 71

1 Introduction

Great effort has been made, since the discovery of Newton's law of gravitation (1687), for explaining how astrophysical objects move at the sky. Deviations of observed motions from the predicted ones always made our knowledge of the Universe deeper. For example, whenever discrepancies arose in the motion of the planets of the Solar system, there were people who would question the validity of the laws of gravitation, but also there existed the ones who would try to postulate yet unseen objects.

The second approach ended up being the correct one in the case of the anomalous motion of Uranus: another planet, called Neptune, was conjectured by U. Le Verrier and John Couch Adams. Neptune was discovered by J.G. Galle in 1846. Nonetheless, when anomalies in the motion of Mercury were observed, one more time people postulated an yet unseen planet, which was called Vulcan. This time, the earlier solution failed and the real solution came with the advent of Einstein's theory of general relativity, which was broader than Newton's gravitation.

The current problem of dark matter is fundamentally very similar to the old problem of orbit anomalies. Present observations, going from the scales of astrophysical systems, such as galaxy clusters, to cosmologic scales, can be explained in principle either by assuming the existence of unseen *dark* matter, or by assuming a deviation from the known theory of general relativity.

The second assumption is more complicated than the first one because it lacks simplicity when compared to the first one. Due to the observation of the collision of galaxies belonging to the cluster 1E0657-558, as explained in the section 2.1, the first solution is favored. Therefore, taking the former assumption as the right one, we are led to the conclusion, through measurements of the CMB via PLANCK sattelite, for example, that the ordinary baryonic matter is not the dominant form of material in the Universe. Although we have yet to detect the dark matter which is roughly five times more abundant than baryonic matter, there exists a lot of evidence which supports its existence, as better explained in section 2.1.

A full understanding of dark matter requires using many branches of physics and astronomy. The creation of dark matter, if thermally created, is understood via statistical mechanics and thermodynamics. Particle physics comes in, when the proposal of candidates for dark matter and the knowledge of its interactions with ordinary matter become necessary. General Relativity, astrophysics and cosmology dictate how dark matter acts on large scales and how the Universe may be viewed as a laboratory to study dark matter. Finally, the appearance of many ground and satellite-based measurements, taking into account direct or indirect detection of dark matter makes the field more attractive and dynamic.

This master thesis is organized as follows: the first chapter is devoted to exposing the discrepancies between data and theory, which led scientific community to propose new matter (in this work, we are going, unless it is explicitly indicated, to assume dark matter, i.e. particles instead of dealing with modifications of General Relativity). Also, we expose some candidates for dark matter.

The second chapter is dedicated to the study of the relic abundance calculation of dark matter which involves: General Relativity, thermodynamics, and cosmology. In a more technical way, in the end, the Boltzmann equation is the differential equation which has to be solved numerically in order to generate the behaviour of the dark matter which was once in thermal equilibrium and eventually decoupled. The physical behaviour of this equation is explained.

In the third chapter, we overview the experiments which are the basis for constraining models which include possible candidates for dark matter. Some direct and indirect detection experiments are briefly reviewed.

In the fourth chapter, a particular B-L model of particles is reviewed. Also, the candidate for dark matter within this model is characterized. In the end of it, we analyze constraints imposed on the studied model via current direct detection experiments on dark matter.

2 Background

Within this chapter, we try to provide the reader an overview to the problem of dark matter, starting from the reasons to believe there was something bad with some observations, and ending with some candidates for this new kind of matter.

2.1 Motivations

Our goal in this section is to review the most important and convincing evidences towards the existence of dark matter. This section is based importantly on [1]. We introduce the following:

- In 1933, Fritz Zwicky measured the mass of the Coma cluster of galaxies outside of our local group [2]. The technique used by Zwicky was to measure the relative velocities of the galaxies in the cluster via their Doppler shift; and use the virial theorem[1] to obtain the gravitational potential in which these galaxies were moving, and then get the mass that must generate the potential. He found for the mass of the cluster the value of about 400 times the mass that could be computed from the visible galaxies in the cluster. The observation was soon confirmed by similar measurements of the Virgo Cluster by Smith [3].

- Evidence for dark matter is also found by relating the X-ray emission from clusters of galaxies to the distribution of the respective cluster masses [4]. Clusters form via the collapse of matter over the region of several megaparsecs (1 parsec= 3.26 light-years). They generate deep gravitational potential wells because of their high masses. This way, hydrogen gas from the galaxies leaks out and fills the whole volume of the cluster. These atoms, with large velocities[2], emit X-rays when they collide. So, in this manner, the X-ray luminosity probes the depth of the cluster gravitational potential. Therefore, we can estimate the mass that generates such a potential, providing this way the contradiction between the observed matter and the matter necessary for accounting for the measured X-ray luminosity.

- In the decade of 1970, astronomers started to measure sistematically the profiles of rotational velocity for many galaxies. At this point people were used to believe that all the mass of the galaxy is made of stars that are visible. This way, we would think

[1] Recall that the virial theorem says the time average of the kinetic and potential energies of the considered system are related by $\langle T\rangle_t = \frac{-1}{2}\langle V\rangle_t$ (-1 for gravitational force) provided that the system remains bounded (spatially and in the sense of finite values of momentum).

[2] For a typical cluster mass of $10^{14} - 10^{15} M_\odot$, the gas reaches temperatures of several $10^7 K$.

that outside of the region with visible matter, the velocities behave the following way

$$F_{\text{centripetal}} = F_{\text{gravitational}} \qquad \therefore \qquad v^2 = \frac{GM_{gal}}{r} \quad \rightarrow \quad v \propto \frac{1}{\sqrt{r}} \quad , \tag{2.1}$$

where M_{gal} is the mass of the visible galaxy, and r is the distance of the object to the center of the galaxy. Here we suppose that the galaxy is spherically symmetric. Something unexpected was observed: the velocities are almost constant or slightly increasing with increasing distance [5]. Particularly, in the galaxy NGC 3067, Rubin, Thonnard and Ford [6] showed that the rotational velocity profile maintains its large value at a distance of 40 Kpc from the center of the galaxy, even though the density of stars outside of 3 Kpc becomes very small if compared to the halo of the galaxy.

Another way to measure the mass of the galaxy, other than rotation curves of stars and X-ray emitting gas belonging to the galaxy, is to take positions and velocities of test particles such as globular clusters of stars, or satellite galaxies. By measurements of the velocities of globular clusters, it was found that there is contribution to the mass of Milky Way up to distances about 100 Kpc from the center [7]. The distance, from where stars of Milky Way begin to become rare, to the center of the galaxy is approximately 15 Kpc (the solar system is at ~ 8.5 Kpc).

- Another source of measurements, concerning the existence of dark matter, comes from the cosmic microwave background [8, 9]. The microwave background was emitted at the time of recombination, epoch when protons and electrons - particles that earlier were not bounded to each other because of high temperatures of the bath of particles that contained them - became bounded and then the Universe became neutral for the photon (at this stage, the photon cannot interact at as high rates as before with proton and electron, because hydrogen is neutral). Recombination ocurred when protons and neutrons were at the temperature of about 1 eV. The most recent measurements from PLANCK satellite require a medium in which a very weakly interacting species in nonrelativistic motion, usually called CDM (Cold Dark Matter), dominates. These measurements can be converted to the fractions of baryonic and dark matter:

$$\Omega_b h^2 = 0.02205 \pm 0.00028 \qquad \Omega_{DM} h^2 = 0.1199 \pm 0.0027 \quad , \tag{2.2}$$

where $\Omega_i = \rho_i / \rho_{crit}$[3] and h is the value of the parameter which multiplies the value 100(km/s)/Mpc to give the value for the Hubble constant, i.e., $H = h \times$ 100(km/s)/Mpc.

[3] ρ_i is the i-species energy density, and ρ_{crit} is the Universe energy density that would make the Universe to be spatially flat.

- Until now, I said some times "dark matter". But that need not be the case. Instead, we could modify the law of gravity [10] and then we wouldn't have to introduce new kind of matter. This approach had great phenomenological success at scales ranging from dwarf spheroidal galaxies to superclusters. However, the interpretation in terms of new matter was encouraged by the observations in Fig. 1, extracted from ref. [11].

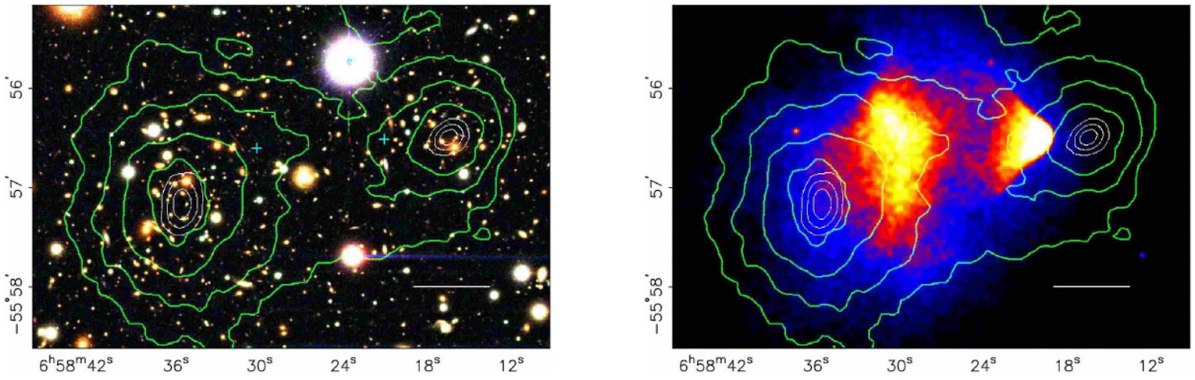

(a) (b)

Figure 1 – In the figure above are shown (a) a color image of the merging cluster 1E0657-558 and (b) a X-ray image of the same cluster. The white bar indicates 200 Kpc. The green contours in both images come from the reconstruction from the weak lensing method: the most inner contour has the highest κ[4]and the most outer one the lowest κ. The white contours show the positions of the κ peaks and correspond to 68.3%, 95.5%, 99.7% confidence levels.

The actual existence of dark matter can be confirmed either by a laboratory detection or by a discovery of a system in which the observed baryons and the inferred dark matter are spatially separated. The galaxy cluster 1E0657-558 is such a system.

During a merger of two clusters, galaxies behave as collisionless particles, while the fluid-like X-ray emitting plasmas belonging to the respective galaxy concentrations collide. So, the two gallaxy concentrations moved ahead of their plasma clouds that suffered ram pressure. In the absence of dark matter, the gravitational potential will depend only on the dominant visible matter component, which is the X-ray plasma. If, on the other hand, the mass is dominated by collisionless dark matter, the potential will trace the distribution of it, which is expected to be spatially coincident with the collisionless galaxies. Hence, by deriving a map of the gravitational potential, we are able to know which possibility we are dealing with.

[4] κ: surface mass density. It is defined simply by the integral of the energy density $\rho(\vec{r})$ over the line of sight distance. Therefore, it is related to the concentration of energy that bends the incoming source light.

2.2 Candidates

Two of the most popular classes of candidates for dark matter are MACHOs and WIMPs[12].

- MACHO is an acronym for MAssive Compact Halo Object and stands for astronomical objects which escape conventional detection (emission or absortion of light). This class includes generally baryonic objects such as neutron and white dwarf stars (stellar remnants). Objects like primordial (big bang epoch) black holes are also included since their detection is difficult.

  Also, some of these objects may consist of balls of hydrogen and helium too light to start nuclear burning. For example, if the Galactic halo were filled with Jupiter mass objects ($10^{-3}M_{\odot}$) they would not have been detected by emission or absorption of light. Brown dwarf stars with masses below $0.08M_{\odot}$ would be similarly invisible.

- WIMP, Weakly Interacting Massive Particle, stands for non-baryonic particles which were created thermally, i.e. particles which interacted with the plasma containing all the other particles after the big bang, and eventually decoupled from it, thus leaving an energy content for the current Universe. The adjective "Weakly Interacting" comes from the observation that particles which interact via the weak force have just the magnitude for the cross section that is necessary for producing the dark matter content that was observed by WMAP and PLANCK sattelite, for example.

  Examples of WIMPs are: standard model neutrinos, neutralino (from SUSY), fermions or bosons from (non-SUSY) extensions of the standard model. Famous examples of non-WIMP particles are the axion and the sterile neutrinos, discussed further below. Thermal and non-thermal candidates will be discussed more carefully now.

Below, we present some particles which make part of the spectrum of possible dark matter candidates.

- Standard Model neutrinos:

  They have already been considered good dark matter candidates because of their very low cross section. However, a direct calculation [13] shows their total relic density is predicted to be

$$\Omega_{\nu}h^2 = \sum_{i=1}^{3} \frac{m_i}{93 \text{ eV}} \quad , \tag{2.3}$$

where m_i is the mass of the ith neutrino, and $h \equiv H_0/(100 \text{ km s}^{-1} \text{ Mpc}^{-1})$. The best laboratory constraint comes from tritium β-decay experiments at Troitsk and Mainz [14], and it is given by the upper limit

$$m_\nu < 2.05 \text{ eV} \quad (95\% \text{ C.L.}) \quad , \tag{2.4}$$

and m_ν means any of the three neutrinos. This implies an upper limit to the total neutrino relic density

$$\Omega_\nu < 0.07 \quad , \tag{2.5}$$

which means that neutrinos are not abundant enough to be the dominant component of dark matter. A more restrictive constraint on the neutrino relic density comes from the data from CMB anisotropies, combined with large-scale structure data, suggesting $\Omega_\nu h^2 < 0.0067$ (95% C.L.). For three degenerate neutrino masses, this latter limit implies $m_\nu < 0.23\ eV$.

In this manner, the neutrinos are relativistic particles, also almost colisionless. Because of this, they don't allow the appearance of fluctuations below the Jeans mass[5] of $4 \times 10^{15} M_\odot \left(\frac{30 \text{ eV}}{m_\nu}\right)^2$ - they can move from high to low density regions, therefore below some radius, which implies a mass for a cloud of gas, the neutrinos would avoid fluctuations - , called the *free streaming length* [15]. This consequently would imply in a scenario of the Universe where big structures form first. This is in apparent contradiction with the fact that the Milky Way appears to be older than the Local Group. Also, there are overall indications that structure formation is done as down-top formation (for example, stars form before galaxies are formed; galaxies form before clusters of galaxies) [16]. These arguments summed, it seems that SM neutrinos are not viable dark matter candidates. At least, we know for sure that they can't compose the total dark matter.

- Sterile Neutrinos:

  Rigorous cosmological and astrophysical constraints on sterile neutrinos come from the analysis of their cosmological abundance and the study of their decay products (see for example [17]).

  These hypothetical particles are similar to SM neutrinos, but without the SM interactions. They were proposed as dark matter candidates in 1993 by Dodelson and Widow [18] via the mechanism of active-sterile neutrino oscillation, leading to warm dark matter, which imply density fluctuations at small galaxy scales ($\sim 1\text{h}^{-1}\text{Mpc}$) that may be too small [19].

[5] Jeans mass is the mass above which the cloud of gas collapses to form some object(s). However, for collapsing, besides its mass, the cloud must suffer from fluctuations of some kind, that's why an analysis must be made on the possible dark matter particles.

Light sterile neutrinos, with masses below a few keV, would be ruled out as dark matter candidates. In fact, if the PLANCK result for the reionization optical depth[6] is correct, then dark matter structures were in place to form massive stars prior to redshift $z \gtrsim 20$, which is a scenario where the dark matter particle can't be of masses smaller than $\sim$ 10 keV [20]. The ionizing sources responsible for reionization can be a variety of astrophysical objects, and work has been done on reionization by for instance the first stars and the first quasars, and dark matter particles would be of importance to the formation of these objects. As an alternative to the stars [21] and quasars [22] being the causes for reionization, heavy sterile neutrinos could generate reionization by their decay [23] (in this case, these heavy sterile neutrinos would not be associated to dark matter) and the former constraint to the masses of dark matter light sterile neutrinos via reionization optical depth can be alleviated. Also, these light sterile neutrinos (i.e. relativistic and colisionless) suffer from the free streaming length constraint, wich cannot be too high.

Another way by which sterile neutrinos could be implemented as dark matter (in this case, CDM) is a picture where there must exist lepton number asymmetries[7] in any of the active neutrino flavors (this is a non-thermal production of dark matter). They are produced via lepton number-driven resonant MSW (Mikheyev-Smirnov-Wolfenstein) conversion of active neutrinos into sterile ones[24]. In this scheme, the range of their masses is between $\sim$ 100 eV and $\sim$ 10 keV. Even though these masses are light, raising questions whether it is cold dark matter indeed, there is the adiabaticity condition[8] of the resonance which favors the production of lower energy sterile neutrinos, and consequently lets the latter respect the constraint that dark matter particles ought to have reasonably small free-streaming lengths in order to respect down-top formation of structures, as cited within the last section.

- Axions:

  this kind of particle was introduced in the attempt to explain the smallness of the CP violating term in the QCD Lagrangian. Axions have never been detected experimentally.

  Laboratory searches, stellar cooling and the dynamics of supernova 1987A constrain axions to be very light ($<$ 10 eV). Also, they are expected to interact very weakly

[6] This term concerns the measurement of the length fraction of our visible Universe that contains ionized hydrogen (better put, reionized because, at recombination, hydrogen became neutral.)

[7] Lepton assymetry in the 'l' family is defined as $\frac{N_l - N_{\bar{l}}}{N_\gamma}$, where l stands for the family lepton, $\bar{l}$ to its respective antilepton, γ means photon, and N_i denotes number of the i particle.

[8] When neutrinos go through the MSW resonance, they have the maximal probability to change their nature. For going through resonance, they must propagate in the adiabatic regime, and the adiabatic condition assures this regime happens. *Adiabaticity* refers to the state when external conditions (density of the medium, in this case) change slowly in such a way that the system has time to adjust itself.

with ordinary particles, consequently they decoupled very early in the early Universe. The calculation of the axion relic density is uncertain and depends on the assumptions made regarding the production mechanism. Nevertheless, it is possible to find a reasonable range of parameters where axions satisfy all current constraints and represent a possible dark matter candidate. For detectability of axions, see for instance [25].

- Supersymmetric candidates

  - Neutralino:

    Supersymmetric models with conserving R-parity[9] are the most studied models among supersymmetric models. Within these models, dark matter particles may arise as the neutralino. In the MSSM, they are formed by a combination of the superpartners of the B, W_3 bosons ($\widetilde{B}$, $\widetilde{W_3}$), together with the superpartners of the neutral Higgs bosons H_1^0 and H_2^0. These four states form four Majorana mass eigenstates, $\widetilde{\chi}_1^0$, $\widetilde{\chi}_2^0$, $\widetilde{\chi}_3^0$, $\widetilde{\chi}_4^0$, called neutralinos. What we usually call *the neutralino* is the one which has the smallest mass among all the four neutralinos.

    As a consequence of R-parity, sparticles can only decay into an odd number of sparticles (plus SM particles). Therefore, if neutralino turns out to be the lightest supersymmetric particle, it cannot decay and can only be destroyed via pair annihilation. Such a property makes it an excellent dark matter candidate. This candidate comes from long time ago and its importance can be seen in ref.[26].

    As of now, it has neither been confirmed nor ruled out - as a Dark Matter candidate - of the space of scenarios which are offered by Supersymmetry.

  - Sneutrino:

    The superpartners of the SM neutrinos in supersymmetric models have been considered as dark matter candidates. It has been shown that sneutrinos will have a cosmologically interesting relic density ($0.1 < \Omega_{\tilde{\nu}} h^2 < 1.0$) if their mass is in the range of $550 - 2300$ GeV. However, the scattering cross section of a sneutrino with nucleons is calculated and is much larger than the limits found by direct dark matter detection experiments [27]. Therefore, in principle, sneutrino is excluded as a dark matter candidate.

  - Gravitino:

    It is the superpartner of the graviton in supersymmetric models. In some supersymmetric scenarios, gauge mediated supersymmetry for example, gravitinos can be the lightest supersymmetric particle and stable. With only gravitational

[9] R-parity was initially introduced to suppress the rate of proton decay.

interactions, gravitinos are very difficult to observe [28]. Long-lived gravitinos can rise some problems for cosmology [29]. As a case in particular, their presence can destroy the abundances of primordial light elements in some scenarios [30]. Another problem with gravitinos is that they may be overproduced in the early Universe if the reheating temperature[10] is not sufficiently low, see for example ref.[30]. But, in some scenarios, these problems can be circumvented, see for instance [31].

- Axino:

  it is the superpartner of the axion. It can act as hot, warm and cold dark matter, or simultaneously some of them together: see ref.[32] for hot and cold, ref.[33] for an examination of the mass spectrum of axinos, ref.[34] for cold or warm, and [35] for cold dark matter.

- Light Scalar Dark Matter:

  If we take into consideration dark matter candidates as being a kind of neutral lepton, we notice relic density arguments don't allow such a WIMP with a mass less than a few GeV [36, 37]. If the dark matter is made of other types of particles, however, this limit can be evaded. A $1-100$ MeV scalar candidate has been proposed [38, 39].

  The latter candidate has become experimentally motivated. In ref. [40](see also [41]), is discussed the possibility that the detection of 511 keV gamma-ray from the galactic bulge by the INTEGRAL satellite might be a consequence of low mass ($\sim$ MeV) dark matter annihilations. Theoretically, dwarf spheroidal galaxies, in addition to the galactic bulge, can be a good source of observation of these signatures of 511 keV gamma-rays due to dark matter anihillation [42].

  In order to account for the observed 511 keV gamma-ray emission, other possibilities for decaying dark matter particles as axinos ($1-300$ MeV) from a R-parity violating model of supersymmetry [43]; and sterile neutrinos ($1-50$ MeV) [44] have also been proposed.

- Dark Matter from Little Higgs Models:

  As an alternative mechanism, other than Supersymmetry, for solving the Hierarchy Problem, the Little Higgs models have been proposed [45, 46, 47, 48]. In these models, the Standard Model Higgs is a pseudo-Goldstone boson and its mass is protected by approximate non-linear global symmetries. The quadratically divergent contributions to the Higgs mass (hierarchy problem) are cancelled by TeV scale new particles.

[10] If we assume inflation ocurred in our Universe, the reheating temperature is the value which the temperature takes after the inflationary period.

At least two varieties of Little Higgs models have been shown to contain possible dark matter candidates. One of these classes, called Theory Space Little Higgs models, provides a possibly stable, scalar particle which can provide the measured density of dark matter [49].

Another kind of Little Higgs model [50] has been developed motivated by the Little Hierarchy Problem[11]. This model solves the problem by introducing a new symmetry at the TeV scale which results in the existence of a stable WIMP candidate with a $\sim$ TeV mass.

- Kaluza-Klein states from Universal Extra Dimensions:

  Although our world seems to consist of $3+1$ dimensions, it is possible that other dimensions exist and appear at higher energy scales. A general feature of extra-dimensional theories is that because of compactification of the extra dimensions, all of the fields propagating in the bulk (bulk: $3+\delta+1$ spacetime, where δ is the number of extra dimensions) have their momentum quantized. The result is that for each bulk field, a set of Fourier expanded modes , called Kaluza-Klein (KK) states, appears. From our point of view in the 4-D world, these KK states appear as a series of states with discrete masses $m_n \sim n$ where n labels the mode number.

  Scenarios in which all the fields are allowed to propagate in the bulk are called universal extra dimensions [51]. There is significant phenomenological motivation to choose the Standard Model fields to propagate in the bulk, for instance

  - Prevention of rapid proton decay;
  - Provides a viable dark matter candidate;
  - Motivation for three families from anomaly cancellation;
  - Attractive dynamical electroweak symmetry breaking.

  Therefore the candidate *Kaluza-Klein state* we are talking about comes from UED scenarios.

  Considering UED, the lightest KK particle (LKP) is associated with the first KK excitation of the photon γ_1 [52]. A calculation of the γ_1 relic density was done [53], and it was found that if the LKP is to take account for the observed quantity of dark matter, its mass must lie in the range $400-1200$ GeV. Direct detection of the

[11] Little Hierarchy Problem: related to the Hierarchy Problem. It arises when the fine tunning of the quadratically divergent quantity M_H^2 (Higgs mass squared) is already done, i.e., the parameter Λ that measures the scale concerning new physics takes the value ~ 1 TeV (so that the physical Higgs mass is ~ 126 GeV). Therefore, new physics is expected at 1 TeV. But data from electroweak precision measurements put a strong constraint that tells us there is no new physics up to $5-7$ TeV. To this incompatibility between these two values, there must be some additional fine tunning, and to this problem we give the name "Little Hierarchy Problem", *little* because the fine tunning is not so severe.

LKP via its elastic scattering with nuclei was investigated in ref. [54] and the main result is that in order to see at least several (several, here, means number of events in the range of $1 - 10^3$. A range is shown because there are different detectors with different materials (for instance, NaI or ^{74}Ge) and different weights.) events per year, heavy (> 100 kg) detectors are needed.

- Superheavy dark matter:

  There exists a limit which constrains the masses of the dark matter particles to be of the order of or below a few hundred TeV. This limit is a consequence of a maximum thermally averaged annihilation cross section - $\langle \sigma v_{møl} \rangle_{\max}$ - (defined in sec.3.5) for a particle of a given mass. This limit is set by the *unitarity bound* [12] [55] (section 3.7 of this reference contains valuable content for the calculation, but see also the paper we refer to in the next sentence). This bound has been applied [56] and the constraint on the relic density has the effect to put an upper limit on the dark matter particle mass

$$m_{DM} \lesssim 340 \text{ TeV} \quad , \tag{2.6}$$

  where it has been used the very general constraint $\Omega_{DM} h^2 \leq 1$ (very general because we know already that $\Omega_{total} h^2 \leq 1$ (for flat Universe) where Ω_{total} is the density of energy regarding radiation (relativistic particles like photon and neutrino) and all kinds of matter (baryonic matter plus dark matter and vacuum energy.). Nowadays, however, if we use the PLANCK constraint on $\Omega_{DM} h^2$, the former constraint can be made as the following

$$m_{DM} \lesssim 100 \text{ TeV} \quad . \tag{2.7}$$

  The above constraints were found by assuming that the dark matter particle is a thermal relic of the early Universe. That's why we can relate $\Omega_{DM} h^2$ and the annihilation cross section.

  Nevertheless, we may define candidates with mass of the order of or above $m_{DM} \sim 10^{11}$ GeV, which we call *Wimpzillas* [57]. Therefore, the relationship between $\Omega_{DM} h^2$ and the annihilation cross section is no longer taken into account, and wimpzillas must not have been in thermal equilibrium during freeze-out. Furthermore, they must be stable against decay and annihilation in order to contribute to the current dark matter density. One way to give rise to wimpzillas is production at the end of the inflation, when the Universe transits from inflationary to matter- or radiation-dominated (see for example refs. [58, 59]).

[12] After some manipulations of the S-matrix and the T operator, $S \equiv 1 + iT$, we are led to an expression which relates $\langle \sigma v_{møl} \rangle_{\max}$ to the mass of the particle.

The motivation behind the research about wimpzillas is the observation of cosmic rays at ultrahigh energies [60] above the GZK cutoff[13] [61, 62]. This cutoff energy is $\sim 5 \times 10^{19}$ eV and because of the existence of this cutoff, the Universe would become opaque to ultra-high energy protons over distances ≥ 50 Mpc. Since no astrophysical sources are known within this range, one possible source of gamma-rays eventually came from superheavy dark matter particles: gamma-rays would be produced via the decay or annihilation of wimpzillas (see for instance [63, 64])

- Q-balls [65, 66]; mirror particles [67, 68, 69, 70, 71]; CHArged Massive Particles (CHAMPs) [72]; self interacting dark matter [73, 74]; D-matter [75]; cryptons [76, 77]; superweakly interacting dark matter [78]; brane world dark matter [79]; heavy fourth generation neutrinos [80, 81], etc.

[13] GZK cutoff: limit of energy above which cosmic rays, constituted by protons, start to interact at a high rate with the photons of the Cosmic Microwave Background. Therefore, above this cutoff, protons as cosmic rays couldn't make their way to earth and then we shouldn't be able to observe the shower of particles to which these rays would give origin.

3 Dark Matter Abundance Calculation

In this chapter, we explain the tools that underlie the calculations of relic abundance for particles which were in thermal equilibrium some time after the big bang and eventually decoupled from it. We provide a little basis of General Relativity, also thermodynamics and finally explain how the Boltzmann equation can shed light on the density of some species which was in thermal equilibrium and currently is or may be present in our Universe.

3.1 Basic General Relativity

3.1.1 Introduction

The Standard Cosmological Model is based on the Einstein equation of gravity

$$R^{ab} - \frac{1}{2}Rg^{ab} + \Lambda g^{ab} = 8\pi G T^{ab} \quad . \tag{3.1}$$

Here, g^{ab} is the metric tensor, which has to be found via the above equation in order for one to know which spacetime he is dealing with. Locally, by the Equivalence Principle, its components are reduced to the Minkowski metric ones $\mathrm{diag}(-1,1,1,1)$ (expressed in any basis of the global inertial coordinate system[1]) which is the metric of special relativity. Λ is the cosmological constant which has to be put by hand to account for the accelerated expansion of the Universe (It can be thought of as the content of dark energy in the Universe). G is the Newton's constant of gravitation. The term T^{ab} is the symmetric energy-momentum tensor of matter and radiation. The Ricci tensor R^{ab} and the Ricci scalar R are defined by

$$R^{ab} = R^{acb}{}_{c}, \qquad R = R^{a}{}_{a} \quad , \tag{3.2}$$

where R^{d}_{abc} is the Riemann tensor,

$$R_{abc}{}^{d} = \partial_b \Gamma^{d}{}_{ac} - \partial_a \Gamma^{d}{}_{bc} + \left(\Gamma^{e}{}_{ac}\Gamma^{d}{}_{eb} - \Gamma^{e}{}_{bc}\Gamma^{d}{}_{ea}\right) \quad . \tag{3.3}$$

[1] The global inertial coordinate system is the map of the spacetime into $\mathbb{R}^4$, i.e., Inertial observers, each one, can set up a rigid grid of metersticks, synchronize clocks places at the gridpoints and label each event by the four numbers (x^0, x^1, x^2, x^3).

The Christoffel symbols $\Gamma^c{}_{ab}$ are given (with the condition of null torsion[2] and $\nabla_a g_{bc} = 0$) by

$$\Gamma^c{}_{ab} = \frac{1}{2} g^{cd} \left(\partial_a g_{bd} + \partial_b g_{ad} - \partial_d g_{ab} \right) \quad . \tag{3.4}$$

They determine the motion of free-falling bodies through the geodesic equation (expressed in a coordinate system basis)

$$\frac{d^2 x^\mu}{d\tau^2} + \Gamma^\mu_{\sigma\nu} \frac{dx^\sigma}{d\tau} \frac{dx^\nu}{d\tau} = 0 \tag{3.5}$$

The *Equivalence Principle*, based on the equality of inertial and gravitational masses, states that a free-falling observer does not experience any gravitational effect (dynamometers attached to his body wouldn't register any acceleration). This means that a free-falling observer can describe spacetime with a metric which is locally flat (Minkowski metric) and has locally vanishing Christoffel symbols. In this case, the geodesic equation reduces locally to the special relativity equation of motion for an inertial body, that is, $d^2 x^\mu / d\tau^2 = 0$.

3.1.2 Robertson-Walker metric

Since observations of the Universe have shown that it is spatially homogeneous and isotropic on large scales ($\gtrsim$ 100 Mpc), the Standard Cosmological Model assumes this is valid for some reference frame. If one takes these considerations ahead, he is led to the following form of the interval

$$ds^2 = -dt^2 + R^2(t) \left[\frac{dr^2}{1 - kr^2} + r^2 \left(d\theta^2 + sin^2\theta d\phi^2 \right) \right] \quad , \tag{3.6}$$

where k specifies three different spatial sections of the Universe:

- $k = 1$ means we have a 3-sphere, defined as the surface in 4-D flat Euclidean space $\Re^4$ whose Cartesian coordinates satisfy

  $$x^2 + y^2 + z^2 + w^2 = R^2 \quad , \tag{3.7}$$

  where R can vary, depending on the 3-sphere.

  In spherical coordinates, the metric of the unit 3-sphere ($R = 1$) is

  $$ds^2 = d\psi^2 + \sin^2\psi \left(d\theta^2 + \sin^2\theta d\phi^2 \right) \quad . \tag{3.8}$$

[2] $\nabla_a \nabla_b f = \nabla_b \nabla_a f$, where f is a function which takes from the manifold M to reals $\mathbb{R}$; and ∇_a is the covariant derivative which acts as $\nabla_a t^b = \partial_a t^b + \Gamma^b{}_{ac} t^c$ on a vector t^b

If one changes variabels in the following way,

$$d\psi \equiv \frac{1}{\sqrt{1-kr^2}} \ , \quad \text{with}\, k=1 \quad , \tag{3.9}$$

he obtains the interval of eq. (3.6).

- $k=0$ means we have a plane, defined in the ordinary 3-D flat Euclidean space $\Re^3$. This plane is generated by not constraining the three coordinates, say x, y and z. In cartesian and spherical coordinates, respectively, the metric of the plane is

$$\begin{aligned} ds^2 &= dx^2+dy^2+dz^2 \\ ds^2 &= d\psi^2+\psi^2\left(d\theta^2+\sin^2\theta d\phi^2\right) \quad . \end{aligned}$$

If one changes variables as in eq. (3.9), with $k=0$, he obtains eq. (3.6).

- $k=-1$ means that the spatial section is a three-dimensional hyperboloid, defined as the surfaces in a 4-D flat Lorentz signature space (i.e., Minkowski spacetime) whose global inertial coordinates satisfy

$$t^2-x^2-y^2-z^2=r^2 \quad , \tag{3.10}$$

where r can vary, depending on the 3-D hyperboloid.

In hyperbolic coordinates, the metric of the unit hyperboloid is

$$ds^2=d\psi^2+\sinh^2\psi\left(d\theta^2+\sin^2\theta d\phi^2\right) \quad . \tag{3.11}$$

If one changes variables as in eq. (3.9), with $k=-1$, he obtains eq. (3.6).

All that is left to determine is the evolution with time of the function $R(t)$. For this, we have to introduce dynamics via Einstein's equation. But there is something missing in order to solve the eq. (3.1), that is, the energy-momentum tensor. Some considerations are necessary. Just considering ordinary matter, we can say that, at the order of large scales we are considering, each galaxy can be considered as a grain of dust. The random velocities of the galaxies are small, so the pressure of the dust galaxies is negligible. Hence, to an approximation, the energy-momentum tensor of the Universe is given by the one of dust (which is perfect fluid, but its pressure is null)

$$T_{ab}=\rho u_a u_b \quad , \tag{3.12}$$

where ρ is the average density of matter, and u_a is the four velocity of each galaxy. However, there are other forms of matter. We have to consider also the content of radiation.

We know that there is radiation at a temperature of about 3K that fills the Universe. This content of radiation can be described by a perfect fluid energy-momentum tensor, with nonzero pressure ($P_{\rm rad} = \rho_{\rm rad}/3$). Therefore, we take the energy-momentum tensor to be of the general perfect fluid form

$$T_{ab} = \rho u_a u_b + P\left(g_{ab} + u_a u_b\right) \quad . \tag{3.13}$$

Well, there is also the content of dark matter that, we know, exists. And will it be a perfect fluid? Luckily this question has an answer: the tensor (3.13) is the most general tensor respecting homogeneity and isotropy because it is formed by the combination of the only tensors which do not specify a privileged direction, i.e., tensors g_{ab} and u_a. Then, assuming the energy-momentum tensor of a perfect fluid, one can solve the Einstein's equation to obtain the so called Friedman equations

$$\frac{\ddot{R}}{R} = -\frac{4\pi G}{3}\left(\rho + 3p\right) + \frac{\Lambda}{3} \quad , \tag{3.14}$$

$$\frac{\dot{R}^2}{R^2} = \frac{8\pi G\rho}{3} - \frac{k}{R^2} + \frac{\Lambda}{3} \quad . \tag{3.15}$$

Now, for sake of completeness, the cosmological constant Λ can be moved to the right side of Einstein's equation as a contribution to the energy-momentum tensor

$$T^{\Lambda}_{ab} = -\frac{\Lambda}{8\pi G} g_{ab} \quad . \tag{3.16}$$

If we identify T^{Λ}_{ab} with the energy-momentum tensor of a perfect fluid, we obtain

$$P_\Lambda = -\frac{\Lambda}{8\pi G} \quad , \tag{3.17}$$

$$\rho_\Lambda = -P_\Lambda = \frac{\Lambda}{8\pi G} \quad . \tag{3.18}$$

If we substitute the energy density of the vacuum into the eqs. (3.14) and (3.15), we obtain as a result

$$\frac{\ddot{R}}{R} = -\frac{4\pi G}{3}\left(\rho - 2\rho_\Lambda + 3p\right) \quad , \tag{3.19}$$

$$\frac{\dot{R}^2}{R^2} = \frac{8\pi G(\rho + \rho_\Lambda)}{3} - \frac{k}{R^2} \quad . \tag{3.20}$$

With them, we can then find how $R(t)$ evolves in time, and consequently know how the geometry of the Universe via the full knowledge of the interval evolves.

3.2 Λ-CDM Cosmological Model

The model on which this work will be based is the Λ-CDM Cosmological Model. It starts assuming that general relativity (GR), with cosmological constant Λ, is the correct theory of gravity on cosmological scales, using the FRW metric. Then, into GR, a field is introduced to describe dark matter, besides the ones that describe usual matter, which is currently mostly baryons. This is the standard Λ-CDM model.

It manages to match with well-established observational tests, examples are:

- the accelerating expansion of the Universe observed in the light from distant type Ia Supernovae (SNe Ia) [82];
- the structure of the cosmic microwave background [83];
- the large-scale structure in the distribution of galaxies [84];
- the baryon acoustic oscillations, which have possibly been formed in the initial plasma via perturbations and have been carried through the epoch of recombination [85];
- the measurements of dark energy parameters through weak lensing [86].

But there are still some challenges the model faces (see Ref. [87]), among which is the most important one:

- the "too big to fail" problem. Simulations for the substructure of the Milky Way and Acquarius halo imply ~ 10 subhalos, that are so massive and dense that they would be too big to fail to form lots of stars. The problem lies on the observation that none of the satellite galaxies of the Milky Way or Andromeda have stars moving as fast as expected in these dense subhalos [88, 89].

There are modifications of it and some of which can be found in Ref. [90]. However, we will assume Λ-CDM throughout this work.

3.3 Thermodynamics of the early Universe

In order to study the early Universe, firstly we have to define some quantities:

$$n_\chi = \frac{g_\chi}{(2\pi)^3}\int f_\chi(\vec{p})\, d^3p \quad , \tag{3.21}$$

$$\rho_\chi = \frac{g_\chi}{(2\pi)^3}\int E_\chi(\vec{p})\, f_\chi(\vec{p})\, d^3p \quad , \tag{3.22}$$

$$p_\chi = \frac{g_\chi}{(2\pi)^3}\int \frac{|\vec{p}|^2}{3E_\chi(\vec{p})} f_\chi(\vec{p})\, d^3p \quad , \tag{3.23}$$

where n_χ, ρ_χ and p_χ denote, respectively, number of the particle species χ per volume, energy of the particle species χ per volume and pressure associated to the particle species χ (the expression for the pressure comes from the same reasoning as in Kinetic Theory of Gases). g_χ is the number of internal degrees of freedom (spin) and $E_\chi(\vec{p}) = \sqrt{|\vec{p}|^2 + m_\chi^2}$ is the energy. The statistical equilibrium distribution $f_\chi(\vec{p})$ depends on the energy E_χ, the chemical potential μ_χ, and the temperature T_χ. It is given by

$$f_\chi(\vec{p}) = \frac{1}{e^{(E_\chi - \mu_\chi)/T_\chi} \pm 1} \quad , \tag{3.24}$$

where the plus sign applies to fermions and the minus sign to bosons.

Nonrelativistic limit. For $m_\chi \gg T_\chi$ and $m_\chi \gg \mu_\chi$, we have for both bosons and fermions

$$f_\chi(\vec{p}) \simeq e^{-m_\chi/T_\chi} e^{-|\vec{p}|^2/2m_\chi T_\chi} \quad , \tag{3.25}$$

which leads to

$$n_\chi \simeq g_\chi \left(\frac{m_\chi T_\chi}{2\pi}\right)^{3/2} \exp\left(-\frac{m_\chi}{T_\chi}\right) \quad , \tag{3.26}$$

$$\rho_\chi \simeq m_\chi n_\chi \left(1 + \frac{3}{2}\frac{T_\chi}{m_\chi}\right) \quad , \tag{3.27}$$

$$p_\chi \simeq n_\chi T_\chi \ll \rho_\chi \quad . \tag{3.28}$$

Relativistic limit. For $T_\chi \gg m_\chi$ and $T_\chi \gg \mu_\chi$, we have

$$f_\chi(\vec{p}) \simeq \frac{1}{e^{|\vec{p}|/T_\chi} \pm 1} \quad , \tag{3.29}$$

which leads to

$$n_\chi(\text{boson}) \simeq \frac{\zeta(3)}{\pi^2} g_\chi T_\chi^3 \quad , \tag{3.30}$$

$$n_\chi(\text{fermion}) \simeq \frac{3}{4}\frac{\zeta(3)}{\pi^2} g_\chi T_\chi^3 \quad , \tag{3.31}$$

$$\rho_\chi(\text{boson}) \simeq \frac{\pi^2}{30} g_\chi T_\chi^4 \quad , \tag{3.32}$$

$$\rho_\chi(\text{fermion}) \simeq \frac{7}{8}\frac{\pi^2}{30} g_\chi T_\chi^4 \quad , \tag{3.33}$$

$$p_\chi \simeq \frac{1}{3}\rho_\chi \quad , \tag{3.34}$$

where $\zeta(3) \simeq 1.20206$ is the Riemann zeta function of 3.

Now we define the total energy density as

$$\rho = \sum_{\chi} \rho_{\chi} = \frac{\pi^2}{30} g_{\rho} T_{\gamma}^4 \tag{3.35}$$

because in the early hot Universe, the energy density is dominated by relativistic particles. T_γ is the photon temperature and the coefficient g_ρ is given by the sum over the contributions of all particles that populate the Universe:

$$g_{\rho} = \sum_{\chi} g_{\rho}^{(\chi)} \quad . \tag{3.36}$$

Thus we obtain

$$\sum_{\chi} \rho_{\chi} = \sum_{\chi} g_{\rho}^{(\chi)} \frac{\pi^2}{30} T_{\gamma}^4 \quad . \tag{3.37}$$

$g_\rho^{(\chi)}$ is then given by

$$g_{\rho}^{(\chi)} = \rho_{\chi} \frac{30}{\pi^2} \frac{1}{T_{\gamma}^4} = g_{\chi} \frac{15}{\pi^4} \left(\frac{T_{\chi}}{T_{\gamma}} \right)^4 \int_{x_{\chi}}^{\infty} dz \, \frac{z^2 \sqrt{z^2 - x_{\chi}^2}}{e^{z - \xi_{\chi}} \pm 1} \quad , \tag{3.38}$$

with $x_\chi \equiv m_\chi / T_\chi$ and $\xi_\chi \equiv \mu_\chi / T_\chi$. The plus sign for fermions and minus sign for bosons. Note that if the particle is relativistic, its $g_\rho^{(\chi)}$ value can be evaluated from (3.32) and (3.33), resulting in

$$g_{\rho}^{(\chi)}(\text{boson}) = g_{\chi} \left(\frac{T_{\chi}}{T_{\gamma}} \right)^4 \quad , \tag{3.39}$$

$$g_{\rho}^{(\chi)}(\text{fermion}) = \frac{7}{8} g_{\chi} \left(\frac{T_{\chi}}{T_{\gamma}} \right)^4 \quad . \tag{3.40}$$

The contribution to g_ρ of relativistic particles is dominant in the early radiation-dominated era as can be seen in the eq. (3.38). Then, eq. (3.36) is well approximated by

$$g_{\rho} = \sum_{\chi = \text{relativistic bosons}} g_{\chi} \left(\frac{T_{\chi}}{T_{\gamma}} \right)^4 + \sum_{\chi = \text{relativistic fermions}} \frac{7}{8} g_{\chi} \left(\frac{T_{\chi}}{T_{\gamma}} \right)^4 \quad . \tag{3.41}$$

The value of g_ρ changes when the temperature drops below the mass of a particle in the plasma (i.e. the particle leaves to be relativistic). Then, this particle does not contribute to the sum (3.41) anymore. The transition between the two values of g_ρ must be calculated numerically using the exact expression (3.38) for the particle that becomes nonrelativistic.

We can now for enlightenment do an example regarding the calculation of the g_ρ value, for the SM, at three different temperature regimes:

- For $m_e/3 \simeq 0.2$ MeV $\ll T_\gamma \ll 35$ MeV $\simeq m_\mu/3$, the relativistic particles within the plasma are the photons, electrons, positrons, and neutrinos (which we will consider to be Majorana and therefore are their own antiparticles), all with the same temperature, yielding

$$g_\rho = 2 + 2\frac{7}{8}2 + 3\frac{7}{8}2 = \frac{43}{4} = 10.75 \quad . \tag{3.42}$$

- For $m_\mu/3 \simeq 35$ MeV $\ll T_\gamma \ll 300$ MeV $\simeq \Lambda_{\rm QCD}$, where $\Lambda_{\rm QCD}$ is the energy scale of the quark-hadron phase transition, there are also muons and anti-muons (contributing equally as electrons: 7/2), thus leading to

$$g_\rho = \frac{57}{4} = 14.25 \quad . \tag{3.43}$$

- For $T_\gamma \gg 300$ MeV , there are tau and anti-tau (contributing 7/2 for $T_\gamma \gg m_\tau/3 \simeq$ 600 MeV); u, anti-u, d, anti-d, s, anti-s quarks (contributing 63/2); c anti-c quarks (contributing 21/2 for $T_\gamma \gg m_c/3 \simeq 400$ MeV) b and anti-b quarks (contributing 21/2 for $T_\gamma \gg m_b/3 \simeq 1.4$ GeV); t and anti-t quarks (contributing 21/2 for $T_\gamma \gg m_t/3 \simeq 60$ GeV); eight gluons (contributing 16) $W^\pm$'s and Z's (contributing 9 for $T_\gamma \gg m_Z/3 \simeq 30$ GeV); H (contributing 1 for $T_\gamma \gg m_H/3 \simeq 100$ GeV) for a total

$$g_\rho = \frac{427}{4} = 106.75 \quad . \tag{3.44}$$

Just as a comment, for $T_\gamma \ll m_e/3 \simeq 0.2$ MeV, neutrinos are already decoupled ($T_{\rm dec} \sim 1$ MeV) and they are at a different temperature than the plasma. This temperature T_ν can be calculated analytically but it won't be done here. The Fig. 2 is a plot for the numerical evaluation of g_ρ as a function of the temperature of the plasma T_γ, using eq. (3.38) and suming over all pertinent particles of the SM within the different temperature regimes.

Now, we are going to deal with entropy, which will be useful when manipulating the Boltzmann equation in the next sections.

We first use the second law of thermodynamics, which says that in the equation

$$đQ = dU + đW \quad , \tag{3.45}$$

the heat differential $đQ$ is given by $đQ = TdS$, where $S(T, V, N)$ is a function of state of the system called entropy. From eq. (3.45), we have

$$\begin{aligned} TdS(T,V,N) &= d\left[\rho(T)V\right] + p(T)dV + \mu(T)dN \\ &= V\frac{d\rho(T)}{dT}dT + \left[\rho(T) + p(T)\right]dV + \mu(T)dN \quad . \end{aligned} \tag{3.46}$$

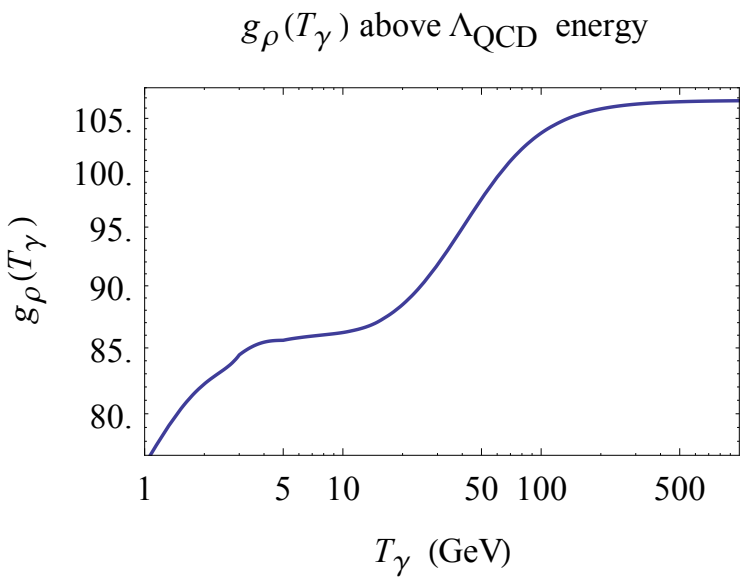

Figure 2 – Plot of g_ρ as a function of the plasma temperature T_γ, in the SM. The range of temperatures is set above 1 GeV because we don't show the fine behaviour of the quark-hadron phase transition that happens, in our case, at 300 MeV.

Notice that the functions μ, p and ρ depend on the temperature T only. First, $\mu = \mu(T)$ can't depend either on the volume or the number of particles because the observable which determines whether the process, for example $\phi_1 + \phi_2 \leftrightarrow \phi_3 + \phi_4$, will happen is the cross section which depends ultimately on the mandelstam variable $s \equiv (p_1 + p_2)^2$. Well, and how is s related to T? Intuitively, T is the one which provides the necessary energy for the above process to happen. When the temperature goes below certain value, the process may not happen anymore and these particles decouple from the other surrounding particles.

Now for the case of $\rho = \rho(T)$ and $p = p(T)$, it is clear from Eqs. (3.22), (3.23) and (3.24), that they can only depend on m_χ, μ_χ and T_χ. m_χ enters as input parameter and as we have explained above, $\mu = \mu(T)$, therefore, one has the three functions μ, p and ρ depending only on T. Hence,

$$\frac{\partial S(T,V,N)}{\partial T} = \frac{V}{T}\frac{d\rho(T)}{dT} \quad , \quad \frac{\partial S(T,V,N)}{\partial V} = \frac{\rho(T)+p(T)}{T} \quad , \quad \frac{\partial S(T,V,N)}{\partial N} = \frac{\mu(T)}{T} \quad .$$

On $S(T,V,N)$ is imposed the condition which assures

$$\frac{\partial^2 S(T,V,N)}{\partial V \partial T} = \frac{\partial^2 S(T,V,N)}{\partial T \partial V} \quad , \tag{3.47}$$

which implies

$$\frac{dp(T)}{dT} = \frac{\rho(T)+p(T)}{T} \quad . \tag{3.48}$$

Also, we may find

$$\frac{\partial^2 S(T,V,N)}{\partial N \partial T} = \frac{\partial^2 S(T,V,N)}{\partial T \partial N} \quad , \tag{3.49}$$

which yields

$$\frac{d\mu(T)}{dT} = \frac{\mu(T)}{T} \quad . \tag{3.50}$$

Putting the last two conditions into (3.46), we obtain

$$\begin{aligned} TdS(T,V,N) &= d\left[\rho(T)V\right] + p(T)dV + \left[V\frac{dp(T)}{dT}dT - V\frac{dp(T)}{dT}dT\right] + \\ &\quad + \mu(T)dN + \left[N\frac{d\mu(T)}{dT}dT - N\frac{d\mu(T)}{dT}dT\right] \end{aligned}$$

$$\begin{aligned} TdS(T,V,N) &= d\left[\rho(T)V\right] + d\left[p(T)V\right] + \left[-V\frac{dp(T)}{dT}dT\right] \\ &\quad + d\left[\mu(T)N\right] + \left[-N\frac{d\mu(T)}{dT}dT\right] \end{aligned}$$

$$\begin{aligned} dS(T,V,N) &= \frac{1}{T}d\left[(\rho(T)+p(T))V + \mu(T)N\right] - \\ &\quad - \frac{1}{T}\left(\frac{\left(\rho(T)+p(T)\right)V + \mu(T)N}{T}\right)dT \\ dS(T,V,N) &= d\left[\frac{p+\rho+\mu\frac{N}{V}}{T}V\right] \equiv d\left[\frac{p+\rho+\mu n}{T}V\right] \quad . \end{aligned} \tag{3.51}$$

Hence, apart from an additive constant, the entropy $S(T,V)$ is given by

$$S(T,V) = \frac{p+\rho+\mu n}{T}V \tag{3.52}$$

We define now the entropy density

$$s \equiv \frac{S}{V} = \frac{p+\rho+\mu n}{T} \quad . \tag{3.53}$$

We will neglect the chemical potential term from now on for the following reasons:

- In thermodynamic equilibrium, the chemical potential for neutral particles is null. In fact, take the reversible processes $\phi_0+\phi_0 \leftrightarrows \phi_+ + \phi_-$ and $\phi_0+\phi_0+\phi_0 \leftrightarrows \phi_+ + \phi_-$ which are allowed by charge conservation. In equilibrium we have $\mu_0 + \mu_0 = \mu_+ + \mu_- \ \therefore\ 2\mu_0 = \mu_+ + \mu_-$ and $\mu_0 + \mu_0 + \mu_0 = \mu_+ + \mu_- \ \therefore\ 3\mu_0 = \mu_+ + \mu_-$. Therefore, $\mu_0 = 0$;
- For charged particles, as indicated in the first item, it yields $\mu_+ = -\mu_-$. Well, this doesn't eliminate their chemical potential terms, $\frac{\mu_+ n_+}{T}$ and $\frac{\mu_- n_-}{T}$, but we have certain indications which can support the negligence of these terms.

First, the evidence that today $n_B - n_{\bar{B}} = 3 \times 10^{-10} n_\gamma = (3 \times 10^{-10}) \times 411.4 \text{ cm}^{-3} = 9.58 \times 10^{-49} \text{ GeV}^3$. Supposing that the baryon numbers corresponding to baryon and antibaryon, respectively, are conserved through thermodynamic equilibrium until today and also that the assymetry $n_B - n_{\bar{B}} \neq 0$ is caused somewhere before the initial condition of our simulations ($x = m_{DM}/T_\gamma \sim 3$), we may arrive to an estimate for the sum $\Delta_{B\bar{B}} \equiv \frac{\mu_B n_B}{T} + \frac{\mu_{\bar{B}} n_{\bar{B}}}{T} = \frac{\mu_B (n_B - n_{\bar{B}})}{T}$ [3] which can be noticed to be negligible before the other contirbutions to the entropy density.

Second, besides baryons, the remaining charged particles which are reasonably asymetric - for hydrogen is the most abundant in number considering visible matter and it is composed by 1 proton and 1 electron. - are the electrons. These will be neglected for the same reasoning as for baryons: the estimate for the sum $\Delta_{e^+e^-}$ is negligible when the equilibrium distributions are considered.

In the end, we just have to calculate

$$s = \frac{p + \rho}{T} \quad . \tag{3.54}$$

As we did for the total energy density ρ, we can do the following definition for the total entropy density of the plasma (thus with T_γ):

$$s = \sum_{\chi=\text{interacting}} s_\chi = \frac{2\pi^2}{45} g_s T_\gamma^3 \quad . \tag{3.55}$$

The sum over interacting particles means we consider all the particles which contribute to the entropy of the plasma when interacting in thermal equilibrium. g_s is given by

$$g_s = \sum_{\chi=\text{interacting}} g_s^{(\chi)} \quad , \tag{3.56}$$

where

$$g_s^{(\chi)} = s_\chi \frac{45}{2\pi^2} \frac{1}{T_\gamma^3} = g_\chi \frac{15}{4\pi^4} \int_{x_\chi}^{\infty} dz \frac{\left(4z^2 - x_\chi^2\right) \sqrt{z^2 - x_\chi^2}}{e^{z - \xi_\chi} \pm 1} \quad , \tag{3.57}$$

where $x_\lambda \equiv m_\chi / T_\gamma$ and $\xi_\chi = \mu_\chi / T_\gamma$. The plus sign for fermions and the minus sign for bosons.We can see from the last equation that relativistic particles contribute much more than nonrelativistic ones to the total entropy density. Note also that if the particle is relativistic, its $g_s^{(\chi)}$ value can be evaluated from (3.32), (3.33), (3.34) and (3.53). Its value can be approximated by

[3] This estimate takes into account the equilibrium regime in the following way: we consider the difference $n_B - n_{\bar{B}}$ of the equilibrium distributions and solve for μ_B; later, we consider a range of temperatures when the baryons and antibaryons were at equilibrium and find the magnitude of μ_B within this range.

$$g_s^{(\chi)}(\text{bosons}) = g_\chi \quad , \tag{3.58}$$

$$g_s^{(\chi)}(\text{fermions}) = \frac{7}{8} g_\chi \quad . \tag{3.59}$$

Hence, we can write

$$g_s = \sum_{\chi=\text{int. rel. bosons}} g_\chi + \sum_{\chi=\text{int. rel. fermions}} \frac{7}{8} g_\chi \quad . \tag{3.60}$$

The value of g_s changes when the temperature drops below the mass of a particle in the plasma (i.e. the particle leaves to be relativistic). Then, this particle does not contribute to the sum (3.60) anymore. The transition between the two values of g_s must be calculated numerically using the exact expression (3.57) for the particle that becomes nonrelativistic.

Examples with g_s won't be necessary because g_s turns out to be identical to g_ρ in the three different regimes discussed before, when $T_\chi = T_\gamma$.

Next, comes a figure in which g_s is plotted and that shows the comparison between g_s and g_ρ.

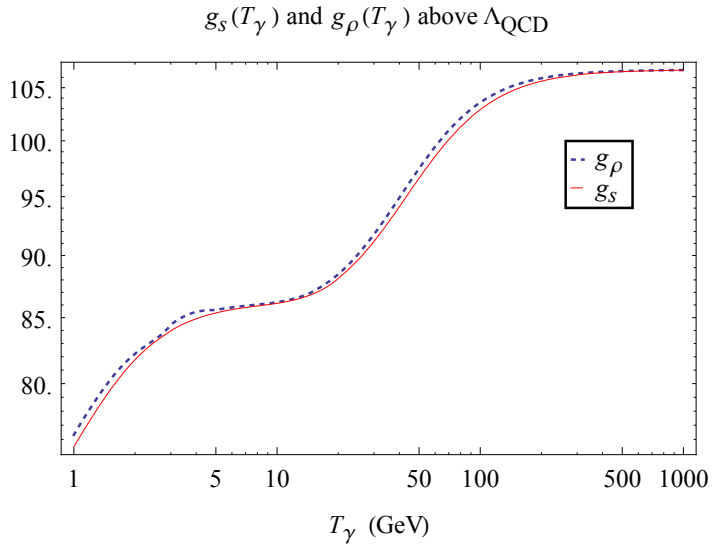

Figure 3 – Plot of g_s and g_ρ as a function of the plasma temperature T_γ. As before, we don't show the fine behaviour of the quark-hadron transition.

The difference between the two curves lies on the feature: the two functions would be equal if every particle were in equilibrium all the time ($T_\chi = T_\gamma$). However, this is not always the case. When particles decouple from the plasma, they don't share the same temperature as before the decoupling. g_ρ can still be calculated with eq.(3.38) if we know T_χ of all decoupled particles, but g_s can no longer be calculated via the formulas from before because the entropy of the decoupled particles and the entropy of the other

particles are conserved separately after the decoupling (before, when all were in thermal equilibrium, the entropy of all particles was conserved). Details about the calculation of g_s and g_ρ with the above considerations can be found in ref.[91].

3.4 The Boltzmann equation

The evolution of the phase space density $f(x, p, t)$ of a particle species is described by the Boltzmann equation, which can be written as [92]

$$L[f] = C[f] \quad , \tag{3.61}$$

where L is the Liouville operator giving the net rate of change in time of the particle phase space density f, and C is the collision operator representing the number of particles per phase space volume that are lost or gained per unit time under interaction with other particles.

In the Friedmann-Robertson-Walker cosmological model, the phase space density is spatially homogeneous and isotropic, so f depends only on the particle energy E and the time t: $f = f(E, t)$. In this case, the Liouville operator becomes

$$L[f] = \frac{\partial f}{\partial t} - H\frac{|p|^2}{E}\frac{\partial f}{\partial E} \quad , \tag{3.62}$$

where $H \equiv \dot{R}/R$ is the Hubble parameter, R is the scale factor of the Universe and dot indicates time derivative.

In fact, the Liouville operator takes the form above with some more considerations than only $f = f(E, t)$. Generically, it is just a time derivative $\frac{d}{dt}$ applied to the relevant function. Said that, we know that in this case the total time derivative can be put as

$$\frac{df}{dt} = \frac{\partial f}{\partial t} + \frac{\partial f}{\partial E}\frac{dE}{dt} \quad . \tag{3.63}$$

The term $\frac{dE}{dt}$ will be dealt with using the geodesic equation

$$\frac{d^2x^\mu}{d\tau^2} + \Gamma^\mu_{\sigma\nu}\frac{dx^\sigma}{d\tau}\frac{dx^\nu}{d\tau} = 0 \quad , \tag{3.64}$$

or, with the zero-component of the four-momentum definition $p^\mu = m\frac{dx^\mu}{d\tau}$,

$$m\frac{dp^0}{d\tau} = -\Gamma^0_{\sigma\nu}p^\sigma p^\nu \quad . \tag{3.65}$$

We know $E \equiv p^0$, hence

$$m\frac{dE}{dt}\frac{dt}{d\tau} = -\Gamma^0_{\sigma\nu}p^\sigma p^\nu \quad , \tag{3.66}$$

$$\frac{dE}{dt}\left(m\frac{dt}{d\tau}\right) = -\Gamma^0_{\sigma\nu}p^\sigma p^\nu \quad , \tag{3.67}$$

$$\frac{dE}{dt} = -\left(\Gamma^0_{\sigma\nu}p^\sigma p^\nu\right)/p^0 \quad . \tag{3.68}$$

Now let's work with the rhs of the last line,

$$\Gamma^0_{\sigma\nu} = \frac{g^{0\alpha}}{2}\left(2\frac{\partial g_{\alpha\sigma}}{\partial x^\nu} - \frac{\partial g_{\sigma\nu}}{\partial x^\alpha}\right) = \frac{g^{00}}{2}\left(2\frac{\partial g_{0\sigma}}{\partial x^\nu} - \frac{\partial g_{\sigma\nu}}{\partial t}\right) = \frac{g^{00}}{2}\left(-\frac{\partial g_{\sigma\nu}}{\partial t}\right) \quad . \tag{3.69}$$

The first term is zero because the term g_{00} is constant. Now, contracting with the momenta, we have for the second term

$$-\frac{\partial g_{\sigma\nu}}{\partial t}p^\sigma p^\nu = -\frac{\partial g_{ij}}{\partial t}p^i p^j = -2R\dot{R}p^i p^j\delta_{ij} \tag{3.70}$$

$$= -2R^2 H\frac{|\vec{p}|^2}{R^2} = -2H|\vec{p}|^2 \quad . \tag{3.71}$$

We have used the definition $|\vec{p}|^2 = g_{ij}p^i p^j = R^2\delta_{ij}p^i p^j$. This way, we obtain

$$\Gamma^0_{\sigma\nu}p^\sigma p^\nu = \frac{g^{00}}{2}\left(-2H|\vec{p}|^2\right) = H|\vec{p}|^2 \quad . \tag{3.72}$$

Thus, finally

$$\frac{dE}{dt} = -H\frac{|\vec{p}|^2}{E} \quad , \tag{3.73}$$

$$\frac{df}{dt} = \frac{\partial f}{\partial t} + \frac{\partial f}{\partial E}\frac{dE}{dt} = \frac{\partial f}{\partial t} - H\frac{|\vec{p}|^2}{E}\frac{\partial f}{\partial E} \quad . \tag{3.74}$$

The particle number density n is the integral of the phase space density over all momenta and the sum over all spins. With g spin degrees of freedom, each with the same distribution $f(E,t)$, we have

$$n = \int dn = \int f(E,t)g\frac{d^3p}{(2\pi)^3} \quad . \tag{3.75}$$

In order to obtain an evolution equation for n, the Boltzmann equation (3.61) must be integrated over the particle momenta and summed over the spin degrees of freedom. For clarity, we present computations for the case of annihilations of two particles, 1 and 2, into two others, 3 and 4. At the end, it will be obvious how to sum over all the possible final channels. The Liouville term becomes

$$g_1\int L[f_1]\frac{d^3p_1}{(2\pi)^3} = \dot{n}_1 + 3Hn_1 \tag{3.76}$$

because

$$
\begin{aligned}
g_1 \int L[f_1] \frac{d^3p_1}{(2\pi)^3} &= g_1 \int \left\{ \frac{\partial f_1}{\partial t} - H \frac{|\vec{p}_1|^2}{E_1} \frac{\partial f_1}{\partial E_1} \right\} \frac{d^3p_1}{(2\pi)^3} \equiv g_1 \int \{(1)-(2)\} \frac{d^3p_1}{(2\pi)^3} \quad , \\
g_1 \int (1) \frac{d^3p_1}{(2\pi)^3} &= \frac{d}{dt} \int g_1 f_1 \frac{d^3p_1}{(2\pi)^3} = \dot{n}_1 \quad , \\
g_1 \int (2) \frac{d^3p_1}{(2\pi)^3} &= H g_1 \int \frac{|\vec{p}_1|^2}{E_1} \frac{\partial f_1}{\partial |\vec{p}_1|} \frac{\partial |\vec{p}_1|}{\partial E_1} \frac{d^3p_1}{(2\pi)^3} = H g_1 \int \frac{|\vec{p}_1|^2}{E_1} \frac{\partial f_1}{\partial |\vec{p}_1|} \frac{E_1}{|\vec{p}_1|} \frac{d^3p_1}{(2\pi)^3} \\
&= \frac{H g_1}{(2\pi)^3} \int_0^\infty |\vec{p}_1|^3 \frac{\partial f_1}{\partial |\vec{p}_1|} d|\vec{p}_1| \int d\Omega_1 \quad \longrightarrow \\
&\quad \longrightarrow \quad \frac{H g_1}{(2\pi)^3} (-3) \int_0^\infty |\vec{p}_1|^2 f_1 d|\vec{p}_1| \int d\Omega_1 \\
&= \frac{-3 H g_1}{(2\pi)^3} \int_0^\infty |\vec{p}_1|^2 f_1 d|\vec{p}_1| \int d\Omega_1 = -3 H g_1 \int \frac{d^3p_1}{(2\pi)^3} f_1 = -3 H n_1 \quad ,
\end{aligned}
$$

where the arrow indicates integration by parts, with the assumptions: $f_1(|\vec{p}_1| = \infty) = 0$ and $f_1(|\vec{p}_1| = 0) < \infty$. Now, integrating the collision term, only the inelastic contributions survive[4] [93]:

$$
\begin{aligned}
g_1 \int C_{\text{inelastic}}[f_1] \frac{d^3p_1}{(2\pi)^3} = \; - \; & \sum_{\text{spins}} \int \left[f_1 f_2 (1 \pm f_3)(1 \pm f_4) |\mathcal{M}_{12\to34}|^2 - \right. \\
& \left. - f_3 f_4 (1 \pm f_1)(1 \pm f_2) |\mathcal{M}_{34\to12}|^2 \right] \times \\
& \times (2\pi)^4 \delta^4 (p_1 + p_2 - p_3 - p_4) \times \\
& \times \frac{d^3p_1}{(2\pi)^3 2E_1} \frac{d^3p_2}{(2\pi)^3 2E_2} \frac{d^3p_3}{(2\pi)^3 2E_3} \frac{d^3p_4}{(2\pi)^3 2E_4} \quad .
\end{aligned}
\tag{3.77}
$$

Notice that an elastic collision term would be given by

$$
\begin{aligned}
g_1 \int C_{\text{elastic}}[f_1] \frac{d^3p_1}{(2\pi)^3} = \; - \; & \sum_{\text{spins}} \int \left[f_1 f_2 (1 \pm f_1)(1 \pm f_2) |\mathcal{M}_{12\to12}|^2 - \right. \\
& \left. - f_1 f_2 (1 \pm f_1)(1 \pm f_2) |\mathcal{M}_{12\to12}|^2 \right] \times \\
& \times (2\pi)^4 \delta^4 (p_1 + p_2 - p_3 - p_4) \times \\
& \times \frac{d^3p_1}{(2\pi)^3 2E_1} \frac{d^3p_2}{(2\pi)^3 2E_2} \frac{d^3p_3}{(2\pi)^3 2E_3} \frac{d^3p_4}{(2\pi)^3 2E_4} \quad ,
\end{aligned}
\tag{3.78}
$$

which is zero.

Let's analyze the collision term above by parts:

- First and second lines. Setting aside the terms $(1 \pm f)$ for now, we see that the rate of producing species 1 is proportional to the initial occupation numbers of species

[4] Therefore, processes dealing with scattering of particles won't be considered. We just need to concern ourselves with processes such as annihilation.

3 and 4, f_3 and f_4. Similarly the loss term is proportional to the initial $f_1 f_2$. The $1 \pm f$ terms, with plus sign for bosons and minus sign for fermions, represent the phenomena of Bose enhancement (consequence of stimulated emission) and Pauli blocking (Pauli's exclusion principle). If particles of type 1 already exist, a reaction producing more such particles is more likely to occur if 1 is a boson and less likely if a fermion. Also, there are weights associated to the processes which create or destroy particle species 1, which are respectively the invariant polarized amplitudes $\mathcal{M}_{34\to 12}$ or $\mathcal{M}_{12\to 34}$ obtained via Feynman rules of the pertinent model. The initial and final polarizations of all the particles must be summed within $\sum_{\text{spins}}$.

- The third line enforces energy-momentum conservation;

- The fourth line simply represents integration over the possible four-momenta of all the particles, thereby introducing the invariant four-volume elements are used.

The eq.(3.77) is valid also when the particles 1 and 2 are identical. No additional factor of $\frac{1}{2}$ should appear in eq.(3.77) in this case for the following reason: we are counting particles twice when we perform the products $f_1 \times f_1$ and $(1 \pm f_1) \times (1 \pm f_1)$, but for identical particles, two equal particles annihilate and are created each time, so that f_1 varies as twice as the rate for different particles. Therefore, factors of $\frac{1}{2}$ and 2 don't need to appear explicitly. For massive particles which decouple in the early Universe while they are a non-degenerate gas, we can neglect the statistical mechanical factors $(1 \pm f)$ in eq.(3.77).

Now, we make a key assumption: we assume that the annihilation products, 3 and 4, go quickly into equilibrium with the thermal background, therefore we replace $f_{3;\,4} = f^{\text{eq}}_{3;\,4}$.

Also we use the principle of detailed balance. In chemical equilibrium, it allows the replacement

$$f_3^{\text{eq}} f_4^{\text{eq}} = f_1^{\text{eq}} f_2^{\text{eq}} \quad , \tag{3.79}$$

since, in equilibrium, there is no preferred sense in the reaction $1 + 2 \longleftrightarrow 3 + 4$.

Another useful assumed property is unitarity (CPT theorem) because if CP is conserved, so is T. It enables us to write

$$\begin{aligned} &\sum_{\text{spins}} \int \left|\mathcal{M}_{34\to 12}\right|^2 (2\pi)^4 \, \delta^4 \left(p_1 + p_2 - p_3 - p_4\right) \frac{d^3 p_3}{(2\pi)^3 \, 2E_3} \frac{d^3 p_4}{(2\pi)^3 \, 2E_4} = \\ &= \sum_{\text{spins}} \int \left|\mathcal{M}_{12\to 34}\right|^2 (2\pi)^4 \, \delta^4 \left(p_1 + p_2 - p_3 - p_4\right) \frac{d^3 p_3}{(2\pi)^3 \, 2E_3} \frac{d^3 p_4}{(2\pi)^3 \, 2E_4} \quad . \end{aligned} \tag{3.80}$$

We then recall the definition of the unpolarized cross section $\sigma_{12\to34}$ for the process $12 \to 34$ which is given by

$$\sum_{\text{spins}} \int |\mathcal{M}_{12\to34}|^2 (2\pi)^4 \delta^4 (p_1 + p_2 - p_3 - p_4) \frac{d^3p_3}{(2\pi)^3 2E_3} \frac{d^3p_4}{(2\pi)^3 2E_4} = 4F g_1 g_2 \sigma_{12\to34} \quad , \tag{3.81}$$

where $F = \left[(p_1 \cdot p_2)^2 - m_1^2 m_2^2\right]^{1/2}$ and the spin factor $g_1 g_2$ comes from the average over initial spins.

At this point then, we know how to include all accessible final states, instead of just two (in this case indicated by 3 and 4.), i.e.,

$$\sigma = \sum_{\text{all f}} \sigma_{12\to f} \quad . \tag{3.82}$$

Hence, we reach the intermediate equations

$$\begin{aligned}
g_1 \int C_{\text{inelastic}}[f_1] \frac{d^3p_1}{(2\pi)^3} = & - \sum_{\text{spins}} \int \left[f_1 f_2 |\mathcal{M}_{12\to34}|^2 - f_3^{\text{eq}} f_4^{\text{eq}} |\mathcal{M}_{12\to34}|^2 \right] \times \\
& \times (2\pi)^4 \delta^4 (p_1 + p_2 - p_3 - p_4) \times \\
& \times \frac{d^3p_1}{(2\pi)^3 2E_1} \frac{d^3p_2}{(2\pi)^3 2E_2} \frac{d^3p_3}{(2\pi)^3 2E_3} \frac{d^3p_4}{(2\pi)^3 2E_4} \\
= & - \int 4F g_1 g_2 \sigma \left(f_1 f_2 - f_1^{\text{eq}} f_2^{\text{eq}} \right) \frac{d^3p_1}{(2\pi)^3 2E_1} \frac{d^3p_2}{(2\pi)^3 2E_2} \\
= & - \int \frac{F}{E_1 E_2} \sigma \left(g_1 f_1 g_2 f_2 - g_1 f_1^{\text{eq}} g_2 f_2^{\text{eq}} \right) \frac{d^3p_1}{(2\pi)^3} \frac{d^3p_2}{(2\pi)^3} \\
= & - \int v_{\text{Møl}} \, \sigma \left(g_1 f_1 \frac{d^3p_1}{(2\pi)^3} g_2 f_2 \frac{d^3p_2}{(2\pi)^3} - g_1 f_1^{\text{eq}} \frac{d^3p_1}{(2\pi)^3} g_2 f_2^{\text{eq}} \frac{d^3p_2}{(2\pi)^3} \right) \\
= & - \int v_{\text{Møl}} \, \sigma \left(dn_1 dn_2 - dn_1^{\text{eq}} dn_2^{\text{eq}} \right) \quad ,
\end{aligned} \tag{3.83}$$

where we've defined $v_{\text{Møl}} \equiv \frac{F}{E_1 E_2}$ (as defined in [94]) and used the eq.(3.75) for the last step.

Here we may comment a little on the physical meaning of $v_{\text{Møl}}$. In terms of the particle velocities $\vec{v}_1 = \vec{p}_1/E_1$ and $\vec{v}_2 = \vec{p}_2/E_2$, the Møller velocity can be written as

$$v_{\text{Møl}} = \left[|\vec{v}_1 - \vec{v}_2|^2 - |\vec{v}_1 \times \vec{v}_2|^2 \right]^{1/2} \quad . \tag{3.84}$$

Therefore, the initial definition of the Møller velocity yields an expression which is not trivial but has to do with the velocities of the initial particles.

Another useful simplification comes from the consideration, [93], that the species 1 and 2 are maintained in kinetic equilibrium through scattering with other particles in the thermal bath during all of their evolution, even after their decoupling when they are out of

chemical equilibrium: the distributions in kinetic (=thermal) equilibrium are proportional to those in chemical equilibrium, with a proportionality factor $e^{-\alpha(t)}$, independent of momentum, - where $\alpha(t)$ is a time-dependent effective chemical potential. Hence, eq.(3.83) can be written, both before and after the decoupling, as

$$\begin{aligned} g_1 \int C_{\text{inelastic}}\left[f_1\right] \frac{d^3p_1}{(2\pi)^3} &= - \int v_{\text{M}\o\text{l}}\, \sigma \left(A\, dn_1^{\text{eq}} dn_2^{\text{eq}} - dn_1^{\text{eq}} dn_2^{\text{eq}}\right) \\ &= - \int v_{\text{M}\o\text{l}}\, \sigma\, dn_1^{\text{eq}} dn_2^{\text{eq}} \left(A - 1\right) \\ &= - \frac{\left(An_1^{\text{eq}} n_2^{\text{eq}} - n_1^{\text{eq}} n_2^{\text{eq}}\right)}{n_1^{\text{eq}} n_2^{\text{eq}}} \int v_{\text{M}\o\text{l}}\, \sigma\, dn_1^{\text{eq}} dn_2^{\text{eq}} \\ &= - \frac{\left(n_1 n_2 - n_1^{\text{eq}} n_2^{\text{eq}}\right)}{n_1^{\text{eq}} n_2^{\text{eq}}} \int v_{\text{M}\o\text{l}}\, \sigma\, dn_1^{\text{eq}} dn_2^{\text{eq}} \\ &= - \left(n_1 n_2 - n_1^{\text{eq}} n_2^{\text{eq}}\right) \frac{\int v_{\text{M}\o\text{l}}\, \sigma\, dn_1^{\text{eq}} dn_2^{\text{eq}}}{\int dn_1^{\text{eq}} dn_2^{\text{eq}}} \\ &\equiv - \left(n_1 n_2 - n_1^{\text{eq}} n_2^{\text{eq}}\right) \left\langle \sigma v_{\text{M}\o\text{l}} \right\rangle \quad , \end{aligned} \tag{3.85}$$

where A is the product of the momentum-independent terms ($e^{-\alpha(t)}$) of the two particles. Finally, we equal the lhs and the rhs of the eq.(3.61)

$$\dot{n}_1 + 3Hn_1 = - \left(n_1 n_2 - n_1^{\text{eq}} n_2^{\text{eq}}\right) \left\langle \sigma v_{\text{M}\o\text{l}} \right\rangle \quad . \tag{3.86}$$

If we are dealing with $1 = 2\,(\equiv \chi)$, we obtain as a result

$$\dot{n}_\chi + 3Hn_\chi = - \left\langle \sigma v_{\text{M}\o\text{l}} \right\rangle \left(n_\chi^2 - n_{\chi,\text{eq}}^2\right) \quad . \tag{3.87}$$

3.5 Thermalized cross section

In this section, we will reach another form for the introduced thermalized cross section $\langle \sigma v_{\text{M}\o\text{l}} \rangle$. Above, it was defined as

$$\left\langle \sigma v_{\text{M}\o\text{l}} \right\rangle = \frac{\int \sigma v_{\text{M}\o\text{l}} e^{-E_1/T} e^{-E_2/T} d^3p_1 d^3p_2}{\int e^{-E_1/T} e^{-E_2/T} d^3p_1 d^3p_2} \quad , \tag{3.88}$$

where $\overrightarrow{p_1}$ and $\overrightarrow{p_2}$ are the three-momenta and E_1 and E_2 are the energies of the two colliding particles, in the cosmic comoving frame.

Notice that we have used Maxwell-Boltzmann statistics for dn_i since, in the computations to be performed, the relevant temperatures are less than the particle mass. A satisfactory explanation is that the x_f for decoupling of a heavy particle has to be ~ 25 in order for its abundance to correspond to the current dark matter results from CMB. Also, we know that for $x \gtrsim 3$, the Fermi-Dirac and the Bose-Einstein statistics can be approximated to the Maxwell-Boltzmann one (see Fig. 4).Therefore, if one starts the

simulations at $x \sim 3$, there is almost no loss in accuracy. The insensitivity of the final abundance of heavy relics on the statistics of the particles was already noticed in ref. [95].

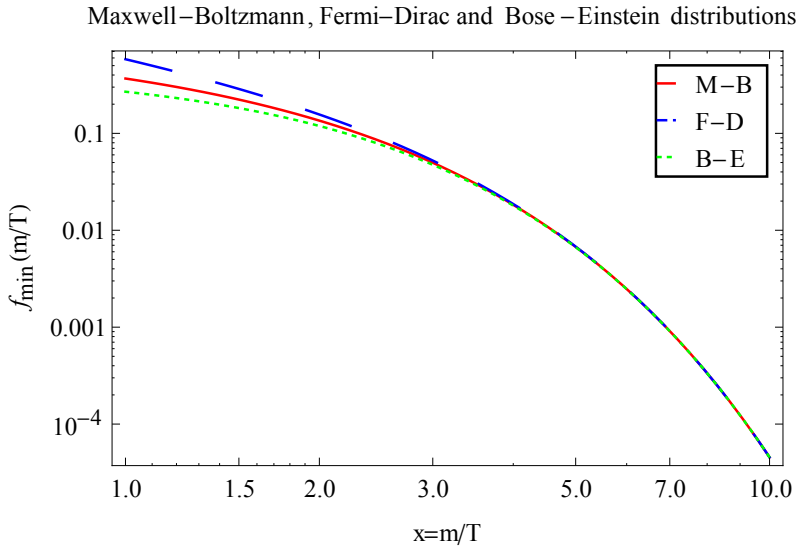

Figure 4 – Plot of $f_{\min}(m/T) \equiv f(E = m, T)$ as a function of $x = m/T$, neglecting chemical potential μ. We can clearly notice that the Fermi-Dirac (F-D) and Bose-Einstein (B-E) equilibrium distributions may be approximated to the Maxwell-Boltzmann (M-B) one above $x \gtrsim 3$.

We can manage to simplify the last expression by working out the momentum volume element $d^3p_1 d^3p_2$. It can be expressed as

$$d^3p_1 d^3p_2 = 4\pi p_1 E_1 dE_1 2\pi p_2 E_2 dE_2 d\cos\theta \quad , \tag{3.89}$$

where we have used the relativistic relation $pdp = EdE$. Also, from now on, the momentum modulus $|\vec{p}|$ will be expressed as p. The trick used above is a picture realization of the collision between the particles with momenta $\overrightarrow{p_1}$ and $\overrightarrow{p_2}$. An illustration comes below

The trick consists on integrating over θ_1 and ϕ_1, maintaining also the angle θ between p_1 and p_2. As a result, we end up integrating also over ϕ_2 because θ remains fixed between the momenta. In the end, the variables θ_1, ϕ_1 and ϕ_2 are integrated, yielding the value $4\pi \times 2\pi$. Therefore, the volume element becomes (3.89).

We know perform change of variables:

$$E_+ = E_1 + E_2 \quad ; \tag{3.90}$$

$$E_- = E_1 - E_2 \quad ; \tag{3.91}$$

$$s = 2m^2 + 2E_1E_2 - 2p_1p_2\cos\theta \quad . \tag{3.92}$$

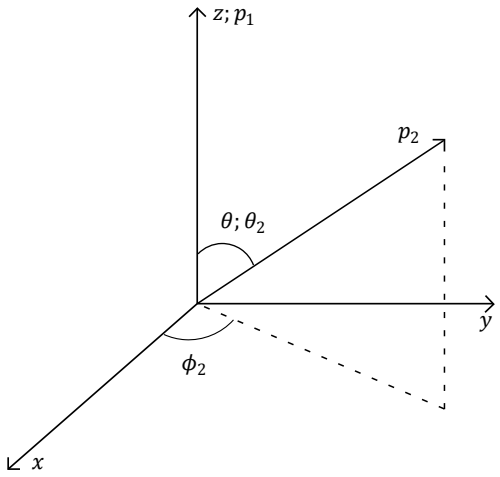

Figure 5 – Illustration for two colliding particles. In this figure, we have $\theta_1 = 0$.

We must evaluate the Jacobian of the transformation

$$J = \begin{vmatrix} \frac{\partial E_1}{\partial E_+} & \frac{\partial E_1}{\partial E_-} & \frac{\partial E_1}{\partial s} \\ \frac{\partial E_2}{\partial E_+} & \frac{\partial E_2}{\partial E_-} & \frac{\partial E_2}{\partial s} \\ \frac{\partial \cos\theta}{\partial E_+} & \frac{\partial \cos\theta}{\partial E_-} & \frac{\partial \cos\theta}{\partial s} \end{vmatrix} = \begin{vmatrix} \frac{1}{2} & \frac{1}{2} & 0 \\ \frac{1}{2} & -\frac{1}{2} & 0 \\ \frac{\partial \cos\theta}{\partial E_+} & \frac{\partial \cos\theta}{\partial E_-} & -\frac{1}{2p_1p_2} \end{vmatrix} = \frac{1}{4p_1p_2} \quad . \tag{3.93}$$

The volume element takes the form

$$\begin{aligned} d^3p_1 d^3p_2 &= 4\pi p_1 dE_1 2\pi p_2 dE_2 d\cos\theta \longrightarrow 8\pi^2 p_1 p_2 E_1 E_2 \left[\frac{1}{4p_1p_2} dE_+ dE_- ds\right] \\ &= 2\pi^2 E_1 E_2 dE_+ dE_- ds \quad . \end{aligned} \tag{3.94}$$

Now, we need to find the new integration limits. For s, it's known that

$$\begin{aligned} s = (p_1+p_2)^2 = (E_1+E_2)^2 - (\overrightarrow{p_1}+\overrightarrow{p_2})^2 &\geq (E_1+E_2)^2 - (p_1+p_2)^2 \quad , \\ (E_1+E_2)^2 - (p_1+p_2)^2 &= \left(\sqrt{p_1^2+m^2}+\sqrt{p_2^2+m^2}\right)^2 - (p_1+p_2)^2 \\ &= 2m^2 + 2\sqrt{p_1^2+m^2}\sqrt{p_2^2+m^2} - 2p_1p_2 \\ &= 4m^2 + 2\sqrt{p_1^2+m^2}\sqrt{p_2^2+m^2} - 2p_1p_2 - 2m^2 \end{aligned} \tag{3.95}$$

Now we are going to prove that $2\sqrt{p_1^2+m^2}\sqrt{p_2^2+m^2} - 2p_1p_2 - 2m^2 \geq 0$:

$$\begin{aligned}
&\sqrt{p_1^2+m^2}\sqrt{p_2^2+m^2} \Leftrightarrow p_1p_2+m^2 \\
&\left(p_1^2+m^2\right)\left(p_2^2+m^2\right) \Leftrightarrow p_1^2p_2^2+m^4+2m^2p_1^2p_2^2 \\
&m^2\left(p_1^2+p_2^2\right) \Leftrightarrow m^2p_1^2p_2^2 \\
&m^2\left(|\overrightarrow{p_1}|-|\overrightarrow{p_2}|\right)^2 \geq 0 \quad .
\end{aligned} \tag{3.96}$$

Finally, we get the limit for s:

$$s \geq 4m^2 \quad . \tag{3.97}$$

For E_+, we know the following

$$s=(E_1+E_2)^2-(\overrightarrow{p_1}+\overrightarrow{p_2})^2=E_+^2-(\overrightarrow{p_1}+\overrightarrow{p_2})^2 \quad \therefore \quad E_+ \geq \sqrt{s} \quad . \tag{3.98}$$

For E_-:

$$\begin{aligned}
s &= 2m^2+2E_1E_2-2p_1p_2\cos\theta \\
s &= 2m^2+\frac{2}{4}\left(E_+^2-E_-^2\right)-2p_1p_2\cos\theta \\
s-2m^2-\frac{2}{4}\left(E_+^2-E_-^2\right) &= -2p_1p_2\cos\theta \quad .
\end{aligned} \tag{3.99}$$

If we consider the extreme cases of $\cos\theta$, we obtain as a result

$$\begin{aligned}
s-2m^2-\frac{2}{4}\left(E_+^2-E_-^2\right) &\geq -2p_1p_2 \quad , \\
s-2m^2-\frac{2}{4}\left(E_+^2-E_-^2\right) &\leq 2p_1p_2 \quad .
\end{aligned} \tag{3.100}$$

p_1p_2 is given by

$$p_1p_2=\sqrt{E_1^2-m^2}\sqrt{E_2^2-m^2}=\sqrt{\frac{\left(E_++E_-\right)^2}{4}-m^2}\sqrt{\frac{\left(E_+-E_-\right)^2}{4}-m^2} \quad . \tag{3.101}$$

If one solves the two inequalities for E_-, one finds the limits

$$-\sqrt{1-\frac{4m^2}{s}}\sqrt{E_+^2-s} \leq E_- \leq +\sqrt{1-\frac{4m^2}{s}}\sqrt{E_+^2-s} \quad . \tag{3.102}$$

Now let's proceed to the integral that expresses the thermal averaging of the cross section:

$$\langle\sigma v_{\text{M}\o\text{l}}\rangle=\frac{\int\sigma v_{\text{M}\o\text{l}}e^{-E_1/T}e^{-E_2/T}d^3p_1d^3p_2}{\int e^{-E_1/T}e^{-E_2/T}d^3p_1d^3p_2} \equiv \frac{\text{Num}}{\text{Den}} \quad . \tag{3.103}$$

Working with the numerator, we obtain

$$\begin{aligned}
\text{Num} &= \int \sigma v_{\text{Møl}} e^{-E_1/T} e^{-E_2/T} d^3p_1 d^3p_2 \\
&= 2\pi^2 \int dE_+ \int ds \int dE_- \quad \sigma v_{\text{Møl}} E_1 E_2 e^{-E_+/T} \\
&= 2\pi^2 \int dE_+ \int ds \left[2\sqrt{1-\frac{4m^2}{s}} \sqrt{E_+^2 - s} \right] \sigma v_{\text{Møl}} E_1 E_2 e^{-E_+/T} \\
&= 4\pi^2 \int ds \quad \sigma v_{\text{Møl}} E_1 E_2 \sqrt{1-\frac{4m^2}{s}} \int dE_+ e^{-E_+/T} \sqrt{E_+^2 - s} \quad .
\end{aligned} \tag{3.104}$$

The above steps have been done thanks to the independence of $v_{\text{Møl}} E_1 E_2$ related to E_+ and E_-. We know from the earlier section that $F = \left((p_1 \cdot p_2)^2 - m_1^2 m_2^2 \right)^{1/2}$. It takes some work to show that F can be cast as $F = \frac{1}{2}\sqrt{s\left(s-4m^2\right)}$. Recall also that the Møller velocity has been defined as

$$F = v_{\text{Møl}} E_1 E_2 \quad , \tag{3.105}$$

,therefore, we reach

$$\begin{aligned}
\text{Num} &= 4\pi^2 \int ds \quad \sigma F \sqrt{1-\frac{4m^2}{s}} \int dE_+ e^{-E_+/T} \sqrt{E_+^2 - s} \\
&= 2\pi^2 \int ds \quad \sigma \left(s-4m^2\right) \int dE_+ e^{-E_+/T} \sqrt{E_+^2 - s} \\
&= 2\pi^2 \int ds \quad \sigma \left(s-4m^2\right) \left[\sqrt{s} T K_1 \left(\frac{\sqrt{s}}{T} \right) \right] \\
&= 2\pi^2 T \int ds \quad \sigma \left(s-4m^2\right) \sqrt{s} K_1 \left(\frac{\sqrt{s}}{T} \right) \quad .
\end{aligned} \tag{3.106}$$

The denominator must now be evaluated. For this task, we use the following volume element: $d^3p_1 d^3p_2 = (4\pi)^2 p_1 E_1 dE_1 p_2 E_2 dE_2$. It's convenient because there is no function other than the exponentials of the energies. Thus,

$$\begin{aligned}
\text{Den} &= \int e^{-E_1/T} e^{-E_2/T} d^3p_1 d^3p_2 \\
&= (4\pi)^2 \int e^{-E_1/T} e^{-E_2/T} p_1 E_1 dE_1 p_2 E_2 dE_2 \\
&= (4\pi)^2 \int e^{-E_1/T} e^{-E_2/T} \sqrt{E_1^2 - m^2} E_1 dE_1 \sqrt{E_2^2 - m^2} E_2 dE_2 \\
&= (4\pi)^2 \left[\int_m^\infty dx \; e^{-x/T} x \sqrt{x^2 - m^2} \right]^2 = (4\pi)^2 \left[m^2 T K_2 \left(\frac{m}{T} \right) \right]^2 \\
&= \left[4\pi m^2 T K_2 \left(\frac{m}{T} \right) \right]^2 \quad .
\end{aligned} \tag{3.107}$$

Finally, the compact expression for $\langle \sigma v_{\text{Møl}} \rangle$ reads as

$$\begin{aligned} \langle \sigma v_{\text{Møl}} \rangle &= \frac{\int \sigma v_{\text{Møl}} e^{-E_1/T} e^{-E_2/T} d^3p_1 d^3p_2}{\int e^{-E_1/T} e^{-E_2/T} d^3p_1 d^3p_2} = \frac{2\pi^2 T \int_{4m^2}^{\infty} ds \quad \sigma\left(s-4m^2\right)\sqrt{s} K_1\left(\frac{\sqrt{s}}{T}\right)}{\left[4\pi m^2 T K_2\left(\frac{m}{T}\right)\right]^2} \\ \langle \sigma v_{\text{Møl}} \rangle &= \frac{1}{8m^4 T\left[K_2\left(\frac{m}{T}\right)\right]^2} \int_{4m^2}^{\infty} ds \quad \sigma\left(s-4m^2\right)\sqrt{s} K_1\left(\frac{\sqrt{s}}{T}\right) \quad . \end{aligned} \tag{3.108}$$

3.5.1 $\langle \sigma v_{\text{Møl}} \rangle$ expansion in x^{-1}

It is convenient to expand $\langle \sigma v_{\text{Møl}} \rangle$ in the variable $x^{-1} = T/m$ because we are assuming that for great part of its history, the dark matter particle satisfies $x \gg 1$.

For achieving that goal, the following steps are done (see details in ref.[96]):

- The LAB frame is defined: one particle is at rest and the other particle with velocity $v_{lab} = v_{lab}(\epsilon)$, where $\epsilon \equiv (s-4m^2)/4m^2$, comes to the interaction with the latter;
- Therefore v_{lab} can be associated to s via ϵ. As a consequence, $\langle \sigma v_{\text{Møl}} \rangle$ is expressed with the new variables $(\sigma \times v_{lab})$ and ϵ (together with $x = m/T$), with $d\epsilon$ as the integration volume .
- Now, the product σv_{lab} is expanded in ϵ about the point $\epsilon = 0$. After that, $\langle \sigma v_{\text{Møl}} \rangle$ is integrated over ϵ, obtaining $\langle \sigma v_{\text{Møl}} \rangle = \langle \sigma v_{\text{Møl}} \rangle (x)$.

The final expression is written as

$$\begin{aligned} \langle \sigma v_{\text{Møl}} \rangle &= a^{(0)} + \frac{3}{2}a^{(1)}x^{-1} + \left[\frac{9}{2}a^{(1)} + \frac{15}{8}a^{(2)}\right]x^{-2} + \left[\frac{15}{16}a^{(1)} + \frac{195}{16}a^{(2)} + \frac{35}{16}a^{(3)}\right]x^{-3} \\ &+ \left[\frac{675}{32}a^{(2)} + \frac{735}{32}a^{(3)} + \frac{315}{128}a^{(4)}\right]x^{-4} + O(x^{-5}) \quad , \end{aligned} \tag{3.109}$$

where $a^{(i)}$ are the coefficients of the expansion of σv_{lab}.

Then, depending on the case, it may be time-saving to solve the Boltzmann equation with the expanded $\langle \sigma v_{\text{Møl}} \rangle$ instead of with the exact one.

3.5.2 Non-relativistic $\langle \sigma v_{\text{Møl}} \rangle$ ($\langle \sigma v_{\text{Møl}} \rangle_{n.r.}$) and its expansion

It is convenient to define the $\langle \sigma v_{\text{Møl}} \rangle_{n.r.}$ as

$$\langle \sigma v_{\text{Møl}} \rangle_{n.r.} = \frac{\int \sigma v_{lab} e^{-E_1/T} e^{-E_2/T} d^3p_1 d^3p_2}{\int e^{-E_1/T} e^{-E_2/T} d^3p_1 d^3p_2} \quad , \tag{3.110}$$

which can be expressed as a single integral over s as is eq.(3.108).

That is, this new definition is just the limit of $\langle \sigma v_{\text{Møl}} \rangle$ when the product of the velocity modules of the particles in the comoving frame is considered negligible, as can be seen (ref.[96]):

$$v_{\text{Møl}} = v_{lab}(1 - \vec{v}_1 \cdot \vec{v}_2) \quad , \tag{3.111}$$

where $\vec{v}_i$ corresponds to the ith particle velocity vector as seen by an observer at rest in the comoving frame.

The definition of $\langle \sigma v_{\text{Møl}} \rangle_{n.r.}$ can be developed to yield a more compact and simpler expression depending on $\sigma \times v_{lab}$ and ϵ - integrating over the last one. Also, it can be expanded following the last step of the earlier section. Thus, one can reach

$$\langle \sigma v_{\text{Møl}} \rangle_{n.r.} = a^{(0)} + \frac{3}{2} a^{(1)} x^{-1} + \frac{15}{8} a^{(2)} x^{-2} + \frac{35}{16} a^{(3)} x^{-3} + \frac{315}{128} a^{(4)} x^{-4} + O(x^{-5}) \quad . \tag{3.112}$$

Comparing the expansions of the relativistic and non-relativistic averages (3.109) and (3.112) we see that they coincide up to order x^{-1}, when σv_{lab} can be expanded.

It is well known that these expansions are not valid when there is resonance via s-channel. As an example, we show a plot, Fig. 6, of the expanded $\langle \sigma v_{\text{Møl}} \rangle_{n.r.}$ and the exact one as a function of the mass of the initial particles. The cross section considered was the one for the tree-level process involving only scalars, $\phi_i + \phi_i \to \phi_f + \phi_f$ with an exchange of a scalar particle ϕ_{ex} through the s-channel. The respective cross section is

$$\sigma_{\text{s-channel}} = \frac{\lambda_s^2}{16\pi s} \frac{1}{\left(s - M_{ex}^2\right)^2 + \left(\Gamma_{ex} M_{ex}\right)^2} \sqrt{\frac{s - 4m_f^2}{s - 4m_i^2}} \quad . \tag{3.113}$$

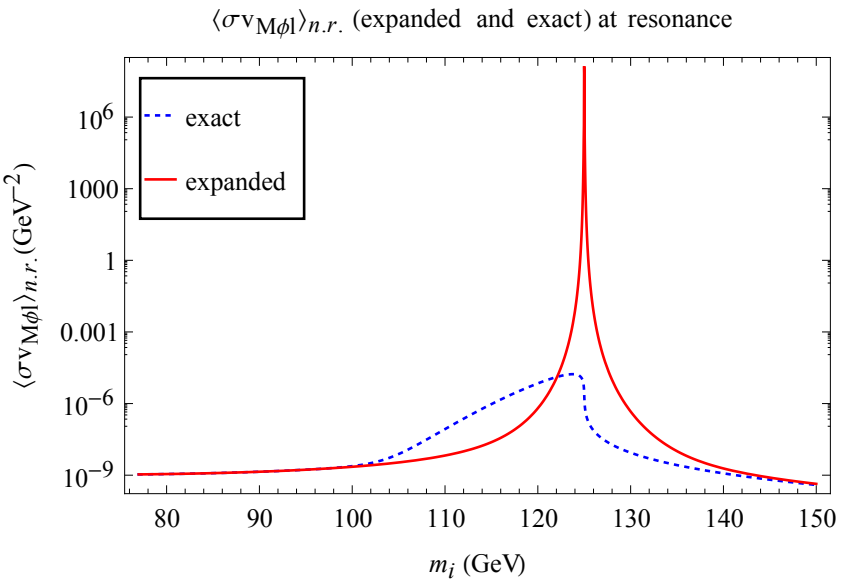

Figure 6 – Comparison of expanded and exact $\langle \sigma v_{\text{M}\o\text{l}} \rangle_{n.r.}$'s near the pole. The parameters considered were: $\Gamma_{ex} = 0.09$ GeV; $M_{ex} = 250$ GeV; $\lambda_s = 10^3$ GeV^2; and $m_f = 0$.

3.6 Obtaining the DM mass density

3.6.1 Numerical solution

As we found at the section 3.4, the rate equation for determining the relic density of some hypothetical stable particle is the Boltzmann equation (3.87)

$$\dot{n}_\chi + 3Hn_\chi = -\langle \sigma v_{\text{M}\o\text{l}} \rangle \left(n_\chi^2 - n_{\chi,\text{eq}}^2 \right) \quad ,$$

where n_χ is the number density of χ particles, $n_{\chi,\text{eq}}$ is the number density the χ particles would have if in thermal equilibrium at temperature T, H is the Hubble constant, and $\langle \sigma v_{\text{M}\o\text{l}} \rangle$ is the thermally averaged cross section as described in sec. 3.5.

It is convenient to replace time in the above equation by the photon temperature. For this, we need our previous definitions for g_s and g_ρ :

$$g_s(T_\gamma) = \frac{45}{2\pi^2} \frac{s(T_\gamma)}{T_\gamma^3} \quad , \tag{3.114}$$

$$g_\rho(T_\gamma) = \frac{30}{\pi^2} \frac{\rho(T_\gamma)}{T_\gamma^4} \quad , \tag{3.115}$$

where $s(T_\gamma)$ and $\rho(T_\gamma)$ are, respectively, the total entropy and energy densities of the Universe, and T_γ is the photon gas temperature.

It is convenient to treat implicitly the decrease in density due to the expansion of the Universe, considering the ratio of number of particles to the entropy density: $Y \equiv n_\chi/s$. Doing so, we may derivate it with respect to time:

$$\begin{aligned} \frac{dY}{dt} &= \frac{1}{s}\frac{dn_\chi}{dt} - \frac{n_\chi}{s^2}\frac{ds}{dt} \quad , \\ & \frac{ds}{dt} = \frac{d}{dt}\left(\frac{S}{R^3}\right) = -\frac{3S}{R^4}\dot{R} = -3sH \quad , \\ s\frac{dY}{dt} &= \dot{n}_\chi + 3Hn_\chi \quad , \end{aligned} \tag{3.116}$$

where we have used the condition of entropy conservation[5]

Thus, the Boltzmann equation gets the form

$$\frac{dY}{dt} = -s\left\langle \sigma v_{\text{Møl}} \right\rangle \left(Y^2 - Y_{eq}^2\right) \quad . \tag{3.117}$$

We may make Y a function of $x \equiv m/T_\gamma$. Hence, we must be able to obtain an expression which takes into account the evolution of Y with respect to x

$$\frac{dY}{dt} = \frac{dY}{dx}\frac{dx}{dt} \quad .$$

Also, we may arrange

$$s = -\frac{1}{3H}\frac{ds}{dt} = -\frac{1}{3H}\frac{ds}{dx}\frac{dx}{dt} \quad . \tag{3.118}$$

This way, we have

$$\frac{dY}{dx} = \frac{1}{3H}\frac{ds}{dx}\left\langle \sigma v_{\text{Møl}} \right\rangle \left(Y^2 - Y_{eq}^2\right) \quad . \tag{3.119}$$

ds/dx can be expressed in another way according to the eq.(3.114),

$$\begin{aligned} \frac{ds}{dx} &= \frac{2\pi^2}{45}\left(\frac{dg_s}{dx}T_\gamma^3 + g_s 3T_\gamma^2\frac{dT_\gamma}{dx}\right) \\ \frac{ds}{dx} &= \frac{2\pi^2}{45}\left(\frac{dg_s}{dT_\gamma}T_\gamma^3 + g_s 3T_\gamma^2\right)\frac{dT_\gamma}{dx} \quad . \end{aligned} \tag{3.120}$$

If we assume a FRW cosmology with no curvature ($k = 0$), then the Hubble constant can be written via one of the Friedmann equations:

$$H = \left(\frac{8}{3}\pi G\rho\right)^{1/2} \quad . \tag{3.121}$$

[5] Before the decoupling of some species, there is entropy ($S_{\text{plasma}} + S_{\text{species}}$) conservation because the rapid interactions of the plasma particles assure that the plasma stays at thermal equilibrium. In order to consider entropy conservation after decoupling, we make an assumption: it is assumed there is no entropy production when the species leaves to interact (decouples from) with the plasma. Consequently, the entropies of the plasma (S_{plasma}) and of the species (S_{species}) are conserved separately.

But ρ is given by eq.(3.115) (we consider just matter and radiation in ρ because the vacuum energy density is more than fourty orders of magnitude smaller than the matter and radiation energy density for $x \lesssim 1000$). Then,

$$H = \left(\frac{4}{45}\pi^3 G g_\rho\right)^{1/2} T_\gamma^2 \quad . \tag{3.122}$$

This way,

$$\frac{1}{3H}\frac{ds}{dx} = \frac{\frac{2\pi^2}{45}\left(\frac{dg_s}{dT_\gamma}T_\gamma^3 + g_s 3T_\gamma^2\right)\frac{dT_\gamma}{dx}}{3\left(\frac{4}{45}\pi^3 G g_\rho\right)^{1/2} T_\gamma^2} = \frac{\frac{2\pi^2}{45}\left(\frac{1}{3}\frac{dg_s}{dT_\gamma}T_\gamma + g_s\right)\frac{dT_\gamma}{dx}}{\left(\frac{4}{45}\pi^3 G g_\rho\right)^{1/2}} \quad .$$

Finally, the Boltzmann equation is written as

$$\begin{aligned}
\frac{dY}{dx} &= \frac{2\pi^2}{45}\frac{\left(\frac{1}{3}\frac{dg_s}{dT_\gamma}T_\gamma + g_s\right)}{\left(\frac{4}{45}\pi^3 G g_\rho\right)^{1/2}}\frac{dT_\gamma}{dx}\langle\sigma v_{\text{Møl}}\rangle\left(q^2 - q_{eq}^2\right) \quad , \\
&\frac{dT_\gamma}{dx} = m\frac{d(T_\gamma/m)}{dx} = m\frac{d(x^{-1})}{dx} = -\frac{m}{x^2} \quad , \\
\frac{dY}{dx} &= -\frac{m}{x^2}\frac{\left(\frac{1}{3}g_s' m x^{-1} + g_s\right)}{\left(\frac{45}{\pi}G g_\rho\right)^{1/2}}\langle\sigma v_{\text{Møl}}\rangle\left(Y^2 - Y_{eq}^2\right) \quad .
\end{aligned} \tag{3.123}$$

Notice that the temperature of the photon gas T_γ may differ from that of the χ particles. To obtain the numerical solution of (3.123), we integrate from $x \sim 3$ (where $Y = Y_{eq}$, for nonrelativistic particles) to $x = x_0 = x_{\text{today}}$, thus finding $Y_0 = Y(x_0)$. Knowing Y_0, we can compute $\Omega = \rho_0/\rho_c = m s_0 Y_0/\rho_c$, where $\rho_c = 3H^2/8\pi G$,

$$\Omega h^2 = 2.8282 \times 10^8 \frac{m}{\text{GeV}} Y_0 \quad , \tag{3.124}$$

where h is the Hubble constant in units of 100 km sec^{-1} Mpc^{-1} (it is currently in the range $0.5 \lesssim h \lesssim 1$). s_0 is found via the knowledge of the g_s function behavior at $T = T_{0,\gamma} \equiv T_\gamma(x = x_0)$.

$T_{0,\gamma} = 2.7K$ is the present photon temperature. Although the detailed calculation of $g_s(T)$ is done in Ref.[91], we may provide some information about the calculation of this quantity. It is calculated regarding all the particles that constitute the matter of the Universe, taking into account the formula (3.57), with some modifications because some particles leave to interact with the early Universe plasma and we must take care of the temperature discrepancies between the decoupled particles and those which are still within the plasma. Something else about its evaluation is discussed below Fig. 3.

3.6.2 Approximated solution

No closed-form solution for the eq. (3.123) is known, and sometimes the numerical calculations demand some time. An approach has been devised in order to save time. We describe it now.

Our initial condition for solving the Boltzmann equation is $x = 1$. In this regime, the particle statistics can be considered to be Maxwell-Boltzmann, as we have already observed earlier. The use of the correct statistics would yield a correction of less than 1% on Y_0 (see ref.[95]). Using Maxwell-Boltzmann statistics, the equilibrium density Y_{eq} is given by

$$Y_{eq} = \frac{45g}{4\pi^4}\frac{x^2 K_2(x)}{g_s(m/x)} \quad , \tag{3.125}$$

where g is number of internal degrees of freedom of the species under consideration, $K_2(x)$ is the modified second order Bessel function, and g_s has been defined in (3.57).

First, we determine the temperature of decoupling (freeze-out) T_f. Before the decoupling, it is convenient to work with the equation for $\Delta \equiv Y - Y_{eq}$,

$$\frac{d\Delta}{dx} = -\left(\frac{45}{\pi}G\right)^{-1/2}\frac{g_*^{1/2}m}{x^2}\langle\sigma v_{\text{Møl}}\rangle\Delta(\Delta + 2Y_{eq}) - \frac{dY_{eq}}{dx} \quad , \tag{3.126}$$

where $g_*^{1/2} \equiv \frac{1}{g_\rho^{1/2}}\left(g_s + \frac{m}{3x}g_s'\right)$. Before the decoupling, we neglect $d\Delta/dx$ because Y follows the equilibrium density Y_{eq}. We define T_f as the temperature at which $\Delta = \delta Y_{eq}$, with δ a chosen number, that must be adjusted in order for the approximate results to match the numerical solution. Therefore, the condition for freeze-out is

$$\left(\frac{45}{\pi}G\right)^{-1/2}\frac{g_*^{1/2}m}{x^2}\langle\sigma v_{\text{Møl}}\rangle Y_{eq}\delta(\delta+2) = -\frac{d(\ln Y_{eq})}{dx} \quad . \tag{3.127}$$

Inserting eq. (3.125) into the last equation yields the transcendental equation

$$\left(\frac{45}{\pi}G\right)^{-1/2}\frac{45g}{4\pi^4}\frac{K_2(x)}{g_s(m/x)}g_*^{1/2}m\langle\sigma v_{\text{Møl}}\rangle\delta(\delta+2) = \frac{K_1(x)}{K_2(x)} - \frac{1}{x}\frac{d(\ln g_s(T))}{d(\ln T)} \quad , \tag{3.128}$$

which must be solved for $x = x_f$. $K_1(x)$ and $K_2(x)$ are the first and second order modified Bessel functions of the second kind, respectively.Comparing the approximate results with those of the numerical integration for several cross sections, we found that $\delta = 1.5$ is a good choice. (coinciding with the choice of ref. [96]).

As the next step, we go back to eq. (3.123). After the decoupling, we can neglect Y_{eq} in that equation and integrate from T_f to T_0. We obtain

$$\frac{1}{Y_0} = \frac{1}{Y_f} + \left(\frac{45}{\pi}G\right)^{-1/2}\int_{T_0}^{T_f} g_*^{1/2}\langle\sigma v_{\text{Møl}}\rangle dT \quad . \tag{3.129}$$

With these steps done, we have the complete solution for the approximate density equation after freeze-out. Since T_0 is very small[6], one may replace it by zero in eq. (3.129), because the integrand does not behave in an abrupt way (extremely high derivatives) between 0 GeV and 10^{-13} GeV. By knowing Y_0, we can use eq. (3.124) to evaluate Ωh^2.

Another more strict approximation towards the calculation of Y_0. Neglecting variations, with temperature, in g_s, the non-relativistic limit ($x \gg 1$) of the condition for freeze-out, eq. (3.128), is

$$\left(\frac{45}{\pi}G\right)^{-1/2} \frac{45g}{4\sqrt{2}\pi^4} \frac{\pi^{1/2}x^{-1/2}e^{-x}}{g_s(T)} g_\rho^{1/2} m\langle\sigma v_{\text{Møl}}\rangle\delta(\delta+2) = 1 \quad . \tag{3.130}$$

Neglecting Y_f in eq. (3.129), which is sometimes unjustified because $1/Y_f$ is necessary for good approximation to Y_0 (within a few percent)[7], we reach

$$\Omega h^2 = 8.7661 \times 10^{-11}\ \text{GeV}^{-2} \left[\overline{g_\rho}^{1/2} \int_{T_0}^{T_f} \langle\sigma v_{\text{Møl}}\rangle \frac{dT}{m}\right]^{-1} \quad , \tag{3.131}$$

where $\overline{g_\rho}^{1/2}$ is a typical value of $g_\rho^{1/2}(T)$ between T_0 and T_f.

Of course we can perform a variation on the calculations, exact or approximated, that is, we can change $\langle\sigma v_{\text{Møl}}\rangle$ by $\langle\sigma v_{\text{Møl}}\rangle_{n.r.}$, or also expand either in a series for x^{-1}, following the method described in section 3.5.

3.7 An example: How Boltzmann equation works

For enlightenment, we now perform an example of numerical computation regarding the decoupling of an species from the plasma, which is in thermal equilibrium. For this task, we assume an effective interaction Lagrangian, for this species, of the kind

$$\mathcal{L}_{\text{eff}} = \frac{\lambda}{4}\chi^2\phi^2 \quad , \tag{3.132}$$

where χ is a real scalar field representing the particle which decouples at some time, or some $x_f = m_\chi/T_f$, and ϕ is some Standard Model real scalar field. First, we need to find an expression for the cross section of this process. Up to tree-level Feynman diagrams, we have just a vertex diagram. Thus, we reach

$$i\,M = -i\,\lambda \quad , \tag{3.133}$$

and for cross section,

$$\left(\frac{d\sigma}{d\Omega}\right)_{CM} = \frac{|M|^2}{64\pi^2 s}\left(\frac{\xi_{34}}{\xi_{12}}\right) \quad , \tag{3.134}$$

[6] $T_0 = 2.7\ \text{K} \rightarrow \text{Natural Units} \rightarrow 2.7 \times \left(8.62 \times 10^{-14}\ \text{GeV}\right) = 2.33 \times 10^{-13}\ \text{GeV}$.

[7] However, for not so fine calculations - as the ones that will be done by the second part of this work which are a first approach of this formalism to the B-L Model that will be analyzed later - , this is reasonable in order to save time with the numerical evaluations.

where

$$\xi_{ij} = \sqrt{s-(m_i+m_j)^2}\sqrt{s-(m_i-m_j)^2} \quad . \tag{3.135}$$

Then, we have

$$\sigma_{\chi\phi} = \frac{|\lambda|^2}{16\pi s}\left(\frac{\sqrt{s-4m_\phi^2}}{\sqrt{s-4m_\chi^2}}\right) \quad . \tag{3.136}$$

Next, we must calculate $\langle\sigma v_{\text{Møl}}\rangle$ (eq.(3.108))in order to describe the evolution of $Y = n_\chi/s$ as in eq. (3.123). We may, of course, use the expansion of $\langle\sigma v_{\text{Møl}}\rangle$ in powers of x (eq.(3.109)), as well as the non-relativistic $\langle\sigma v_{\text{Møl}}\rangle_{\text{n.r.}}$ (eq.(3.110)) and respective expansion (eq.(3.112)).

We are going to numerically calculate Y from the Boltzmann equation for $Y = n_\chi/s$,

$$\frac{dY}{dx} = -\frac{m}{x^2}\frac{\left(\frac{1}{3}g_s' m x^{-1} + g_s\right)}{\left(\frac{45}{\pi}G g_\rho\right)^{1/2}}\langle\sigma v_{\text{Møl}}\rangle\left(Y^2 - Y_{eq}^2\right) \quad , \tag{3.137}$$

using the expansion of $\langle\sigma v_{\text{Møl}}\rangle_{\text{n.r.}}$, since there are no resonances.

What comes in the figure 7 is a plot of the evolution of Y with $x = m_\chi/T$.

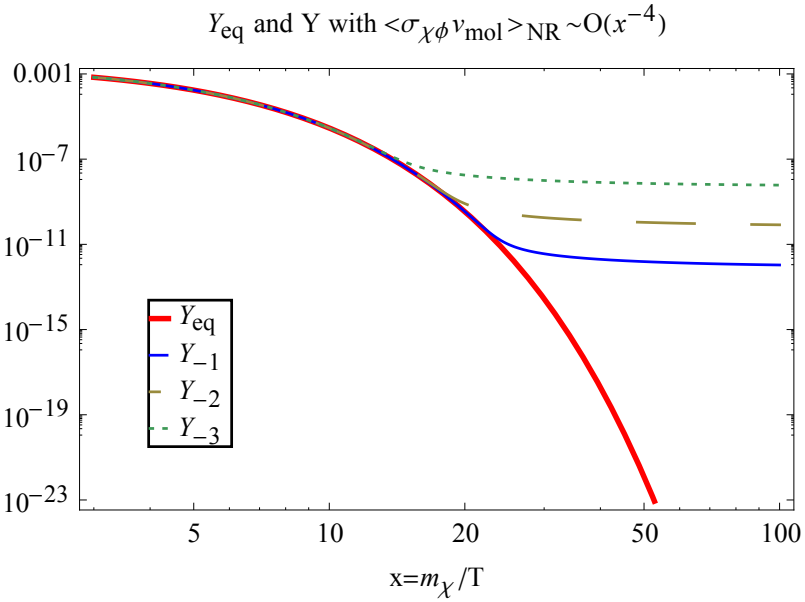

Figure 7 – This figure shows how a nonrelativistic particle decouples. In it, are shown the equilibrium distribution, Y_{eq}; numerical solutions for $\lambda = 10^{-1}$, Y_{-1}; $\lambda = 10^{-2}$, Y_{-2}; and $\lambda = 10^{-3}$, Y_{-3}. The n.r. particle has mass $m_\chi = 100$ GeV and the scalar particles into which it annihilates have $m_\phi = 0$.

As one can notice, there is an x_f when the particle decouples, i.e., it leaves to interact with the other particles. Before this event, the particle distribution followed the equilibrium one; after it, its distribution - after settling on a value of Y - becomes constant. This behavior can be explained in two ways:

- **Technical way**

  Using the modified Boltzmann equation, 3.119,

$$\frac{dY}{dx} = \frac{1}{3H}\frac{ds}{dx}\left\langle \sigma v_{\text{Møl}} \right\rangle \left(Y^2 - Y_{eq}^2\right) \quad , \tag{3.138}$$

  we may arrange it as

$$\frac{dY}{dx} = -\frac{1}{H}\left[-\frac{1}{3}\frac{ds}{dx}\left\langle \sigma v_{\text{Møl}} \right\rangle\right]\left(Y^2 - Y_{eq}^2\right) \equiv -\frac{\Gamma}{H}\left(Y^2 - Y_{eq}^2\right) \quad . \tag{3.139}$$

  Notice that $\Gamma > 0$ because $ds/dx < 0$. The function Γ can be called "interaction rate"[8] at which pertinent relic particles collide, because it contains $\langle \sigma v_{\text{Møl}} \rangle$. The term Γ/H tells us the time around which the decoupling of the relic particle occurs.

  Said that, we may probe how some particle evolves in time and eventually decouples from the initial plasma considering two extreme regimes, in the perspective of the evolution of the eq.3.139:

  - $\Gamma \gg H$. This regime will be analyzed in three steps. First, we begin at $x = x_0$, where $Y = Y_{eq}$, therefore it yields $dY/dx = 0$. At the next step, $x = x_1 > x_0$, Y hasn't changed and Y_{eq} has evolved as $\sim x^2 K_2(x)$[9]. Therefore, $Y > Y_{eq}$ and consequently $dY/dx \ll 0$. Finally, at $x = x_2 > x_1 > x_0$, Y has changed in order to follow the behavior of Y_{eq}, which is decreasing and now Y may be either $> Y_{eq}$ or $< Y_{eq}$. If $Y > Y_{eq}$ still, $dY/dx \ll 0$ will try to bring Y close to Y_{eq}; if $Y < Y_{eq}$ instead, $dY/dx \gg 0$ will try to bring Y close to Y_{eq}. The steps go on following this pattern in which Y follows Y_{eq} until the regime $\Gamma \gg H$ is no longer valid.

  - $\Gamma \ll H$. For the analysis of this regime, also three steps are detailed. First, we begin at $x = x_0$, where $Y = Y_{eq}$, therefore it yields $dY/dx = 0$. At the following step, $x = x_1 > x_0$, Y hasn't changed and Y_{eq} has evolved as $\sim x^2 K_2(x)$. Hence, $Y > Y_{eq}$, but since $\Gamma/H \approx 0$, it yields $dY/dx \approx 0$. Finally, at $x = x_2 > x_1 > x_0$, Y hasn't changed largely enough to follow Y_{eq}. As the steps succeed, and x increases, Y_{eq} goes to zero and Y essentially becomes constant after some iterations, since $dY/dx \approx 0$.

  In summary, if for some x, $\Gamma \ll H$, the decoupling is about to happen, however if $\Gamma \gg H$, the particle distribution follows th one of equilibrium and its decoupling does not happen.

[8] Some authors don't define it mathematically as we did for Γ, and just introduce it as the interaction rate at which particles collide, as we do below for R_{int}. With R_{int}, also one is able to estimate when particles decouple, when comparing R_{int} to the expansion rate H.

[9] See eq.3.125. The function $x^2 K_2(x)$ decreases as x increases.

Nevertheless, in realistic simulations, the particle decouples when $\Gamma < H$ simply and the condition $\Gamma \ll H$ may be satisfied only after decoupling, therefore the complete treatment - taking into account regimes between the two described above - is necessary and must be done via Boltzmann equation.

- **Physical way**

  From the physical point of view, a particle decouples from the primordial plasma when its interaction rate, which we will call R_{int}[10], becomes smaller than the expansion rate H. When this happens, the interactions are not fast enough to maintain chemical and thermal equilibrium[11] and the particle decouples. Thus, the relation

$$R_{int} \sim H \tag{3.140}$$

  gives us the decoupling condition.

  We may understand the above relation in another way. We will consider the mean free path of the particle as R_{int}^{-1}. Since the particle horizon in a radiation-dominated Universe (see ref.[97], eq.(16.123) within) is given by H^{-1}, when $R_{int} \lesssim H$, the mean free path becomes larger than the particle horizon, leading to decoupling due to the lack of collisions.

Done this background on decoupling, we can surely say that the solutions in the last figure correspond to what has been explained above: the highest cross section $\sigma_{\chi\phi}$ (interaction rate), $\lambda = 10^{-1}$, corresponds to the solution which shows the highest x_f, and therefore decouples at the latest time; and the lowest $\sigma_{\chi\phi}$ represents the solution which shows the lowest x_f, and therefore decouples at the earliest time.

[10] In the literature R_{int} is often defined with the Greek letter Γ, but in this case, since we have already used it in order to elucidate the technical way to the understanding of decoupling, we prefer not to use it again, since the two are not equal a priori (Γ does not take into account just $\langle\sigma v_{\text{Møl}}\rangle$, but also ds/dx). However, they are connected via cross section, therefore it makes sense to call them with the term *interaction rate*.

[11] For the process $A + B \leftrightarrows C + D$, chemical equilibrium means $\mu_A + \mu_B = \mu_C + \mu_D$. Thermal equilibrium means $T_\chi = T_\gamma$, where T_χ is the particle species temperature and T_γ is the plasma temperature.

4 Detection of Dark Matter

This chapter is dedicated to the overview of experiments which are the basis for eliminating some models which include possible candidates for dark matter; also some theoretical tools will be provided. In our case, these experiments will be important to the constraint of some free parameters which are present in our model. Direct and indirect detection experiments are explained next.

4.1 Direct detection of Dark Matter

Although WIMPS are only weakly coupled to baryons, they can occasionally scatter elastically off atomic nuclei. Several experiments [98] try to look for possible direct detection signals. Examples of such experiments are:

- **LUX** (**L**arge **U**nderground **X**enon) **experiment**

  LUX uses as its target 368 kilograms of liquefied ultra-pure xenon, which is a scintillator: interactions inside the xenon will create an amount of light proportional to the amount of energy deposited. That light can be collected on arrays of light detectors sensitive to a single photon, providing the LUX detector a low enough energy threshold to stand a good chance of detecting the tiny bump of a dark matter particle with an atom of xenon.

  For very rare events such as dark matter detection, the shielding that LUX provides is a necessity. However some backgrounds are harder to shield against, for example cosmic rays. These very high energy, charged subatomic particles are extremely penetrating and kilometers of material between them and the detector are put for diminishing the flux of these particles. Also, because xenon is three times denser than water, it can stop a lot of the radiation originating from outside the detector before it can reach the very center.

- **CDMS** (**C**ryogenic **D**ark **M**atter **S**earch)

  It uses cryogenic germanium detectors to search for direct interactions of WIMPs with ordinary matter. The detectors are operated at a temperature of ~ 40 mK. At this temperature a WIMP interaction would cause a measurable (even though tiny) increase in temperature. The thermal signal from an interaction is used to determine the energy deposited.

  The CDMS detectors are germanium disks with a diameter of 3 inches and a thickness of 1 cm (~ 250 g each). If some WIMP comes and shocks with some nucleus of

the germanium crystal, it will cause a recoil on the former one and as a consequence this deposited energy of it can be described as phonons going through the crystal. How can one measure phonons? Well, there is a thermal sensor (also called phonon sensor) that works in the following way. It is a superconducting thin film at the crystal (germanium) surface. At the critical temperature (below which the superconductor loses its electrical resistance), the electrical resistance shows a very strong dependence on the temperature. This way, if the film is reached by the phonons, these transfer their energy to it and if some current is present in the film, one is able to notice the occurence of initial collision events on the germanium crystal[1].

The CDMS experiment takes place in the Soudan Underground Laboratory to reduce the background from cosmic radiation.

- **PICASSO** (**P**roject **I**n **CA**nada to **S**earch for **S**upersymmetric **O**bjects)

  The sensitive material of PICASSO detectors are millions of tiny droplets (diameter of $50 - 100\ \mu m$) of a superheated liquid (C_4F_{10}) in a polymerized or viscous medium. A superheated liquid is a liquid heated well above its boiling point. Such a liquid is extremely unstable, since any slight perturbation will trigger an explosive transformation of the liquid into vapor.

  If a dark matter particle, not necessarily a supersymmetric one, hits a nucleus, e.g. a F-atom, in a tiny superheated droplet, the atom recoils and deposits its energy in a heat spike - proto-bubble which grows violently - which in turn triggers a phase transition, liquid into gas, over the entire initial bubble.

In summary, the direct detection experiments try to measure the recoil energies of nuclei, which are the result from interactions. The energies involved are estimated to be of order 10 keV, which is well below the typical nuclear energy scales, therefore the non-relativistic limit ($v \ll c$) may be taken within the calculations. The magnitude of the WIMP-nucleus scattering cross section is sensitive to the exact form of the interactions of the dark matter particle with the individual nucleons. Because of that, we need to distinguish spin-dependent from spin-independent interactions for the experimental data are separated into these two classes.

For spin-dependent interactions, the scattering amplitude changes sign with spin direction so that, although the interaction with a nucleus is still coherent - in the sense that the scattering amplitudes are summed - paired (null total spin) nucleons contribute zero to the full scattering amplitude and only the residual unpaired (non-null total spin) nucleons contribute. Thus only nuclei with an odd number of protons plus neutrons can probe spin-dependent interactions. For spin-independent interactions, all the partial scattering amplitudes (related to each nucleon) are summed no matter the pairing of nuclear spins. The three collaborations above probe these two types of interactions.

[1] I won't go into the details of the origin of the current inside the film.

Below, we classify the interactions [99], relevant to direct detection, for complex scalar dark matter ϕ in the low velocity regime (because we consider cold dark matter):

- **Vector-vector** interaction. $\phi^\dagger \overleftrightarrow{\partial_\mu} \phi \bar{q}\gamma^\mu q \approx 2m\phi^\dagger \overleftrightarrow{\partial_\mu} \phi \left[a^\dagger a + b^\dagger b\right] \delta^{\mu 0}$ is spin-independent because no spin operators appear inside of it;

- **Vector-axial vector** interaction. $\phi^\dagger \overleftrightarrow{\partial_\mu} \phi \bar{q}\gamma^\mu\gamma_5 q \approx 2m\phi^\dagger \overleftrightarrow{\partial_\mu} \phi \left[a^\dagger a \left(\xi^\dagger \sigma^i \xi\right) + b^\dagger b \left(\eta^\dagger \sigma^i \eta\right)\right] \delta^{\mu i}$ is spin-dependent because σ^i are spin operators;

- **Scalar-pseudoscalar** interaction. $\phi^\dagger \phi \bar{q}\gamma_5 q \approx \phi^\dagger \phi \times 0 = 0$ is spin-independent for it is null in this limit;

- **Scalar-scalar** interaction. $\phi^\dagger \phi \bar{q} q \approx 2m\phi^\dagger \phi \left[a^\dagger a + b^\dagger b\right]$ is spin-independent for the same reason as in the first item,

where q represents a quark field; γ^μ is a dirac matrix; and $\sigma^{\mu\nu} = \frac{i}{2}\left[\gamma^\mu, \gamma^\nu\right]$.

The scalar and vector bilinears just yield the number operator. Therefore, when these operators are evaluated in the nuclear state, they add coherently. The axial-vector on the other hand yields the spin-operator, and hence couple to the net spin of the nucleus. The sum over the entire nucleus for the two cases is given in Ref. [99].

There are no bilinear tensor terms, i.e. tensor interactions in the spinor part, because interactions of the type $\phi^\dagger \partial_\mu \partial_\nu (\phi)\, \bar{q}\sigma^{\mu\nu} q$ (two derivatives coupled to a totally antisymmetric tensor) are zero. Even if the operation of the derivatives was different, like $\partial_\mu \phi^\dagger \partial_\nu \phi$ or $\partial_\mu \partial_\nu \left(\phi^\dagger\right) \phi$, the result would be null. (Because of hermiticity of the Lagrangian, the last term is zero. It can be shown that the hermitian conjugate of it is minus it, therefore it must be zero since the beginning.)

Since the experiments try to identify direct detections, their results are expressed via the data concerning cross section and WIMP mass values (essentially WIMP energy values). For better understanding, the figure 4.1.1 is drawn with results from the experiments briefly described above. It is better understood if one reads the following section.

4.1.1 Theoretical description

In order to describe direct detection of WIMPs against nuclei theoretically, we need to introduce some tools.

First of all, we need to identify, in the model described in the chapter 5, the effective couplings which would yield interactions between the dark matter and the nuclei (quarks). As will be seen in that chapter, the only effective coupling will be due to the Higgs propagator, i.e., its form will be given by

$$\phi^\dagger_{DM} \phi_{DM} \bar{q} q \tag{4.1}$$

because of the couplings $\phi^{\dagger}_{DM}\phi_{DM}H$ and $H\bar{q}q$. Since the interaction between dark matter and nuclei is of the scalar-scalar kind, it is spin-independent in the non-relativistic limit.

We show now the dark matter-nucleus cross section for spin-independent elastic scattering, see Ref. [99] for a greater understanding,

$$\sigma_{\chi N} = \frac{4}{\pi}\frac{m_N^2 M_\chi^2}{(m_N + M_\chi)^2}\left[(A-Z)f_n + Z f_p\right]^2 \quad , \tag{4.2}$$

where A and Z are the mass and the atomic numbers of the target nuclei, respectively. For example, xenon has $Z = 54$ and $A = 131$. m_N is the nucleon mass which is equal to $m_p \simeq 938.27$ GeV for the proton and $m_n \simeq 939.57$ GeV for the neutron.

The effective coupling to neutrons and protons, $f_{p,n}$, can be written in terms of the dark matter's couplings to quarks. In the case of a scalar interaction,

$$f_{p,n} = \sum_{q=u,d,s}\frac{G_q}{\sqrt{2}} f_{Tq}^{(p,n)}\frac{m_{p,n}}{m_q} + \frac{2}{27} f_{TG}^{(p,n)}\sum_{q=c,b,t}\frac{G_q}{\sqrt{2}}\frac{m_{p,n}}{m_q} \quad , \tag{4.3}$$

where G_q denotes the dark matter's effective Fermi coupling for a given quark species. The first term reflects scattering with light quarks, while the second term accounts for interactions with gluons through a heavy quark loop. The values of $f_{Tq}^{(p,n)}$ have been measured to be (only average values exposed here)

$$\begin{aligned}
f_{Tu}^p = 0.020,\ f_{Td}^p = 0.026,\ f_{Ts}^p = 0.118 \rightarrow \sum_{q-u,d,s} f_{Tq}^p = 0.164 \quad , \\
f_{Tu}^n = 0.014,\ f_{Td}^n = 0.036,\ f_{Ts}^n = 0.118 \rightarrow \sum_{q-u,d,s} f_{Tq}^n = 0.168 \quad , \\
f_{TG}^p = 1 - \sum_{q-u,d,s} f_{Tq}^p = 0.836, \text{ and, } f_{TG}^n = 1 - \sum_{q=u,d,s} f_{Tq}^n = 0.832 \quad ,
\end{aligned} \tag{4.4}$$

where $f_{TG}^{(p,n)}$ is related to the gluons and is given by $f_{TG}^{(p,n)} = 1 - \sum\limits_{q=u,d,s} f_{Tq}^{(p,n)}$, which is approximately 0.84 and 0.83 for protons and neutrons, respectively.

The effective Fermi coupling for a given quark species is given by

$$\begin{aligned}
G_q &= \frac{C_{DM^2H}\times C_{H\bar{q}q}}{m_H^2} = \\
&= \frac{C_{DM^2H}}{m_H^2}\times\frac{m_q}{V_H} = \frac{C_{DM^2H}}{V_H\times m_H^2}\times m_q \equiv G_0 \times m_q \quad ,
\end{aligned} \tag{4.5}$$

where C_{DM^2H} is the coupling related to the term $\phi^{\dagger}_{DM}\phi_{DM}H$ and $C_{H\bar{q}q}$ to $H\bar{q}q$. Therefore, we can simplify $f_{p,n}$ as follows

$$
\begin{aligned}
f_{p,n} &= \frac{G_0 m_{p,n}}{\sqrt{2}} \sum_{q=u,d,s} f_{Tq}^{(p,n)} + \frac{2}{27} f_{TG}^{(p,n)} \frac{G_0 m_{p,n}}{\sqrt{2}} \sum_{q=c,b,t} 1 \\
&= \frac{G_0 m_{p,n}}{\sqrt{2}} \left\{ \sum_{q=u,d,s} f_{Tq}^{(p,n)} + \frac{2}{9} f_{TG}^{(p,n)} \right\} \\
&= \frac{G_0 m_{p,n}}{\sqrt{2}} \left\{ \sum_{q=u,d,s} f_{Tq}^{(p,n)} + \frac{2}{9} \left(1 - \sum_{q=u,d,s} f_{Tq}^{(p,n)} \right) \right\} \\
&= \frac{G_0 m_{p,n}}{\sqrt{2}} \left\{ \left(1 - \frac{2}{9} \right) \sum_{q=u,d,s} f_{Tq}^{(p,n)} + \frac{2}{9} \right\} \\
&= \frac{G_0 m_{p,n}}{9\sqrt{2}} \left\{ 2 + 7 \sum_{q=u,d,s} f_{Tq}^{(p,n)} \right\} \quad .
\end{aligned}
\tag{4.6}
$$

Since $\sum_{q=u,d,s} f_{Tq}^{p} \simeq \sum_{q=u,d,s} f_{Tq}^{n}$, consequently $f_p \simeq f_n$ and we can write in an approximate form

$$
\begin{aligned}
\sigma_{\chi N} &= \frac{4}{\pi} \frac{m_N^2 M_\chi^2}{(m_N + M_\chi)^2} \left[(A - Z) f_n + Z f_p \right]^2 \\
&\simeq \frac{4}{\pi} \frac{m_N^2 M_\chi^2}{(m_N + M_\chi)^2} A^2 f_p^2 \quad .
\end{aligned}
\tag{4.7}
$$

Hence, we may define the cross section per nucleon

$$
\sigma_{\chi,p} \equiv \frac{\sigma_{\chi N}}{A^2} = \frac{4}{\pi} \frac{m_N^2 M_\chi^2}{(m_N + M_\chi)^2} f_p^2 \quad , \tag{4.8}
$$

with

$$
\begin{aligned}
f_p &= \frac{G_0 m_p}{9\sqrt{2}} \left\{ 2 + 7 \sum_{q=u,d,s} f_{Tq}^{p} \right\} \\
f_p &\simeq \frac{938 \times 10^{-3}}{9\sqrt{2}} \left\{ 2 + 7 \times 0.164 \right\} \times G_0 \\
f_p &\simeq 0.23 \times G_0 \ \mathrm{GeV}^{-1} \quad .
\end{aligned}
\tag{4.9}
$$

Now, substituing the value of f_p above, it yields

$$
\begin{aligned}
\sigma_{\chi,p} &= \frac{4}{\pi} \frac{m_N^2 M_\chi^2}{(m_N + M_\chi)^2} f_p^2 \\
&\simeq 0.07 \times \frac{m_N^2 M_\chi^2}{(m_N + M_\chi)^2} G_0^2 \ \mathrm{GeV}^{-2} \quad .
\end{aligned}
\tag{4.10}
$$

Now, using the conversion factors

$$1 \text{ pbarn} = 10^{-36} \text{ cm}^2 = 2.5681 \times 10^{-9} \text{ GeV}^{-2} \quad , \tag{4.11}$$

we have

$$\begin{aligned} \sigma_{\chi,p} &\simeq \frac{0.07}{2.5681 \times 10^{-9}} \times \frac{m_N^2 M_\chi^2}{(m_N + M_\chi)^2} G_0^2 \text{ pbarn} \\ &\simeq 2.7 \times 10^7 \frac{m_N^2 M_\chi^2}{(m_N + M_\chi)^2} G_0^2 \text{ pbarn} \quad . \end{aligned} \tag{4.12}$$

Thus, in the end, we have the cross section per nucleon dependent on the coupling G_0 which is dependent on the coupling C_{DM^2H}. Therefore, the direct detection experiments will constrain the latter in a way that the cross section per nucleon will be below the limits set by them.

In the chapter 5, we do this kind of analysis via the most stringent data on spin-independent interactions.

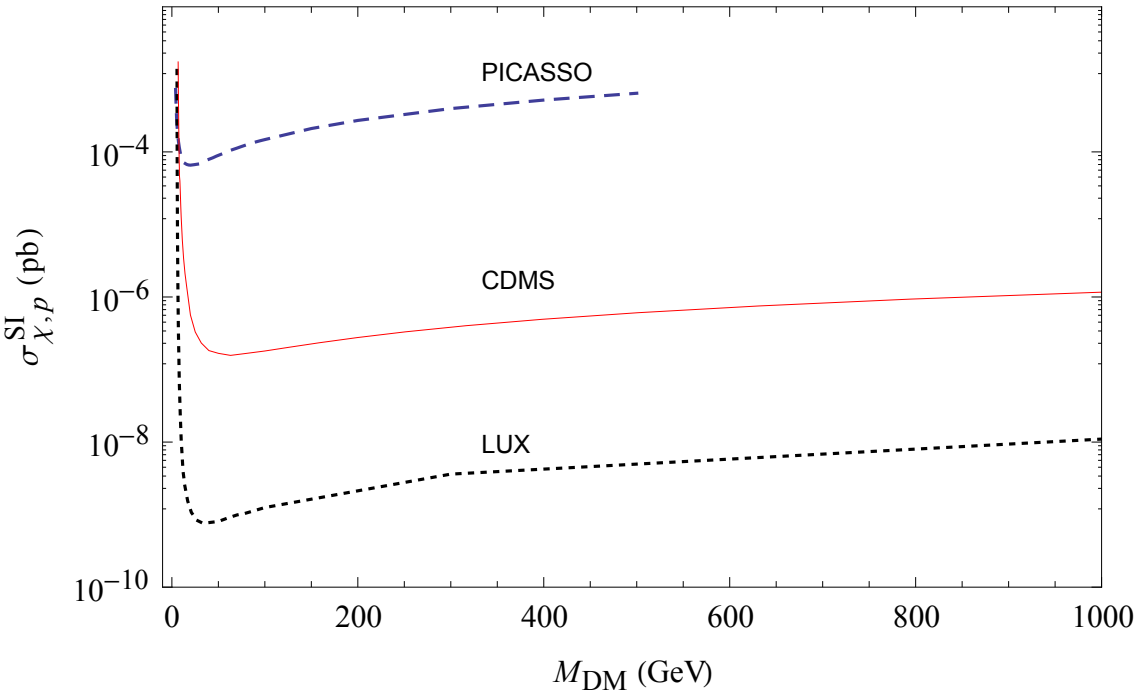

Figure 8 – Spin-independent limits from PICASSO ([100]), LUX ([101]) and CDMS ([102]) experiments. Data courtesy of [103].

4.2 Indirect detection of Dark Matter

The philosophy behind indirect detection of dark matter consists in detecting the signatures of the annihilations or decays of dark matter particles in the fluxes of cosmic rays, for

example: charged particles (electrons and postirons, protons and antiprotons, deuterium and antideuterium), photons (radio to gamma rays, synchroton radiation), neutrinos.[2]

We must know that the pertinent experiments look for channels and ranges of energy where it is possible to distinguish the background from usual astrophysical processes. Note for instance that searches for antiparticles (positrons, antiprotons, antideuterons) are "cleaner" because they are much less abundant in the Universe than the corresponding particles. We won't detail the process for obtaining data in each case, but references will be given:

- Neutrinos (DMν). Large neutrino detectors such as IMB [104], Kamiokande [105], Baksan [106], Macro [107], Super-Kamiokande [108], AMANDA [109] and BAIKAL [110] already obtained constraints on DMν fluxes.

- Charged particles. Results have already been obtained with PAMELA [111], Fermi-LAT [112] and AMS [113] (all related to positron measurements).

- Photons. Currently, the most productive observatory for dark-matter related publications with a focus on gamma-ray observations is the Fermi-LAT with currently $\sim$200 such refereed publications. A recent one is ref. [114].

[2] Also classified into the category of indirect detection, the measurements made by PLANCK, WMAP, and COBE satellites probe the anisotropies of the CMB (Cosmic Microwave Background). Through the detailed study of them, it is then possible to determine the amount of energy density of the Universe which is contained in the form of dark matter. This kind of measurement won't be detailed here because it has been already explained in the section 2.1. Later, in the last chapter, this kind of indirect detection of dark matter will impose constraints to our particular B-L model of particles.

5 Scalar Dark Matter in a B-L Model

In this chapter, we are going to verify if one particular B-L Model can contain a possible candidate for dark matter, respecting certain conditions explained in the first and second sections below. For this task, we first review some general features of the B-L Model we are going to deal with; later we display the vacuum structure and the scalar sector spectrum, characterizing this way the dark matter candidate; next, we handle the gauge bosons; and in the end we analyze the constraints imposed on this model via current direct detection experiments on dark matter. The content of this chapter is in the Ref. [115], still to be published.

5.1 Brief review of the $B - L$ model

We briefly summarize here the model in Refs. [116, 117]. It is an extension of the SM based on the gauge symmetry $SU(2)_L \otimes U(1)_{Y'} \otimes U(1)_{B-L}$ where B and L are the usual baryonic and leptonic numbers, respectively, and Y' is a new charge different from the hypercharge Y of the SM. The values of Y' are chosen to obtain the hypercharge Y through the relation $Y = [Y' + (B - L)]$, after the first spontaneous symmetry breaking. Assuming a generation-independent charge assignment, the non-existence of mirror fermions and restricting ourselves to integer quantum numbers for the Y' charge, the anomaly cancellation constrains the number of right-handed neutrinos, $n_R \geq 3$ [116]. Considering $n_R = 3$, there is an exotic charge assignment for the Y' charge where $Y'_{n_{R1},n_{R2}} = -4$ and $Y'_{n_{R3}} = 5$ besides the usual one where $Y'_{n_{Ri}} = 1$ with $i = 1, 2, 3$. The model under consideration has that exotic Y' charge assignment. The respective fermionic charge assignment of the model is shown in Table 1.

Fermion	I_3	I	Q	Y'	$B - L$
ν_{eL}, e_L	$1/2, -1/2$	$1/2$	$0, -1$	0	-1
e_R	0	0	-1	-1	-1
u_L, d_L	$1/2, -1/2$	$1/2$	$2/3, -1/3$	0	$1/3$
u_R	0	0	$2/3$	1	$1/3$
d_R	0	0	$-1/3$	-1	$1/3$
n_{1R}, n_{2R}	0	0	0	4	-4
n_{3R}	0	0	0	-5	5

Table 1 – Quantum number assignment for the fermionic fields.

In the scalar sector the model has three $SU(2)_L$ doublets, H, Φ_1, Φ_2, and four $SU(2)_L$ singlets, ϕ_1, ϕ_2, ϕ_3, ϕ_X. The scalar charge assignments are shown in Table 2. The H doublet is introduced to give mass to the lighter massive neutral vector boson $Z_{1\mu}$, the charged vector bosons $W^{\pm}_{\mu}$, and the charged fermions, as in the SM. Besides giving mass to the extra neutral vector boson $Z_{2\mu}$, which is expected to be heavier than $Z_{1\mu}$, the other scalars are mainly motivated to generate mass for both the left and the right handed neutrinos. In order to be more specific, the other Φ_1 and Φ_2 doublets are introduced to give Dirac mass terms at tree level through the renormalizable Yukawa interactions $\mathcal{D}_{im}\overline{L}_{Li}n_{Rm}\Phi_1$ and $\mathcal{D}_{i3}\overline{L}_{Li}n_{R3}\Phi_2$ in the Lagrangian. The ϕ_1, ϕ_2 and ϕ_3 singlets are introduced to generate Majorana mass terms at tree level ($\mathcal{M}_{mn}\overline{(n_{Rm})^c}n_{Rn}\phi_1$, $\mathcal{M}_{33}\overline{(n_{R3})^c}n_{R3}\phi_2$, $\mathcal{M}_{m3}\overline{(n_{Rm})^c}n_{R3}\phi_3$). Finally, the ϕ_X singlet is introduced to avoid dangerous Majorons when the symmetry is broken down as shown in Ref. [117]. These extra scalars allow the model to implement a seesaw mechanism at $\mathcal{O}$ (TeV) energy scale, and the observed mass-squared differences of the neutrino are obtained without resorting to fine-tuning the neutrino Yukawa couplings [117]. Other studies about the possibility that the model accommodates different patterns for the neutrino mass matrix using discrete symmetries (S_3, A_4) together with the SM ones have been done [118, 119].

Scalar	I_3	I	Q	Y'	$B-L$
$H^{0,+}$	$\mp 1/2$	$1/2$	$0,1$	1	0
$\Phi_1^{0,-}$	$\pm 1/2$	$1/2$	$0,-1$	-4	3
$\Phi_2^{0,-}$	$\pm 1/2$	$1/2$	$0,-1$	5	-6
ϕ_1	0	0	0	-8	8
ϕ_2	0	0	0	10	-10
ϕ_3	0	0	0	1	-1
$\phi_{\rm X}$	0	0	0	3	-3

Table 2 – Quantum number assignment for the scalar fields.

With the above matter content we can write the most general Yukawa Lagrangian respecting the gauge invariance as follows

$$\begin{aligned} -\mathcal{L}_{\rm Y} &= Y_i^{(l)}\overline{L}_{Li}e_{Ri}H + Y_{ij}^{(d)}\overline{Q}_{Li}d_{Rj}H + Y_{ij}^{(u)}\overline{Q}_{Li}u_{Rj}\widetilde{H} + \mathcal{D}_{im}\overline{L}_{Li}n_{Rm}\Phi_1 + \mathcal{D}_{i3}\overline{L}_{Li}n_{R3}\Phi_2 \\ &\quad + \mathcal{M}_{mn}\overline{(n_{Rm})^c}n_{Rn}\phi_1 + \mathcal{M}_{33}\overline{(n_{R3})^c}n_{R3}\phi_2 + \mathcal{M}_{m3}\overline{(n_{Rm})^c}n_{R3}\phi_3 + \text{H.c.}, \end{aligned} \tag{5.1}$$

where $i,j = 1,2,3$ are lepton/quark family numbers; $m,n = 1,2$, and $\widetilde{H} = i\tau_2 H^*$ (τ_2 is the Pauli matrix). Also, we have omitted summation symbols over repeated indices.

Finally, the most general renormalizable scalar potential obtained by the addition of

all these above mentioned scalar fields is given by

$$
\begin{aligned}
V_{B-L} \;=\; & -\mu_H^2 H^\dagger H + \lambda_H \left|H^\dagger H\right|^2 - \mu_{11}^2 \Phi_1^\dagger \Phi_1 + \lambda_{11} \left|\Phi_1^\dagger \Phi_1\right|^2 - \mu_{22}^2 \Phi_2^\dagger \Phi_2 + \lambda_{22} \left|\Phi_2^\dagger \Phi_2\right|^2 \\
& -\mu_{s\alpha}^2 \left|\phi_\alpha\right|^2 + \lambda_{s\alpha} \left|\phi_\alpha^* \phi_\alpha\right|^2 + \lambda_{12} \left|\Phi_1\right|^2 \left|\Phi_2\right|^2 + \lambda'_{12} (\Phi_1^\dagger \Phi_2)(\Phi_2^\dagger \Phi_1) + \Lambda_{H\gamma} \left|H\right|^2 \left|\Phi_\gamma\right|^2 \\
& +\Lambda'_{H\gamma} (H^\dagger \Phi_\gamma)(\Phi_\gamma^\dagger H) + \Lambda_{Hs\alpha} \left|H\right|^2 \left|\phi_\alpha\right|^2 + \Lambda'_{\gamma\alpha} \left|\Phi_\gamma\right|^2 \left|\phi_\alpha\right|^2 + \Delta_{\alpha\beta} (\phi_\alpha^* \phi_\alpha)(\phi_\beta^* \phi_\beta) \\
& + \Big[\beta_{123} \phi_1 \phi_2 (\phi_3^*)^2 + \Phi_1^\dagger \Phi_2 (\beta_{13} \phi_1 \phi_3^* + \beta_{23} \phi_2^* \phi_3) - i\kappa_{H1X} \Phi_1^T \tau_2 H \phi_X \\
& -i\kappa_{H2X} (\Phi_2^T \tau_2 H)(\phi_X^*)^2 + \beta_X (\phi_X^* \phi_1)(\phi_2 \phi_3) + \beta_{3X} (\phi_X^* \phi_3^3) + \text{H.c.}\Big] \,, \qquad (5.2)
\end{aligned}
$$

where $\gamma = 1, 2$; $\alpha, \beta = 1, 2, 3, \text{X}$; and $\alpha \neq \beta$ in the $\Delta_{\alpha\beta}(\phi_\alpha^* \phi_\alpha)(\phi_\beta^* \phi_\beta)$ terms.

5.2 The vacuum structure and the scalar sector spectrum

In general, DM must be stable to provide a relic abundance in agreement with the one measured by WMAP and PLANCK, $\Omega_{\text{DM}} h^2 = 0.1199 \pm 0.0027$ [8, 9]. Although the DM stability could result from the extreme smallness of its couplings to ordinary particles, we restrict ourselves to search for a discrete, or continuous, symmetry such as Z_2, or $U(1)$, to protect DM candidates to decay. If they decayed, for example, through the channel $DM \to \phi_1 + \phi_2$, which is forbidden due to the Z_2 invariance, where ϕ_i represent whatever SM fields or BSM not yet discovered fields, they would, with reasonable couplings, not be present in satisfactory density in the current Universe.

First, we consider the scalar potential in Eq. 5.2 looking for an accidental symmetry that naturally stabilizes the DM candidate. Doing so, we find that the scalar potential has just the $SU(2) \otimes U(1)_{Y'} \otimes U(1)_{B-L}$ initial symmetry. However, none of these gauge groups can generate a stable neutral scalar when they are spontaneously broken down to $U(1)_Q$. Therefore, we impose a discrete symmetry in the following way: $Z_2(\phi_2) = -\phi_2$ and the other scalar fields being even under this Z_2 symmetry. As a result, the $\beta_{23} \Phi_1^\dagger \Phi_2 \phi_2^* \phi_3$, $\beta_{123} \phi_1 \phi_2 (\phi_3^*)^2$ and $\beta_X (\phi_X^* \phi_1)(\phi_2 \phi_3)$ terms are prohibited from appearing in the scalar potential, Eq. 5.2. Actually, when these terms are eliminated from Eq. 5.2, the true global symmetry in the potential is $SU(2) \otimes U(1)_{Y'} \otimes U(1)_{B-L} \otimes U(1)_\chi$, where the last one is $U(1)_\chi : \phi_2 \to \exp(-i\chi_{\phi_2})\phi_2$, where χ_{ϕ_2} is the ϕ_2 quantum number under the $U(1)_\chi$ symmetry, and the rest of the fields being invariant. It is important to say that we have taken into account the simplicity and some phenomenological criteria to choose the Z_2 symmetry above. For example, if we impose $Z_2(\phi_1) = -\phi_1$ (and the other fields being even), the model has a massless right handed neutrino, say N_R, at tree level. That poses a tension with the experimental data of the invisible Z_μ decay width [120], since $Z_\mu \to \bar{N_R} + N_R$ would be allowed to exist [121]. Other simple choices such as $Z_2(\phi_3) = -\phi_3$ or $Z_2(\phi_X, \Phi_1) = -\phi_X, -\Phi_1$ should be avoided due to the appearance of Majorons, Js, in the scalar spectra. As it is well known, the major challenges to models with Majorons come from the energy loss in stars, through the process $\gamma + e^- \to e^- + J$, and the invisible Z_μ decay width, through $Z_\mu \to RJ \to JJJ$, being R a scalar [122].

For the general case of the scalar potential with the $U(1)_\chi$ symmetry, we have the minimization conditions given in the Appendix A. In general, those conditions lead to different breaking symmetry patterns and to a complex vacuum structure because the scalar potential has several free parameters. In this paper, however, we restrict ourselves to find a (some) viable scalar DM candidate(s) and to study its (their) properties in a relevant subset of the parameter space.

First, we impose the necessary conditions for all real neutral components of the scalar fields, except ϕ_{2R}, to obtain nontrivial vacuum expectation values (VEVs), i.e. $\langle H_R^0\rangle = V_H$, $\langle \Phi_{1R}^0\rangle = V_{\Phi_1}$, $\langle \Phi_{2R}^0\rangle = V_{\Phi_2}$, $\langle \phi_{1R}\rangle = V_{\phi_1}$, $\langle \phi_{2R}\rangle = 0$, $\langle \phi_{3R}\rangle = V_{\phi_3}$, $\langle \phi_{XR}\rangle = V_{\phi_X}$. For the sake of simplicity, we set $V_{\Phi_1} = V_{\Phi_2} = V_\Phi$ and $V_{\phi_1} = V_{\phi_3} = V_{\phi_X} = V_\phi$. Thus, the $U(1)_\chi$ symmetry is not spontaneously broken and the model possesses two neutral stable scalars which are the real (CP-even) and the imaginary (CP-odd) parts of the ϕ_2 field with the same mass given by

$$M_{\rm DM}^2 = \frac{1}{2}\Big[\Lambda_{Hs2}V_{\rm SM}^2 + (\Lambda_{12}^{'} + \Lambda_{22}^{'} - 2\Lambda_{Hs2})V_\Phi^2 + (\Delta_{12}+\Delta_{23}+\Delta_{2X})V_\phi^2 - 2\mu_{s2}^2\Big]; \quad (5.3)$$

where we have defined $V_{\rm SM}^2 \equiv V_H^2 + V_{\Phi_1}^2 + V_{\Phi_2}^2 = V_H^2 + 2V_\Phi^2 = (246)^2$ GeV^2. From here on, we work with $M_{\rm DM}^2$ as an input parameter, thus we solve Eq. 5.4 for μ_{s2}^2

$$\mu_{s2}^2 = \frac{1}{2}\Big[\Lambda_{Hs2}V_{\rm SM}^2 + (\Lambda_{12}^{'} + \Lambda_{22}^{'} - 2\Lambda_{Hs2})V_\Phi^2 + (\Delta_{12}+\Delta_{23}+\Delta_{2X})V_\phi^2 - 2M_{\rm DM}^2\Big]. \quad (5.4)$$

If we allow $\langle\phi_2\rangle \neq 0$, the real part of the ϕ_2 field obtains mass and its imaginary part is massless and stable. In that case, the DM candidate would be the Goldstone boson related to the breakdown of the $U(1)_\chi$ symmetry. In general, such massless DM has severe constraints from the big bang nucleosynthesis [123, 124] and the bullet cluster [125, 126], also massless DM would have a too high *free streaming length*, which would make the down-top structure formation impossible, as said in the section 2.2. Here we do not consider this case.

Also, we work in the context of $\zeta \equiv \frac{V_\Phi}{V_\phi} \ll 1$. This assumption allows us to implement a stable and natural see-saw mechanism for neutrino masses at low energies, as shown in Ref. [117]. Once $V_H^2 + 2V_\Phi^2 = (246)^2$ GeV^2 and V_H is the mainly responsible to give the top quark mass at tree level, we have $V_H^2 \gg V_\Phi^2$. Choosing $V_\phi \sim 1$ TeV and $V_\Phi \sim 1$ MeV, as in Ref. [117], we have that the ζ parameter is $\sim 10^{-6}$.

In general, we solve numerically the minimization conditions, and using standard procedures we construct numerically the mass-squared matrices for the charged, CP-even and CP-odd scalar fields. We choose the parameters in the potential such that they satisfy simultaneously the minimization conditions, the positivity of the squared masses and the lower boundedness of the scalar potential. In order to satisfy this last condition, we choose the parameters such that the quartic terms in the scalar potential are positive

for all directions. Although, all those constraints are checked numerically, let us give an insight into some constraints coming from the minimization conditions and the positivity of the squared masses when we do some simplifying assumption on the parameters. First, we solve the Eqs. A.1 and (A.7) in the limit $\zeta \to 0$. Doing so, we have

$$\mu_H = \pm \sqrt{\lambda_H V_{\rm SM}^2 + \frac{1}{2}(\Lambda_{Hs1} + \Lambda_{Hs3} + \Lambda_{HsX})V_\phi^2} + \mathcal{O}(\zeta); \tag{5.5}$$

$$\kappa_{H1X} = \mathcal{O}(\zeta); \qquad \kappa_{H2X} = \mathcal{O}(\zeta); \tag{5.6}$$

$$\mu_{s1} = \pm \frac{\sqrt{\Lambda_{Hs1} V_{\rm SM}^2 + (\Delta_{13} + \Delta_{1X} + 2\lambda_{s1})V_\phi^2}}{\sqrt{2}} + \mathcal{O}(\zeta); \tag{5.7}$$

$$\mu_{s3} = \pm \frac{\sqrt{\Lambda_{Hs3} V_{\rm SM}^2 + (3\beta_{3X} + \Delta_{13} + \Delta_{3X} + 2\lambda_{s3})V_\phi^2}}{\sqrt{2}} + \mathcal{O}(\zeta); \tag{5.8}$$

$$\mu_{sX} = \pm \frac{\sqrt{\Lambda_{HsX} V_{\rm SM}^2 + (\beta_{3X} + \Delta_{1X} + \Delta_{3X} + 2\lambda_{sX})V_\phi^2}}{\sqrt{2}} + \mathcal{O}(\zeta); \tag{5.9}$$

From Eq. 5.6, we see that $\kappa_{H1X} \to 0$ and $\kappa_{H2X} \to 0$ when $\zeta \to 0$ (and keeping V_ϕ finite). Thus, in our calculations we choose $\kappa_{H1X} \sim V_\Phi$ and $\kappa_{H2X} \sim V_\Phi / V_\phi$.

To simplify the squared masses and obtain useful analytical expressions, let us consider $\lambda_{11} = \lambda_{22} = \lambda_{s1} = \lambda_{s3} = \lambda_{sX}$; $\Lambda_{H1} = \Lambda_{H2} = \Lambda_{Hs1} = \Lambda_{Hs3} = \Lambda_{HsX} = \Lambda'_{H1} = \Lambda'_{H2}$; $\Lambda'_{11} = \Lambda'_{13} = \Lambda'_{1X} = \Lambda'_{21} = \Lambda'_{23} = \Lambda'_{2X} = \lambda_{12} = \lambda'_{12} = \Delta_{13} = \Delta_{1X} = \Delta_{3X}$; $\Lambda'_{12} = \Lambda'_{22} = \Delta_{12} = \Delta_{23} = \Delta_{2X}$ and the other parameters without restrictions. The previous constraints have been inspired by the similitude of the respective potential terms. We have left free the parameters that involve the DM candidates. Also, we have assumed that the H scalar field is the Higgs-like field in this model. Doing these considerations, we have, apart from the Goldstone bosons that are eaten by the $W^\pm$ bosons, two charged scalars, $C_{1,2}^\pm$, with masses given by

$$m^2_{C_1^\pm, C_2^\pm} = \frac{1}{4}\left[2\Lambda_{H1} V_{\rm SM}^2 + \left(1+\sqrt{2}\right) V_{\rm SM} V_\phi \right. \\ \left. \mp V_\phi \left(\sqrt{\left(3 - 2\sqrt{2}\right) V_{\rm SM}^2 + 4\beta_{13}^2 V_\phi^2} + 2\beta_{13} V_\phi \right) \right] + \mathcal{O}(\zeta); \tag{5.10}$$

In the CP-odd scalar sector, we have, besides the two Goldstone bosons which give mass to the $Z_{1\mu}$ and $Z_{2\mu}$ gauge bosons, the following mass eigenvalues:

$$m^2_{I_3} = \mathcal{O}(\zeta); \quad m^2_{I_4} = M^2_{\rm DM}; \; m^2_{I_7} = -5\beta_{3X} V_\phi^2 + \mathcal{O}(\zeta); \tag{5.11}$$

$$m^2_{I_5, I_6} = \frac{1}{4} V_\phi \left[\left(1+\sqrt{2}\right) V_{\rm SM} - 2\beta_{13} V_\phi \mp \sqrt{4\beta_{13}^2 V_\phi^2 + \left(3 - 2\sqrt{2}\right) V_{\rm SM}^2} \right] + \\ + \mathcal{O}(\zeta); \tag{5.12}$$

Finally, in the CP-even scalar sector we have $m^2_{R_4} = M^2_{\rm DM}$, and

$$m^2_{R_5,R_6} = \frac{1}{4}V_\phi\left[\left(1+\sqrt{2}\right)V_{\rm SM} - 2\beta_{13}V_\phi \mp \sqrt{4\beta^2_{13}V^2_\phi + \left(3-2\sqrt{2}\right)V^2_{\rm SM}}\right] + \mathcal{O}(\zeta)\,; \quad (5.13)$$

the other mass eigenvalues are not shown for shortness. As shown in the above expressions in the $\mathcal{O}(\zeta)$ we have three degenerate mass eigenstates, i.e. $m^2_{R_4} = m^2_{I_4}$, $m^2_{R_5} = m^2_{I_5}$ and $m^2_{R_6} = m^2_{I_6}$. Imposing that all these masses are positive, we find the following conditions:

$$\begin{aligned} &M_{\rm DM} > 0 \wedge \beta_{3X} < 0 \\ &\wedge\left[\left(\Lambda'_{H2} > 0 \wedge \beta_{13}V_\phi + \sqrt{2}V_{\rm SM} < 2V_{\rm SM}\right) \vee \right. \\ &\left.\left(V_\phi > -2\left(\sqrt{2}-1\right)\Lambda'_{H2}V_{\rm SM} \wedge \beta_{13} < \frac{V_{\rm SM}\left(\Lambda'_{H2}V_{\rm SM}+V_\phi\right)\left(\Lambda'_{H2}V_{\rm SM}+\sqrt{2}V_\phi\right)}{V^2_\phi\left(2\Lambda'_{H2}V_{\rm SM}+\left(1+\sqrt{2}\right)V_\phi\right)} \wedge \Lambda'_{H2} \leq 0\right)\right]. \end{aligned} \quad (5.14)$$

Despite the fact that the Eqs. 5.5-5.15 are only valid in the limit $\zeta \to 0$, these relations will be useful in our analysis, at least as a starting point.

5.3 Gauge Bosons

In this model the gauge symmetry breaking proceeds in two stages. In the first stage, the real components of the ϕ_1, ϕ_3, ϕ_X fields obtain VEVs, say V_ϕ, as discussed in the previous section. Once this happens, the gauge symmetry is broken down to $SU(2)_L \otimes U(1)_Y$, where Y is the usual hypercharge of the SM. In the second stage, the electrically neutral components of the H, $\Phi_{1,2}$ obtain VEVs, V_H and V_Φ, respectively, thus, breaking down the symmetry to $U(1)_Q$.

The mass terms for the three electrically neutral $SU(2)_L \otimes U(1)_{Y'} \otimes U(1)_{B-L}$ gauge bosons (W^3_μ, $B^{Y'}_\mu$, and B^{B-L}_μ) arise from the kinetic terms for the scalar fields upon replacing H, $\Phi_{1,2}$, $\phi_{1,2,3,X}$ by their respective VEVs ($\langle\phi_{2R}\rangle = 0$). In general the mass-square matrix for W^3_μ, $B^{Y'}_\mu$, and B^{B-L}_μ can be written as follows:

$$\mathcal{M}^2_{\text{Gauge Bosons}} = \begin{bmatrix} g^2(K+P+2N) & -gg_{Y'}(K+N) & -gg_{B-L}(P+N) \\ -gg_{Y'}(K+N) & g^2_{Y'}K & g_{Y'}g_{B-L}N \\ -gg_{B-L}(P+N) & g_{Y'}g_{B-L}N & g^2_{B-L}P \end{bmatrix} \quad (5.15)$$

where g, $g_{Y'}$ and g_{B-L} are the $SU(2)_L$, $U(1)_{Y'}$, $U(1)_{B-L}$ coupling constants, respectively. K, P, N are defined by $K \equiv \frac{1}{4}\sum_a V^2_a Y'^2_a$, $P \equiv \frac{1}{4}\sum_a V^2_a (B-L)^2_a$, $N \equiv \frac{1}{4}\sum_a V^2_a Y'_a (B-L)_a$; with Y'_a and $(B-L)_a$ being the quantum numbers given in the Tables 1 and 2. Considering our aforementioned assumptions we have:

$$K = \frac{1}{4}\left(V^2_H + 41V^2_\Phi + 74V^2_\phi\right),\ P = \frac{1}{4}\left(45V^2_\Phi + 74V^2_\phi\right),\ N = -\frac{1}{4}\left(42V^2_\Phi + 74V^2_\phi\right). \quad (5.16)$$

In order to obtain the relation between the neutral gauge bosons $\left(W_\mu^3,\, B_\mu^{Y'},\, B_\mu^{B-L}\right)$ and the corresponding mass eigenstates, we diagonalize $\mathcal{M}^2_{\text{Gauge Bosons}}$. Doing so, we have:

$$\gamma_\mu = \frac{1}{N_\gamma}\left[\frac{1}{g}W_\mu^3 + \frac{1}{g_{Y'}}B_\mu^{Y'} + \frac{1}{g_{B-L}}B_\mu^{B-L}\right]; \tag{5.17}$$

$$\begin{aligned} Z_{1\mu} &= \frac{1}{N_{Z_1}}\Big[g\left(Pg_{B-L}^2 - Ng_{Y'}^2 - M_{Z_1}^2\right)W_\mu^3 - g_{Y'}\left(\left(P+N\right)g^2 + Pg_{B-L}^2 - M_{Z_1}^2\right)B_\mu^{Y'} \\ &\quad + g_{B-L}\left(\left(P+N\right)g^2 + Ng_{Y'}^2\right)B_\mu^{B-L}\Big]; \end{aligned} \tag{5.18}$$

$$\begin{aligned} Z_{2\mu} &= \frac{1}{N_{Z_2}}\Big[g\left(Pg_{B-L}^2 - Ng_{Y'}^2 - M_{Z_2}^2\right)W_\mu^3 - g_{Y'}\left(\left(P+N\right)g^2 + Pg_{B-L}^2 - M_{Z_2}^2\right)B_\mu^{Y'}\Big] \\ &\quad + g_{B-L}\left(\left(P+N\right)g^2 + Ng_{Y'}^2\right)B_\mu^{B-L}\Big]; \end{aligned} \tag{5.19}$$

where N_γ, N_{Z_1}, N_{Z_2} are the corresponding normalization constants. Also, γ_μ corresponds to the photon, and $Z_{1\mu}$ and $Z_{2\mu}$ are the two massive neutral vector bosons of the model, and their squared masses are given by $M_\gamma^2 = 0$, and

$$M^2_{Z_{1\mu},Z_{2\mu}} = \frac{1}{2}R \mp \frac{1}{2}\left[R^2 - 4\left(KP - N^2\right)\left(g^2\left(g_{Y'}^2 + g_{B-L}^2\right) + g_{Y'}^2 g_{B-L}^2\right)\right]^{1/2}, \tag{5.20}$$

where $R \equiv (K+P+2N)g^2 + Kg_{Y'}^2 + Pg_{B-L}^2$. After some manipulations [1] , the Z_μ and Z'_μ bosons may be expressed as

$$Z_\mu = \cos\theta_W\, W_\mu^3 - \sin\theta_W\, \sin\alpha\, B_\mu^{Y'} - \sin\theta_W\, \cos\alpha\, B_\mu^{B-L}; \tag{5.21}$$

$$Z'_\mu = \cos\alpha\, B_\mu^{Y'} - \sin\alpha\, B_\mu^{B-L}; \tag{5.22}$$

where Z_μ is the neutral massive gauge boson described theoretically in the SM. and the γ_μ defined as in Eq. 5.17. The α angle is given by

$$\tan\alpha = \frac{g_{B-L}}{g_{Y'}}. \tag{5.23}$$

This angle must be understood as the parameter of a particular $SO\left(2\right)$ transformation on the two gauge bosons, $B_\mu^{Y'}$ and B_μ^{B-L}, that rotates the $U\left(1\right)_{Y'} \otimes U\left(1\right)_{B-L}$ gauge group into the $U\left(1\right)_Y \otimes U\left(1\right)_{Z'}$ gauge group. In the last expression, $U\left(1\right)_Y$ is the usual hypercharge gauge group. Also, we have that $g^2\sin^2\theta_W = e^2 = \left(\frac{1}{g^2} + \frac{1}{g_{Y'}^2} + \frac{1}{g_{B-L}^2}\right)^{-1}$. The $U\left(1\right)_{Z'}$ can be understood as the gauge group with the coupling $g_{Z'}^2 = g_{Y'}^2 + g_{B-L}^2$. If we diagonalize the gauge bosons squared mass matrix as a whole, we are able to compare the final eigenstates $Z_{1\mu}$ and $Z_{2\mu}$ to the mixed states Z_μ and Z'_μ indicated in the Footnote

[1] We have the $\mathcal{M}^2_{\text{Gauge Bosons}}$ expressed in the basis $W_\mu^3, B_\mu^{Y'}, B_\mu^{B-L}$. We rotate the two states $B_\mu^{Y'}$ and B_μ^{B-L} and define the new ones as W_μ^3, B'_μ, Z'_μ. Later, we rotate W_μ^3 and B'_μ to find $\gamma_\mu, Z_\mu, Z'_\mu$, where γ is the photon and this last $\mathcal{M}'^2_{\text{Gauge Bosons}}$ is diagonal for the photon, meaning that we have mixture in the block composed by Z_μ and Z'_μ. In the end, a final rotation in the two states Z_μ and Z'_μ is necessary for obtaining the mass eigenstates $Z_{1\mu}$ and $Z_{2\mu}$.

1, and consequently we can write the two massive gauge bosons $Z_{1\mu}$ and $Z_{2\mu}$ in terms of Z_μ and Z'_μ as follows:

$$Z_{1\mu} = \cos\beta\, Z_\mu + \sin\beta\, Z'_\mu; \tag{5.24}$$

$$Z_{2\mu} = -\sin\beta\, Z_\mu + \cos\beta\, Z'_\mu; \tag{5.25}$$

where

$$\tan\beta = \frac{\sqrt{g^2\left(g_{Y'}^2+g_{B-L}^2\right)+g_{Y'}^2 g_{B-L}^2}\left(g_{B-L}^2 L - g_{Y'}^2 N - M_{Z_2}^2\right)}{g^2\left(g_{Y'}^2+g_{B-L}^2\right)(L+N)+g_{Y'}^2\left(g_{B-L}^2(L+N)-M_{Z_2}^2\right)} \quad . \tag{5.26}$$

Thus, we notice that our model in principle allows Z_μ, which is the one described in the SM, to be mixed with Z'_μ to form the boson $Z_{1\mu}$ which would be measured experimentally. From Eqs. 5.20), (5.24 and 5.25, we can see that $\tan\beta = 0$ when $V_\phi \to \infty$ or $V_H^2 = \left(g_{Y'}^2+3g_{B-L}^2\right)V_\Phi^2/g_{Y'}^2$. However, this last solution is not allowed since in our case we have $V_H \gg V_\Phi$ and $\mathcal{O}(g_{Y'}) \sim \mathcal{O}(g_{B-L})$.

In this work, we use the following gauge couplings, $g \simeq 0.65$, $g_{Y'} = g_{B-L} \simeq 0.505$, such that $\tan\beta \simeq 4\times10^{-4}$. Doing so, we have $Z_{1\mu} \simeq Z_\mu$ and $Z_{2\mu} \simeq Z'_\mu$. In general, the β angle must be quite small, $\beta \lesssim 10^{-3}$, to be in agreement with precision electroweak studies [127, 128, 129] since a new neutral boson $Z_{2\mu}$ which mixes with the SM Z_μ distorts its properties, such as couplings to fermions and mass relative to electroweak inputs. Using those parameters for the gauge couplings and the VEVs discussed in the previous section, we obtain $M_{Z'} \simeq 3.1$ TeV besides the already known masses for the SM gauge bosons. In general, a new neutral vector boson must have a mass in the order of few TeV, or be very weakly coupled to the known matter to maintain consistency with the present phenomenology [127, 128, 129, 130, 131]. Doing a phenomenological study of the bounds on the parameter space imposed by data coming from LEP II, Tevatron and LHC in the present model is out of the scope of this work. However, we see that the $M_{Z'}$ value above is consistent with the relation $M_{Z'}/g_{B-L} \simeq 6.13 \gtrsim 6$ TeV [130, 131].

Finally, the charged gauge bosons $W_\mu^\pm$ are not affected by the presence of one additional neutral gauge boson $Z_{2\mu}$. These have the same form as in the SM, $W_\mu^\pm = \frac{1}{\sqrt{2}}\left(W_\mu^1 \mp iW_\mu^2\right)$ with masses given by $M_{W^\pm}^2 = \frac{1}{4}g^2V_{\rm SM}^2 = \frac{1}{4}g^2\left(V_H^2+2V_\Phi^2\right)$.

5.4 Dark Matter

In order to verify if our model satisfies current constraints given by experimental measurements, we take one indirect detection experiment - the Dark Matter relic density obtained by the PLANCK and WMAP satellites, Refs. [8, 9] - and two direct detection experiments - XENON100 and LUX, Ref. [132] and Ref. [101] respectively.

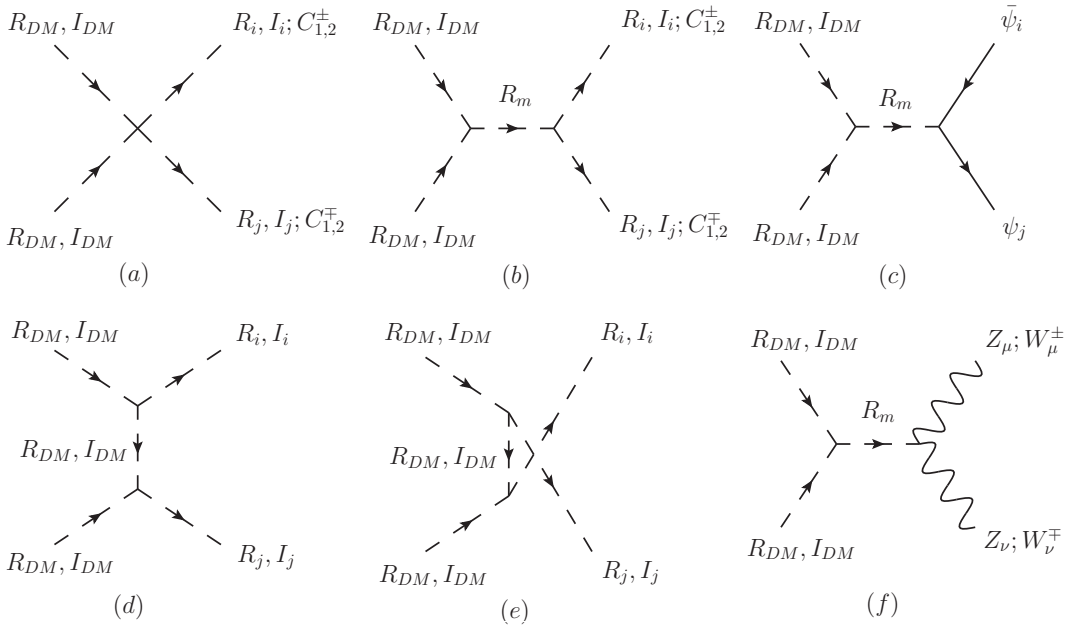

Figure 9 – Main annihilation processes that contribute to $\langle \sigma v_{\text{Møl}} \rangle$.

5.4.1 Thermal Relic Density

In order to calculate the present-day DM mass density, $\Omega_{\text{DM}}h^2$, arising from R_{DM} ($R_4 \equiv R_{\text{DM}}$) and I_{DM} ($I_4 \equiv I_{\text{DM}}$) scalars which freeze out (i.e., leave thermodynamic equilibrium), we follow the procedure outlined in the section 3.6. Thus, we should find the solution to the Boltzmann equations for the $Y_{R_{\text{DM}}}$ and $Y_{I_{\text{DM}}}$, which were defined as the ratio of the number of particles ($n_{R_{\text{DM}}}$ and $n_{I_{\text{DM}}}$) to the entropy, $Y_i \equiv n_i/s$ ($i = R_{\text{DM}}$, I_{DM}), with s being the total entropy density of the Universe. Actually, in our case, due to the $U(1)_\chi$ symmetry introduced in the Sec. 5.2, $M_{I_{\text{DM}}} = M_{R_{\text{DM}}} \equiv M_{\text{DM}}$, $Y_{R_{\text{DM}}} = Y_{I_{\text{DM}}} \equiv Y$, and $\Omega_{\text{DM}}h^2 = \Omega_{R_{\text{DM}}}h^2 + \Omega_{I_{\text{DM}}}h^2 = 2\Omega_{R_{\text{DM}}}h^2 = 2\Omega_{I_{\text{DM}}}h^2$.

The equation we have to solve is the Boltzmann equation given in the eq. 3.123,

$$\frac{dY}{dx} = -\frac{m}{x^2}\frac{\left(\frac{1}{3}g_s' m x^{-1} + g_s\right)}{\left(\frac{45}{\pi}G g_\rho\right)^{1/2}} \langle \sigma v_{\text{Møl}} \rangle \left(Y^2 - Y_{eq}^2\right) \quad , \tag{5.27}$$

whose elements were explained in the section 3.6. In the end, once the Y is numerically calculated for the present time, Y_0, we can obtain $\Omega_{\text{DM}}h^2 = 2.82 \times 10^8 \times (2 \times Y_0) \times \frac{M_{\text{DM}}}{\text{GeV}}$, this formula given in that earlier section.

For calculating σ, we have taken into account all dominant annihilation processes which are shown in the Fig. 9. In our case, the dominant annihilation contributions come from the scalar exchange. That is because our DM candidates, R_{DM} and I_{DM}, couple neither to Z_μ nor to W_μ gauge bosons at tree level. Also, we have found that contributions coming from Z'_μ exchange are negligible for the parameter set considered here.

Taking into account all previously mentioned, we have solved numerically Eq. 3.123 for a representative set of parameters. Although the scalar potential in this model has

many free parameters, we have found that the most relevant parameters in determining the correct DM relic density and in satisfying the currently direct experimental limits are Λ_{Hs2}, $\Delta_{\alpha 2}$ (with $\alpha = 1, 3, X$) and $\Lambda'_{\gamma 2}$ (with $\gamma = 1, 2$). The Λ_{Hs2} coupling strongly controls the direct detection signal, since in our case both the Higgs-like scalar is almost totally the neutral CP-even component of the H field and as discussed below, the direct detection is mainly mediated by the $t-$channel Higgs exchange. In order to obtain the correct direct detection limits without resorting to resonances, we found that $\Lambda_{Hs2} \sim 10^{-4}$. The $\Delta_{\alpha 2}$ and $\Lambda'_{\gamma 2}$ parameters are also crucial in obtaining the correct $\Omega_{\rm DM}h^2$ because they mostly control the $DM - DM - R_i\,(I_i) - R_i\,(I_i)$ and $DM - DM - R_i$ couplings and, therefore, the σ. The latter is not allowed to vary in a wide range since, roughly, $\Omega_{\rm DM}h^2 \sim 1/\langle \sigma v_{\rm M\o l}\rangle$ and we aim to obtain values close to $\Omega_{\rm DM}h^2 \sim 0.11$. In other words, the larger $\Delta_{\alpha 2}$ and $\Lambda'_{\gamma 2}$ parameters are, the smaller the $\Omega_{\rm DM}h^2$ is. In Fig. 10, we have used $\Lambda'_{\gamma 2} \simeq 10^{-2}$ and $\Delta_{\alpha 2} \simeq 9 \times 10^{-2}$. It is also important here to mention that the dominant process is the $DM + DM \to I_3 + I_3$ annihilation, where I_3 refers to the lightest CP-odd scalars, as in Sec. 5.2. Although the other parameters in the scalar potential are not as critical in determining the $\Omega_{\rm DM}h^2$, they give the other quantitative characteristics appearing in Fig. 10. In order to be more specific, we have chosen the other parameters such that the mass scalar spectrum is given by: 1437.6, 1016.9, 631.7, 544.9, 379.6, 125 GeV and 707.1, 544.9, 379.6, 2.3×10^{-6} GeV for the CP-even and CP-odd scalars, respectively (see Table 3 for more clarity).

Sector	Masses (GeV)
Neutral CP-even	$1437.6, 1016.9, 544.9, 379.6, 125$
Neutral CP-odd	$707.1, 544.9, 379.6, 2.3 \times 10^{-6}$
Charged	$545.2, 380.0$

Table 3 – Scalar sector masses, without Goldstone bosons.

The CP-even scalars with masses 1437.6, 1016.9, 631.7 GeV have components only in the singlets $\phi_{1,3,X}$ and the CP-even scalars with 544.9, 379.6 GeV have components only in the scalar doublets $\Phi_{1,2}$. The CP-even scalar with 125 GeV has component in the H doublet and it is the Higgs-like scalar in our model. In Fig. 10, we can also observe three resonances in $\simeq$ 315.8, 508.5, 718.8 GeV corresponding to the $s-$channel exchange of CP-even scalars with components in the singlets. Let us also mention that the processes via the $s-$channel due to the exchange of the CP-even scalars with masses 125, 379.6, 544.9 GeV are highly suppressed because of the smallness of their couplings. Thus, their resonances do not appear in Fig. 10.

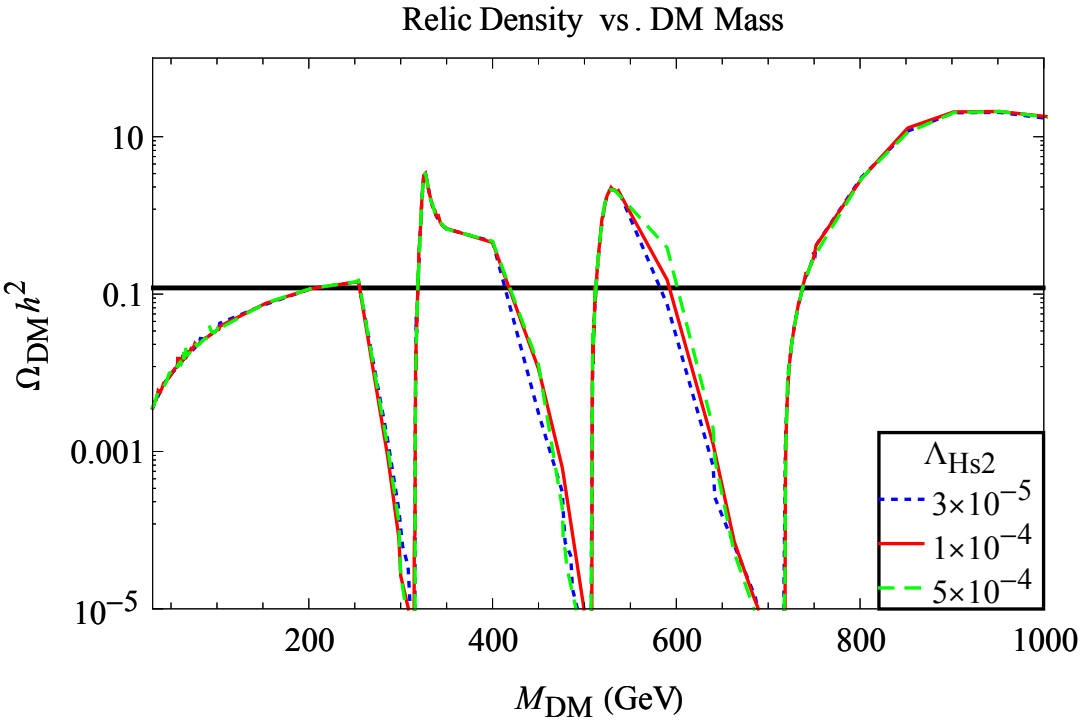

Figure 10 – The total thermal relic density of the $I_{\rm DM}$ and $R_{\rm DM}$ as a function of $M_{\rm DM}$. We have used three different parameters for $\Lambda_{Hs2} = 0.3\times10^{-4}$, 1×10^{-4}, 5×10^{-4}.

5.4.2 Direct Detection

As said earlier, despite weakly coupled to baryons, WIMPs can scatter elastically off atomic nuclei, providing the opportunity for direct detection. Currently, there are several experiments which aim to directly observe WIMP dark matter, the experiments in Refs. [132, 133, 101] are the ones which provide the most stringent limits. In general, the WIMP-nucleus interactions can be classified as either spin-independent or spin-dependent, as explained in the Sec. 4.1. In our case, these interactions are spin-independent because the two DM candidates are scalars, and therefore interact with nucleons via the effective interaction term $\phi^\dagger_{DM}\phi_{DM}\bar{q}q$. The relevant WIMP-nucleus scattering process for direct detection in the case considered here takes place mainly through the $t-$channel elastic scattering due to Higgs exchange:$(I_{\rm DM}, R_{\rm DM}) + N \to (I_{\rm DM}, R_{\rm DM}) + N$ (N refers to the atomic nucleus). The spin-independent cross section is given by

$$\sigma^{\rm SI}_{\chi N} = \frac{4}{\pi}\frac{M^2_{\rm DM}m^2_N}{(M_{\rm DM}+m_N)^2}\left[Zf_p + (A-Z)\,f_n\right]^2; \tag{5.28}$$

where the effective couplings to protons and neutrons, $f_{p,n}$, are

$$f_{p,n} = \sum_{q=u,d,s}\frac{G_{{\rm eff},q}}{\sqrt{2}}f^{(p,n)}_{Tq}\frac{m_{p,n}}{m_q} + \frac{2}{27}f^{(p,n)}_{TG}\sum_{q=c,b,t}\frac{G_{{\rm eff},q}}{\sqrt{2}}\frac{m_{p,n}}{m_q}. \tag{5.29}$$

By using $f_{Tq}^{(p,n)}$ and $f_{TG}^{(p,n)}$ given in Ref. [99] and the fact that, in our case, $G_{\text{eff},q} = G_0 \times m_q \equiv \frac{C_{DM^2H}}{V_H M^2_{\text{Higgs}}} \times m_q$ (with C_{DM^2H} being the coupling $DM - DM -$ Higgs which depends on the parameters of the model), we arrive at the cross section per nucleon of

$$\sigma^{\text{SI}}_{\chi,p} \approx 2.7 \times 10^7 \times \frac{M^2_{\text{DM}} m^2_N}{(M_{\text{DM}} + m_N)^2} \times G_0^2 \text{ in pbarn.} \tag{5.30}$$

Recently, the Large Underground Xenon (LUX) experiment [101] has reported its first results, setting limits on spin-independent WIMP-nucleon elastic scattering with a minimum upper limit on the cross section of 7.6×10^{-10} pbarn at a WIMP mass of 33 GeV/c^2. We have found that choosing $\Lambda_{Hs2} \sim 10^{-4}$ we obtain the LUX bound without resorting to resonances. It is clear that values of Λ_{Hs2} larger can be considered. However, we have chosen this conservative value for Λ_{Hs2}. Our results are shown in Fig. 11. The parameters are the same as in Fig. 10.

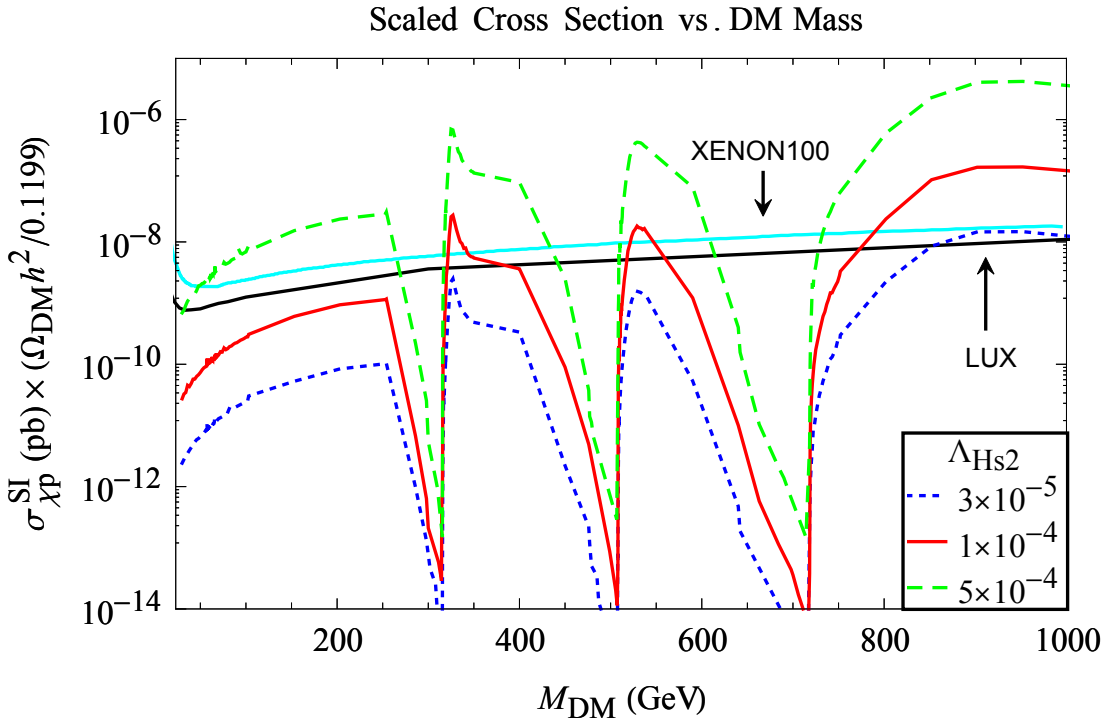

Figure 11 – The spin-independent elastic scattering cross section, $\sigma^{\text{SI}}_{\chi,p}$, off a proton p as a function of M_{DM} for the same parameters as in the Fig.10, appropriately scaled to relic density. We also show the XENON100 and LUX exclusion limits [132, 101].

From Figs. (10) and (11), we see that for a DM candidate with mass around 200 GeV and $\Lambda_{Hs2} = 0.3 \times 10^{-4}$, 1×10^{-4}, the two conditions, $\Omega_{\text{DM}}h^2$ and the direct detection, are satisfied outside the resonance regions. We also have verified that this is a general characteristic of this model. Due to the existence of the light I_3 scalar the annihilation process $DM + DM \to I_3 + I_3$ Fig. 9(a) is the dominant one so that we do not have

to appeal to resonances to get compatibility with experiments. Other $M_{\rm DM}$ values which satisfy the experimental bounds are shown in Figs (10) and (11). Specifically, $M_{\rm DM} \approx$ 319, 410, 511, 590, 737 GeV are also possible solutions. However, these are within regions with resonances.

Let us now do some important remarks about the impact of the existence of I_3 in this model. First of all, we have a tree level contribution to the Higgs invisible decay, $\Gamma_h^{\rm Inv}$, due to the coupling of the Higgs field with the light pseudo-scalar field, $c_{hI_3I_3}$, which comes from the Lagrangian terms of the form $|H|^2|\phi_{1,2,X}|^2$, and gives $\Gamma_{hI_3I_3}^{\rm Inv} = c_{hI_3I_3}^2/32\pi m_{\rm h}$ for $m_{I_3} \ll m_{\rm h}$. Actually, when $2M_{\rm DM} < m_{\rm h}$ the $h \to I_{\rm DM}\, I_{\rm DM}$ and $h \to R_{\rm DM}\, R_{\rm DM}$ decays are also allowed, thus, further contributing to $\Gamma_h^{\rm Inv}$ according to $\Gamma_{h\rm DMDM}^{\rm Inv} = \Gamma_{hI_{\rm DM}I_{\rm DM}}^{\rm Inv} + \Gamma_{hR_{\rm DM}R_{\rm DM}}^{\rm Inv} = 2 \times c_{h\rm DMDM}^2/(32\pi m_{\rm h}) \times \sqrt{1-4M_{DM}^2/m_{\rm h}^2}$ with $c_{h\rm DMDM} \approx \Lambda_{Hs2} V_H$. The current limit on the branching ratio into invisible particles of the Higgs, $BR_h^{\rm Inv}$, is around $10\% - 15\%$ [134, 135]. A stronger bound of $BR_h^{\rm Inv} < 5\%$ at 14 TeV LHC has been claimed [136]. From the set of parameters used to obtain Fig. 10 and Fig. 11 we have that $BR_h^{\rm Inv} = \left(\Gamma_{hI_3I_3}^{\rm Inv} + \Gamma_{h\rm DMDM}^{\rm Inv}\right) / \left(\Gamma_h^{\rm Vis} + \Gamma_{hI_3I_3}^{\rm Inv} + \Gamma_{h\rm DMDM}^{\rm Inv}\right) \simeq 3.78\%$ for $M_{\rm DM} = 50$ GeV. For different $M_{\rm DM}$ values we have found $BR_h^{\rm Inv} < 5\%$. Also, we have used $\Gamma_h^{\rm Vis} = 4.07$ MeV for $m_{\rm H} = 125$ GeV. The model is also safe regarding the severe existing constraints on the invisible decay width of Z_μ boson since there is no process like $Z_\mu \to RI_3 \to I_3I_3I_3$ [121] due to the fact that I_3 has only components in the SM singlets. (It would be kinetically forbidden anyway once all real scalar fields of the model are heavier than the Z_μ boson.) For the same reason, there is no issue with the energy loss in stars astrophysical constraint since there is no tree level coupling inducing the $\gamma + e^- \to e^- + I_3$ [122]. Finally, some last comments are necessary. In general, the I_3 could also contribute to the $\Omega_{\rm DM}h^2$ because it is massive. However, the I_3 pseudo-scalar is not stable. It decays mainly in active neutrinos, ν's, with $\Gamma_{I_3\to\nu\nu} \approx \frac{m_{I_3}}{16\pi}\frac{\sum_i m_{\nu i}^2}{V_\phi^2}$ [137]. For the parameter set used here, we have $\tau_{I_3} \simeq 1/\Gamma_{I_3\to\nu\nu} \approx 10^9\,$s, where we have used $\sum_i m_{\nu i}^2 \lesssim 0.01\,{\rm eV}^2$. With τ_{I_3} given here and $t_U \simeq 4.3 \times 10^{17}$s (age of the Universe), the $\Omega_{I_3}h^2 \simeq \frac{m_{I_3}}{1.25\ {\rm keV}} \exp\left(-t_{\rm U}/\tau_{I_3}\right) \simeq 0$. In the last expression for $\Omega_{I_3}h^2$ we have considered that the $T_{DI_3} > 175$ GeV (where T_{DI_3} is the decoupling temperature of the I_3). There is also a constraint which comes from the observed large scale structure of the Universe [138, 139]. Roughly speaking, this last condition imposes $r_{I_3}\frac{m_{I_3}}{1\ {\rm keV}}\left(\frac{\tau_{I_3}}{1\ {\rm s}}\right)^{1/2} \lesssim 4 \times 10^3$ [138]. In the last expression $r_{I_3} = g_{\rm eff}(T_0)/g_{\rm eff}(T_{DI_3}) \approx 1/25$, being $g_{\rm eff}$ the effective number of the relativistic degrees of freedom. With our parameter set this condition is satisfied.

6 Conclusions

In this work we verified the compatibility of a particular B-L Model, described in the final chapter, to accomodate candidates to dark matter. For this task, in the first chapter, we exposed dark matter motivations, comparing superficially theory and experiment, and later some proposed candidates to this new kind of matter were shown.

In the second chapter, we have studied the relic abundance calculation when one assumes thermal equilibrium at the early Universe. We have spent most of the time working on the understanding of the methods involved in this calculation and on how to implemment them inside numerical calculations. The following subjects have been studied or reviewed: Basics of GR, Λ-CDM Cosmological Model, Thermodynamics of the Early Universe, arriving in the end at the Boltzmann equation (its properties have been analyzed carefully) and how it generates the current relic abundance for a generic particle.

In the following chapter, an introduction to direct and indirect detection experiments was provided, where different techniques were exposed and discussed. Also, the necessary theoretical background on direct detection was provided because the final chapter would have to deal with the limits coming from these experiments and comparison to theory becomes necessary.

Finally a scenario where a complex DM candidate is possible was discussed. In particular, the model studied here is a gauge extension of the SM based on a $SU(2)_L \otimes U(1)_{Y'} \otimes U(1)_{B-L}$ symmetry group. This model contents three right handed neutrinos and some extra scalars, doublets and singlets, with different quantum numbers. In principle, those scalars are introduced to generate Majorana and Dirac mass terms at the tree level and to allow the implementation of a see-saw mechanism at the TeV scale as shown in Ref. [117]. The non-standard doublets and singlets introduce two new energy scales, besides the electoweak one given by $V_H = 246$ GeV: V_Φ (the VEVs of the extra doublet neutral scalars) and V_ϕ (the VEVs of the extra singlet neutral scalars). If $\zeta \equiv V_\Phi/V_\phi \ll 1$ the see-saw mechanism becomes natural [117]. In this context, we have studied the scalar spectrum and imposed a Z_2 symmetry on the ϕ_2 singlet scalar (which accidentally became a $U(1)_\chi$ symmetry : $\phi_2 \to \exp(-i\chi_{\phi_2})\phi_2$) in order to allow a complex DM candidate. Before studying the constraints coming from the thermal relic density ($\Omega_{\rm DM}h^2$) and direct detection experiments on this DM candidate, we have done a brief analysis of the gauge sector concerning the Z_μ, Z'_μ mixing angle ($\tan\beta \simeq 4\times10^{-4}$) which satisfies the $\beta \lesssim 10^{-3}$ electroweak precision constraint, and we have verified that the Z'_μ mass emerging from the model is consistent with the relation $M_{Z'}/g_{B-L} \simeq 6.13 \gtrsim 6$ TeV. Then, we have chosen some parameters that simultaneously allow us to have a compatible $\Omega_{\rm DM}h^2$ and satisfy the direct detection experiments. Although the scalar potential has many parameters, we have found that the Λ_{Hs2}, $\Delta_{\alpha 2}$ (with $\alpha = 1, 3, X$) and $\Lambda'_{\gamma 2}$ (with $\gamma = 1, 2$) parameters

mostly control these two constraints. The Λ_{Hs2} parameter is fundamental in satisfying the limits coming from direct detection, since in our case it takes place through the $t-$channel elastic scattering due to the Higgs exchange. Choosing $\Lambda_{Hs2} \sim 10^{-4}$ roughly satisfies the bounds from the LUX experiment and allows a $\Omega_{\rm DM}h^2$ in agreement with the WMAP and PLANCK experiments. The $\Delta_{\alpha 2}$ and $\Lambda'_{\gamma 2}$ parameters control $\sigma_{\rm ann}$ mostly and, therefore $\Omega_{\rm DM}h^2$. As an example, we have shown $\Omega_{\rm DM}h^2$ and $\sigma^{\rm SI}_{\chi,p}$, for $\Lambda'_{\gamma 2} \simeq 10^{-2}$ and $\Delta_{\alpha 2} \simeq 9\times 10^{-2}$, in Figs. (10) and (11). It is interesting to note that this model, for the same set of parameters fixed, except $M_{\rm DM}$'s, has several $M_{\rm DM}$ values satisfying the experimental bounds. In other words, we have found solutions in the region outside and inside of the resonances for the same parameters, varying $M_{\rm DM}$ only. As previously mentioned, the presence of a light scalar, I_3, in this model makes the process $DM + DM \to I_3 + I_3$ to be dominant for $\Omega_{\rm DM}h^2$. However, I_3 may bring some potential problems, so that we have discussed some constraints imposed on I_3 coming from the Higgs and the Z_μ invisible decay widths, the energy loss in stars and the observed large scale structure of the Universe. We have found that in our context all of these constraints are satisfied. Finally, we would like to point out the recent work studying the possibility of having a Majoron DM candidate [140].

A The Minimization Conditions

The general minimization conditions coming from $\partial V_1/\partial R_i = 0$, where V_1 is the scalar potential with $U(1)_\chi$ symmetry and $R_i = \{H_R^0,\, \Phi_{1R}^0,\, \Phi_{2R}^0,\, \phi_{1R},\, \phi_{2R},\, \phi_{3R},\, \phi_{XR}\}$ are the neutral real components of the scalar fields, can be written as:

$$
\begin{aligned}
0 &= V_H \left(2\lambda_H V_H^2 + \Lambda_{\rm H1} V_{\Phi_1}^2 + \Lambda_{\rm H2} V_{\Phi_2}^2 + \Lambda_{\rm Hs1} V_{\phi_1}^2 + \Lambda_{\rm Hs2} V_{\phi_2}^2 + \Lambda_{\rm Hs3} V_{\phi_3}^2 + \right. \\
&\quad \left. + \Lambda_{\rm HsX} V_{\phi_X}^2 - 2\mu_H^2\right) - \sqrt{2}\kappa_{\rm H1X} V_{\Phi_1} V_{\phi_X} - \kappa_{\rm H2X} V_{\Phi_2} V_{\phi_X}^2 ; \qquad \text{(A.1)} \\
0 &= V_{\Phi_1} \left(\Lambda_{\rm H1} V_H^2 + 2\lambda_{11} V_{\Phi_1}^2 + (\lambda'_{12} + \lambda_{12}) V_{\Phi_2}^2 + \Lambda'_{11} V_{\phi_1}^2 + \Lambda'_{12} V_{\phi_2}^2 + \Lambda'_{13} V_{\phi_3}^2 + \right. \\
&\quad \left. + \Lambda'_{1X} V_{\phi_X}^2 - 2\mu_{11}^2\right) - \sqrt{2}\kappa_{\rm H1X} V_H V_{\phi_X} + \beta_{13} V_{\Phi_2} V_{\phi_1} V_{\phi_3} ; \qquad \text{(A.2)} \\
0 &= V_{\Phi_2} \left(\Lambda_{\rm H2} V_H^2 + (\lambda_{12} + \lambda'_{12}) V_{\Phi_1}^2 + 2\lambda_{22} V_{\Phi_2}^2 + \Lambda'_{21} V_{\phi_1}^2 + \Lambda'_{22} V_{\phi_2}^2 + \Lambda'_{23} V_{\phi_3}^2 + \right. \\
&\quad \left. + \Lambda'_{2X} V_{\phi_X}^2 - 2\mu_{22}^2\right) - \kappa_{\rm H2X} V_H {V_{\phi_X}}^2 + \beta_{13} V_{\Phi_1} V_{\phi_1} V_{\phi_3} ; \qquad \text{(A.3)} \\
0 &= V_{\phi_1} \left(\Lambda_{\rm Hs1} V_H^2 + \Lambda'_{11} V_{\Phi_1}^2 + \Lambda'_{21} V_{\Phi_2}^2 + 2\lambda_{\rm s1} V_{\phi_1}^2 + \Delta_{12} V_{\phi_2}^2 + \Delta_{13} V_{\phi_3}^2 + \Delta_{1X} V_{\phi_X}^2 - \right. \\
&\quad \left. - 2\mu_{\rm s1}^2\right) + \beta_{13} V_{\Phi_1} V_{\Phi_2} V_{\phi_3} ; \qquad \text{(A.4)} \\
0 &= V_{\phi_2} \left(\Lambda_{\rm Hs2} V_H^2 + \Lambda'_{12} V_{\Phi_1}^2 + \Lambda'_{22} V_{\Phi_2}^2 + \Delta_{12} V_{\phi_1}^2 + 2\lambda_{\rm s2} V_{\phi_2}^2 + \Delta_{23} V_{\phi_3}^2 + \Delta_{2X} V_{\phi_X}^2 - \right. \\
&\quad \left. - 2\mu_{\rm s2}^2\right) ; \qquad \text{(A.5)} \\
0 &= V_{\phi_3} \left(\Lambda_{\rm Hs3} V_H^2 + \Lambda'_{13} V_{\Phi_1}^2 + \Lambda'_{23} V_{\Phi_2}^2 + \Delta_{13} V_{\phi_1}^2 + \Delta_{23} V_{\phi_2}^2 + 2\lambda_{\rm s3} V_{\phi_3}^2 + \Delta_{3X} V_{\phi_X}^2 + \right. \\
&\quad \left. + 3\beta_{3X} V_{\phi_3} V_{\phi_X} - 2\mu_{\rm s3}^2\right) + \beta_{13} V_{\Phi_1} V_{\Phi_2} V_{\phi_1} ; \qquad \text{(A.6)} \\
0 &= V_{\phi_X} \left(\Lambda_{\rm Hsx} V_H^2 + \Lambda'_{1X} V_{\Phi_1}^2 + \Lambda'_{2X} V_{\Phi_2}^2 + \Delta_{1X} V_{\phi_1}^2 + \Delta_{2X} V_{\phi_2}^2 + 2\lambda_{\rm sx} V_{\phi_X}^2 - \right. \\
&\quad \left. - 2\kappa_{\rm H2X} V_H V_{\Phi_2} - 2\mu_{\rm sx}^2\right) - \sqrt{2}\kappa_{\rm H1X} V_H V_{\Phi_1} + \beta_{3X} V_{\phi_3}^3 + \Delta_{3X} V_{\phi_3}^2 V_{\phi_X} ; \qquad \text{(A.7)}
\end{aligned}
$$

In the Eqs. (A.1)-(A.7) above, V_H, V_{Φ_1}, V_{Φ_2}, V_{ϕ_1}, V_{ϕ_2}, V_{ϕ_3}, V_{ϕ_X} are the VEVs of H_R^0, Φ_{1R}^0, Φ_{2R}^0, ϕ_{1R}, ϕ_{2R}, ϕ_{3R} , ϕ_{XR}, respectively.

References

[1] M. Peskin, J. Phys. Soc. Jpn. **76** (2007) 111017.

[2] F. Zwicky, Helv. Phys. Acta **6** (1933) 124.

[3] S. Smith, Ap. J. **83** (1936) 23.

[4] P. Rosati, S. Borgani and C. Norman, Ann. Rev. Astron. Astrophys. **40** (2002) 539 [arXiv:astro-ph/0209035].

[5] Y. Sofue and V. Rubin, Ann. Rev. Astron. Astrophys. **39** (2001) 137 [arXiv:astro-ph/0010594].

[6] V.C. Rubin, N. Thonnard, and W.K. Ford, Jr., Ap. J. **87** (182) 477.

[7] V. Trimble, Ann. Rev. Astron. Astrophys. **25** (1987) 425.

[8] C.L. Bennett et al. [WMAP Collaboration], ApJS **208** (2013) 20B.

[9] P. Ade, et al. [Planck Collaboration], arXiv:1303.5076 [astro-ph.CO].

[10] R.H. Sanders and S.S. McGaugh, Ann. Rev. Astron. Astrophys. **40** (2002) 263 [arXiv:astro-ph/0204521].

[11] D. Clowe, M. Bradac, A.H. Gonzalez, M. Markevitch, S.W. Randall, et al., Astrophys. J. **648** (2006) L109–L113 [arXiv:astroph/0608407].

[12] K. Griest, arXiv:hep-ph/9303253.

[13] L. Bergstrom, Rep. Prog. Phys. **63** (2000) 793 [arXiv:hep-ph/0002126].

[14] C. Weinheimer, Proceedings of 10th International Workshop on Neutrino Telescopes, Venice, Italy, 2003 [arXiv:hep-ex/0306057].

[15] J.R. Bond, G. Efstathiou, J. Silk, Phys. Rev. Lett. **45** (1980) 1980.

[16] P.J.E. Peebles, Science **224** (1984) 1385.

[17] K. Abazajian, G.M. Fuller, M. Patel, Phys. Rev. D **64** (2001) 023 501 [arXiv:astro-ph/0101524].

[18] S. Dodelson, L.M. Widrow, Phys. Rev. Lett. **72** (1994) 17 [arXiv:hep-ph/9303287].

[19] S. Colombi, S. Dodelson, and L.M. Widrow, Astrophys. J. **458** (1996) 1.

[20] N. Yoshida, A. Sokasian, L. Hernquist, V. Springel, Astrophys. J. **591** (2003) L1 [arXiv:astro-ph/0303622].

[21] Z. Haiman, A. Loeb, Astrophys. J. **483** (1997) 21 [arXiv:astro-ph/9611028].

[22] Z. Haiman, A. Loeb, Astrophys. J. **503** (1998) 505 [arXiv:astro-ph/9710208].

[23] S.H. Hansen, Z. Haiman, Astrophys. J. **600** (2004) 26 [arXiv:astro-ph/0305126].

[24] X.D. Shi, G.M. Fuller, Phys. Rev. Lett. **82** (1999) 2832 [arXiv:astro-ph/9810076].

[25] L.J. Rosenberg, K.A. van Bibber, Phys. Rep. **325** (2000) 1.

[26] J.R. Ellis, J.S. Hagelin, D.V. Nanopoulos, K.A. Olive, M. Srednicki, Nucl. Phys. B **238** (1984) 453.

[27] T. Falk, K.A. Olive, M. Srednicki, Phys. Lett. B **339** (1994) 248 [arXiv:hep-ph/9409270].

[28] J.L. Feng, A. Rajaraman, F. Takayama, Phys. Rev. Lett. **91** (2003) 011 302 [arXiv:hep-ph/0302215].

[29] S. Weinberg, Phys. Rev. Lett. **48** (1982) 1303.

[30] T. Moroi, H. Murayama, M. Yamaguchi, Phys. Lett. B **303** (1993) 289.

[31] W. Buchmuller, K. Hamaguchi, M. Ratz, Phys. Lett. B **574** (2003) 156 [arXiv:hep-ph/0307181].

[32] S.A. Bonometto, F. Gabbiani, A. Masiero, Phys. Rev. D **49** (1994) 3918 [arXiv:astro-ph/9305010].

[33] T. Goto, M. Yamaguchi, Phys. Lett. B **276** (1992) 103.

[34] L. Covi, H.B. Kim, J.E. Kim, L. Roszkowski, JHEP **0105** (2001) 033 [arXiv:hep-ph/0101009].

[35] L. Covi, L. Roszkowski, R.R. de Austri, M. Small, arXiv:hep-ph/0402240.

[36] B.W. Lee, S. Weinberg, Phys. Rev. Lett. **39** (1977) 165.

[37] P. Hut, Phys. Lett. B **69** (1977) 85.

[38] C. Boehm, T.A. Ensslin, J. Silk, arXiv:astro-ph/0208458.

[39] C. Boehm, P. Fayet, arXiv:hep-ph/0305261.

[40] C. Boehm, D. Hooper, J. Silk, M. Casse, Phys. Rev. Lett. **92** (2004) 101 301 [arXiv:astro-ph/0309686].

[41] Ji-Haeng Huh, Jihn E. Kim, Jong-Chul Park, Seong Chan Park, AIP Conf.Proc. **1078** (2009) 554-556 [arXiv:hep-ph/0809.1953].

[42] D. Hooper, F. Ferrer, C. Boehm, J. Silk, J. Paul, N.W. Evans, M. Casse, arXiv:astro-ph/0311150.

[43] D. Hooper, L.T. Wang, arXiv:hep-ph/0402220.

[44] C. Picciotto, M. Pospelov, arXiv:hep-ph/0402178.

[45] N. Arkani-Hamed, A.G. Cohen, H. Georgi, Phys. Lett. B **513** (2001) 232 [arXiv:hep-ph/0105239].

[46] N. Arkani-Hamed, A.G. Cohen, T. Gregoire, J.G. Wacker, JHEP **0208** (2002) 020 [arXiv:hep-ph/0202089].

[47] N. Arkani-Hamed, A.G. Cohen, E. Katz, A.E. Nelson, JHEP **0207** (2002) 034 [arXiv:hep-ph/0206021].

[48] N. Arkani-Hamed, A.G. Cohen, E. Katz, A.E. Nelson, T. Gregoire, J.G. Wacker, JHEP **0208** (2002) 021 [arXiv:hep-ph/0206020].

[49] A. Birkedal-Hansen, J.G. Wacker, arXiv:hep-ph/0306161.

[50] H.C. Cheng, I. Low, JHEP **0309** (2003) 51 [arXiv:hep-ph/0308199].

[51] T. Appelquist, H.C. Cheng, B.A. Dobrescu, Phys. Rev. D **64** (2001) 035 002 [arXiv:hep-ph/0012100].

[52] H.C. Cheng, K.T. Matchev, M. Schmaltz, Phys. Rev. D **66** (2002) 036 005 [arXiv:hep-ph/0204342].

[53] G. Servant, T.M. Tait, Nucl. Phys. B **650** (2003) 391 [arXiv:hep-ph/0206071].

[54] G. Servant, T.M. Tait, New J. Phys. **4** (2002) 99 [arXiv:hep-ph/0209262].

[55] S.Weinberg, *The Quantum Theory of Fields*, vol. 1, Foundations, Cambridge University Press, Cambridge, 1995.

[56] K. Griest, M. Kamionkowski, Phys. Rev. Lett. **64** (1990) 615.

[57] D.J. Chung, E.W. Kolb, A. Riotto, Phys. Rev. D **59** (1999) 023 501 [arXiv:hep-ph/9802238].

[58] E.W. Kolb, D.J. Chung, A. Riotto, Proceedings of the 2nd International Conference on Dark Matter in Astro and Particle Physics (DARK98), Heidelberg, Germany, 1998 [arXiv:hep-ph/9810361].

[59] D.J.H. Chung, Edward W. Kolb, and A. Riotto, arXiv:hep-ph/9802238.

[60] AGASA Homepage, www.icrr.u-tokyo.ac.jp/as/as.html; HIRES Homepage, www2.keck.hawaii.edu:3636/realpublic/inst/hires/hires.html .

[61] K. Greisen, Phys. Rev. Lett. **16** (1966) 748.

[62] G.T. Zatsepin, V.A. Kuzmin, Pis'ma Zh. Eksp. Teor. Fiz. **4** (1966) 114 [JETP. Lett. **4** (1966) 78].

[63] V. Berezinsky, M. Kachelriess, A. Vilenkin, Phys. Rev. Lett. **79** (1997) 4302 [arXiv:astro-ph/9708217].

[64] M. Birkel, S. Sarkar, Astropart. Phys. **9** (1998) 297 [arXiv:hep-ph/9804285].

[65] A. Kusenko, V. Kuzmin, M.E. Shaposhnikov, P.G. Tinyakov, Phys. Rev. Lett. **80** (1998) 3185 [arXiv:hep-ph/9712212].

[66] A. Kusenko, M.E. Shaposhnikov, Phys. Lett. B **418** (1998) 46 [arXiv:hep-ph/9709492].

[67] R. Foot, Phys. Rev. D **69** (2004) 036 001 [arXiv:hep-ph/0308254].

[68] R. Foot, Z.K. Silagadze, arXiv:astro-ph/0404515.

[69] H.M. Hodges, Phys. Rev. D **47** (1993) 456.

[70] A.Y. Ignatiev, R.R. Volkas, Phys. Rev. D **68** (2003) 023 518 [arXiv:hep-ph/0304260].

[71] R.N. Mohapatra, S. Nussinov, V.L. Teplitz, Phys. Rev. D **66** (2002) 063 002 [arXiv:hep-ph/0111381].

[72] A. De Rujula, S.L. Glashow, U. Sarid, Nucl. Phys. B **333** (1990) 173.

[73] R. Dave, D.N. Spergel, P.J. Steinhardt, B.D.Wandelt, Astrophys. J. **547** (2001) 574 [arXiv:astro-ph/0006218].

[74] D.N. Spergel, P.J. Steinhardt, Phys. Rev. Lett. **84** (2000) 3760 [arXiv:astro-ph/9909386].

[75] G. Shiu, L.T. Wang, arXiv:hep-ph/0311228.

[76] J.R. Ellis, G.B. Gelmini, J.L. Lopez, D.V. Nanopoulos, S. Sarkar, Nucl. Phys. B **373** (1992) 399.

[77] J.R. Ellis, J.L. Lopez, D.V. Nanopoulos, Phys. Lett. B **247** (1990) 257.

[78] J.L. Feng, A. Rajaraman, F. Takayama, Phys. Rev. Lett. **91** (2003) 011302 [arXiv:hep-ph/0302215].

[79] J.A.R. Cembranos, A. Dobado, A.L. Maroto, Phys. Rev. Lett. **90** (2003) 241301 [arXiv:hep-ph/0302041].

[80] K. Kainulainen, K.A. Olive, arXiv:hep-ph/0206163.

[81] P. Roy, ICNAPP 1994:0225-237 [arXiv:hep-ph/9501209].

[82] S. Perlmutter et al. [SNCP Collaboration], Astrophys. J. **517** (1999) 565 [arXiv:astro-ph/9812133]; A. G. Riess et al. [Supernova Search Team Collaboration], Astron. J. **116** (1998) 1009 [arXiv:astro-ph/9805201].

[83] E. Komatsu et al. [WMAP Collaboration], Astrophys. J. Suppl. **192** (2011) 18 [arXiv:1001.4538 [astro-ph.CO]].

[84] M. Tegmark et al. [SDSS Collaboration], Phys. Rev. D **69** (2004) 103501 [arXiv:astro-ph/0310723]; U. Seljak et al. [SDSS Collaboration], Phys. Rev. D **71** (2005) 103515 [arXiv:astro-ph/0407372].

[85] D.J. Eisenstein et al. [SDSS Collaboration], Astrophys. J. **633** (2005) 560 [arXiv:astro-ph/0501171].

[86] B. Jain and A. Taylor, Phys. Rev. Lett. **91** (2003) 141302 [arXiv:astro-ph/0306046].

[87] J.R. Primack, Ann. Phys. (Berlin) **524**, No. 9-10, (2012) 535.

[88] A. Klypin , A.V. Kravtsov , O.Valenzuela and F.Prada, The Astrophysical Journal **522** (1999) 82.

[89] B. Moore et al, Astrophys.J. **524** (1999) L19 [arXiv:astro-ph/9907411].

[90] K. Bamba, S. Capozziello, S. Nojiri, S.D. Odintsov, Astrophysics and Space Science **342** (2012) 155 [arXiv:1205.3421 [gr-qc]].

[91] R. Watkins, K. A. Olive and M. Srednicki, Nucl. Phys. B **310** (1988) 693.

[92] E.W. Kolb and M.S. Turner, *The Early Universe* (Addison-Wesley, Reading, MA 1990) and references within.

[93] J. Bernstein, L.S. Brown and G. Feinberg, Phys. Rev. D **32** (1985) 3261; J. Bernstein, *Kinetic theory in the expanding Universe* (Cambridge Univ. Press, Cambridge, 1988).

[94] S.R. de Groot, W.A. van Leeuwen and Ch.G. van Weert, Relativistic kinetic theory (North-Holland, Amsterdam, 1980).

[95] R.J. Scherrer and M.S. Turner, Phys. Rev. D **33** (1986) 1585.

[96] P. Gondolo and G. Gelmini, Nucl. Phys. B **360** (1991) 145.

[97] C. Giunti and C.W. Kim, *Fundamentals of Neutrino Physics and Astrophysics*, Oxford University Press (2007).

[98] L. Baudis, arXiv:0711.3788 [astro-ph].

[99] P. Agrawal, Z. Chacko, C. Kilic, R.K. Mishra, arXiv:1003.1912 [hep-ph].

[100] PICASSO Collaboration, Phys. Lett. B **711** (2012) 153 [arXiv:1202.1240 [hep-ex]].

[101] D.S. Akerib et al. (LUX Collaboration), [arXiv:1310.8214 [astro-ph.CO]].

[102] CDMS Collaboration, Phys. Rev. Lett. **102** (2009) 011301 [arXiv:0802.3530 [astro-ph]].

[103] http://dmtools.brown.edu/ .

[104] J.M. LoSecco et al., Phys. Lett. B **188** (1987) 388.

[105] M. Mori et al., Phys. Rev. D **48** (1993) 5505.

[106] M.M. Boliev et al., Proc. of Int. Workshop on Aspects of Dark Matter in Astrophysics and Particle Physics, Heidelberg, Germany, 16-20 Sep 1996. Published in Heidelberg 1996, Dark matter in astro and particle physics, 711-717.

[107] M. Ambrosio et al., Phys. Rev. D **60** (1999) 082002 [arXiv:hep-ex/9812020].

[108] S. Desai et al., Phys. Rev. D **70** (2004) 083523 [arXiv:hep-ex/0404025].

[109] J. Ahrens et al., Phys. Rev. D **66** (2002) 032006 [arXiv:astro-ph/0202370].

[110] V. Aynutdinov et al., Nucl. Phys. Proc. Suppl. **143** (2005) 335.

[111] PAMELA Collaboration, Phys. Rev. Lett. **111** (2013) 081102 [arXiv:1308.0133 [astro-ph.HE]].

[112] M. Ackermann et al. (Fermi LAT Collaboration), Phys. Rev. Lett. **108** (2012) 011103.

[113] M. Aguilar et al. (AMS Collaboration) Phys. Rev. Lett. **110** (2013) 141102.

[114] The Fermi-LAT Collaboration, arXiv:1310.0828 [astro-ph.HE].

[115] B.L. Sánchez-Vega, J.C. Montero, E.R. Schmitz, arXiv:1404.5973 [hep-ph].

[116] J.C. Montero and V. Pleitez, Phys. Lett. B **675** (2009) 64.

[117] J.C. Montero and B.L. Sánchez-Vega, Phys. Rev. D **84** (2011) 053006.

[118] A.G. Dias, A.C.B. Machado, and C.C. Nishi, Phys. Rev. D **86** (2012) 093005.

[119] A.C.B. Machado and V. Pleitez, J. Phys. G: Nucl. Part. Phys. **40** (2013) 035002.

[120] K. Nakamura et al. (Particle Data Group), J. Phys. G **37** (2010) 075021.

[121] M.C. Gonzalez-Garcia and Yosef Nir, Phys. Lett. B **232** (1989) 383.

[122] R.N. Mohapatra and P.B. Pal, *Massive Neutrinos in Physics and Astrophysics* (World Scientific, Singapore, 2004), 3rd. ed..

[123] V. Barger, J.P. Kneller, H.S. Lee, D. Marfatia, and G. Steigman, Phys. Lett. B **566** (2003) 8.

[124] R.H. Cyburt, B.D. Fields, K.A. Olive, and E. Skillman, Astropart. Phys. **23** (2005) 313.

[125] S.W. Randall, M. Markevitch, D. Clowe, A. H. Gonzalez, and M. Bradac, arXiv:0704.0261.

[126] V. Barger, P. Langacker, M. McCaskey, M. Ramsey-Musolf, and G. Shaughnessy, Phys. Rev. D **79** (2009) 015018.

[127] J. Erler, P. Langacker, S. Munir and E. Rojas, JHEP **0908** (2009) 017 [arXiv:1108.0685 [hep-ph]].

[128] F. del Aguila, J. de Blas and M. Perez-Victoria, JHEP **2010** (2010) 9 [arXiv:1005.3998 [hep-ph]].

[129] R. Diener, S. Godfrey, and I. Turan, Phys. Rev. D **86** (2012) 115017.

[130] T. Appelquist, B.A. Dobrescu and A.R. Hopper, Phys. Rev. D **68** (2003) 035012.

[131] M. Carena, A. Daleo, B.A. Dobrescu, and T.M.P. Tait, Phys. Rev. D **70** (2004) 093009.

[132] E. Aprile et al. (XENON100 Collaboration), Phys. Rev. Lett. **109** (2012) 181301 [arXiv:1207.5988 [astro-ph.CO]].

[133] R. Agnese et al. (SuperCDMS Collaboration), Phys. Rev. Lett **112** (2014) 091303.

[134] G. Belanger et al., Phys. Rev. D **88** (2013) 075008.

[135] J. Ellis and T. You, JHEP **1306** (2013) 103.

[136] M.E. Peskin, arXiv:1207.2516v3.

[137] M. Lattanzi and J.W.F. Valle, Phys. Rev. Lett. **99** (2007) 121301.

[138] E.Kh. Akhmedov et al., Phys. Lett. B **299** (1993) 90.

[139] G. Steigman and M.S. Turner, Nucl. Phys. B **253** (1985) 375.

[140] F.S. Queiroz and K. Sinha, arXiv:1404.1400v2.